ConocoPhillips School of Geology & Geophysics, The University of Oklahoma

GPHY 5513
3D Seismic Interpretation

Zonghu Liao (China University of Petroleum)

Curvature, Reflector Rotation, and Reflector Convergence

Volumetric Curvature

Sign convention for 2D curvature attributes:

Anticline: k > 0
Plane: k = 0
Syncline: k < 0

$$k = \frac{1}{R} = \frac{\dfrac{d^2 z}{dx^2}}{\left[1 + \left(\dfrac{dz}{dx}\right)^2\right]^{3/2}}$$

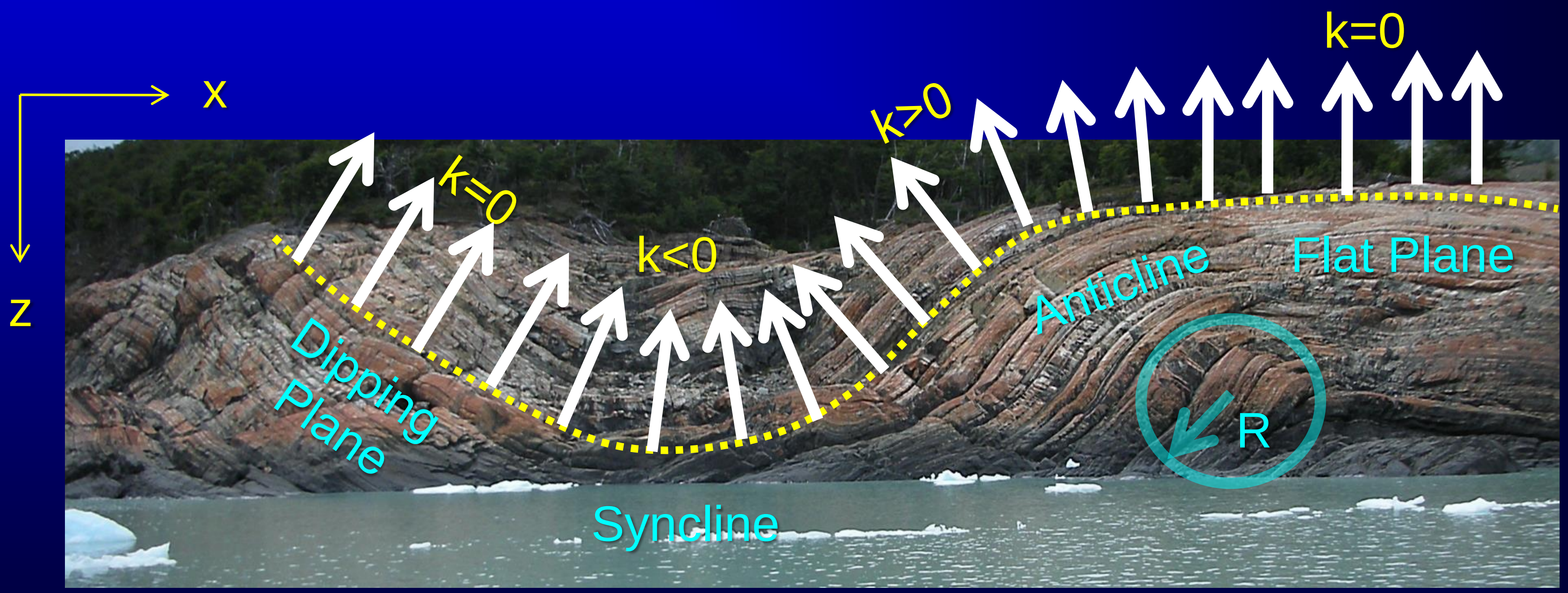

3D Curvature and Topographic Mapping

Bent Creek Experimental Forest

Ecology and Management of Southern Appalachian Hardwoods

Southern Research Station

- Bent Creek GIS Data
- Classification of the Vegetation of the southern Appalachians
- LFI and TSI: Topographic Variables to Quantify Meso- and Micro-scale Landforms
  - Terrain Shape Index
  - Landform Index
  - C+ Program

(http://www.srs.fs.usda.gov/bentcreek)

3D Curvature and Molecular Docking

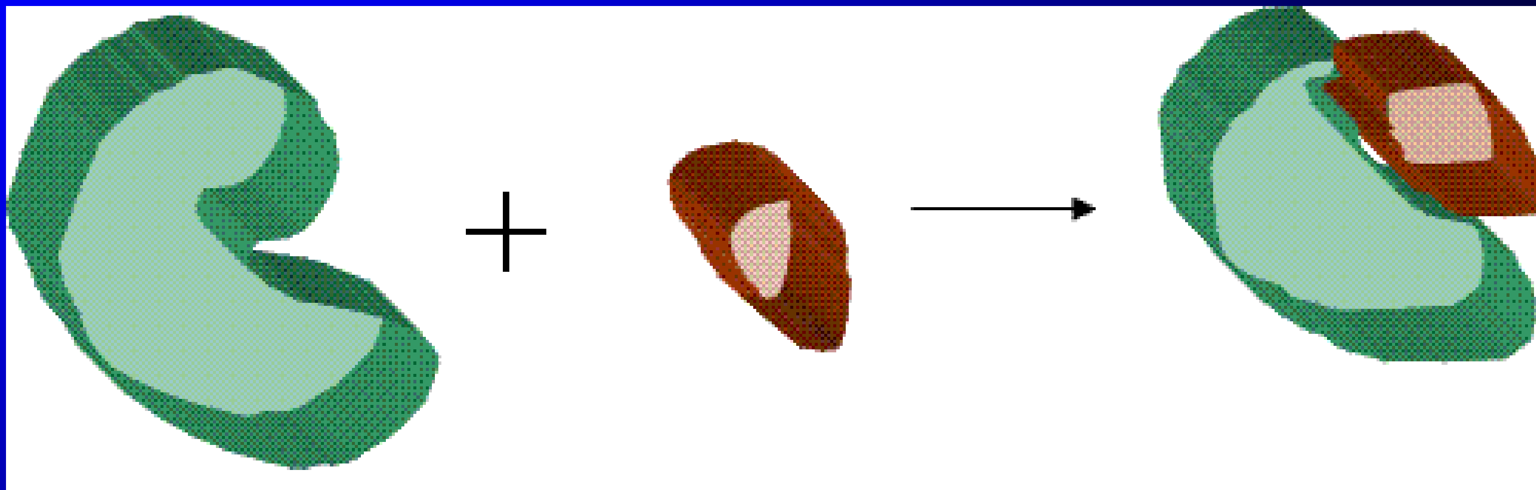

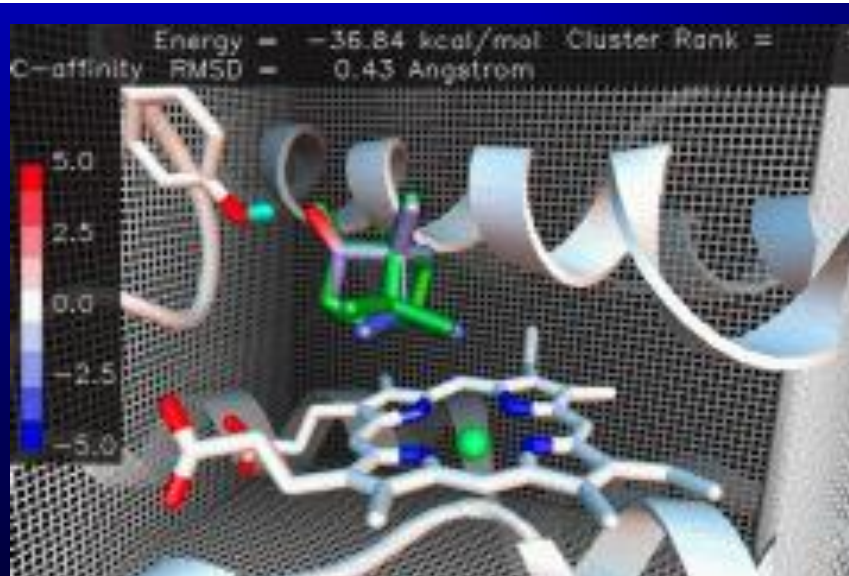

(http://en.wikipedia.org/wiki/Molecular_docking

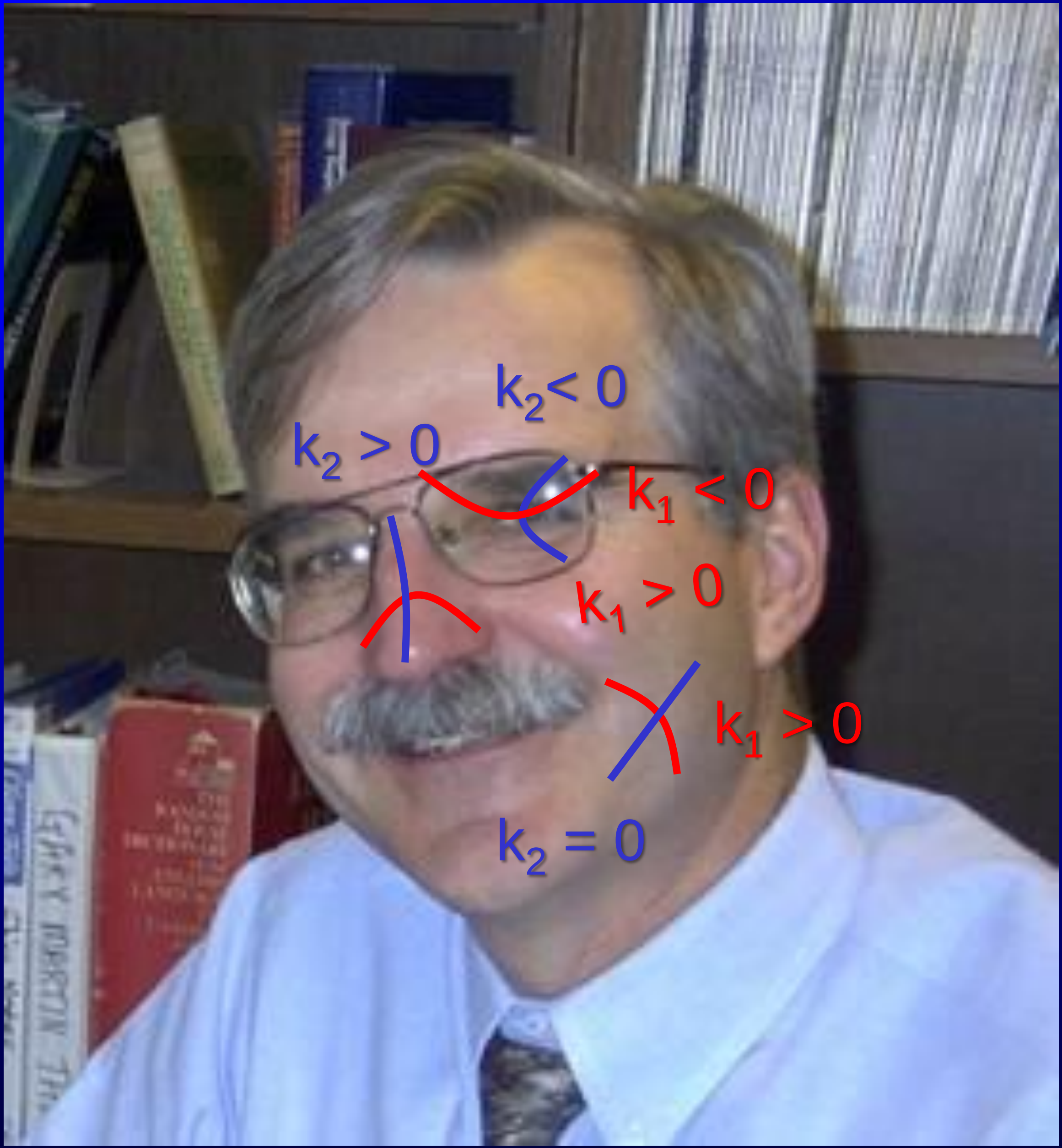

3D Curvature and Biometric Identification of Suspicious Travelers

Circles in perpendicular planes tangent to a quadratic surface

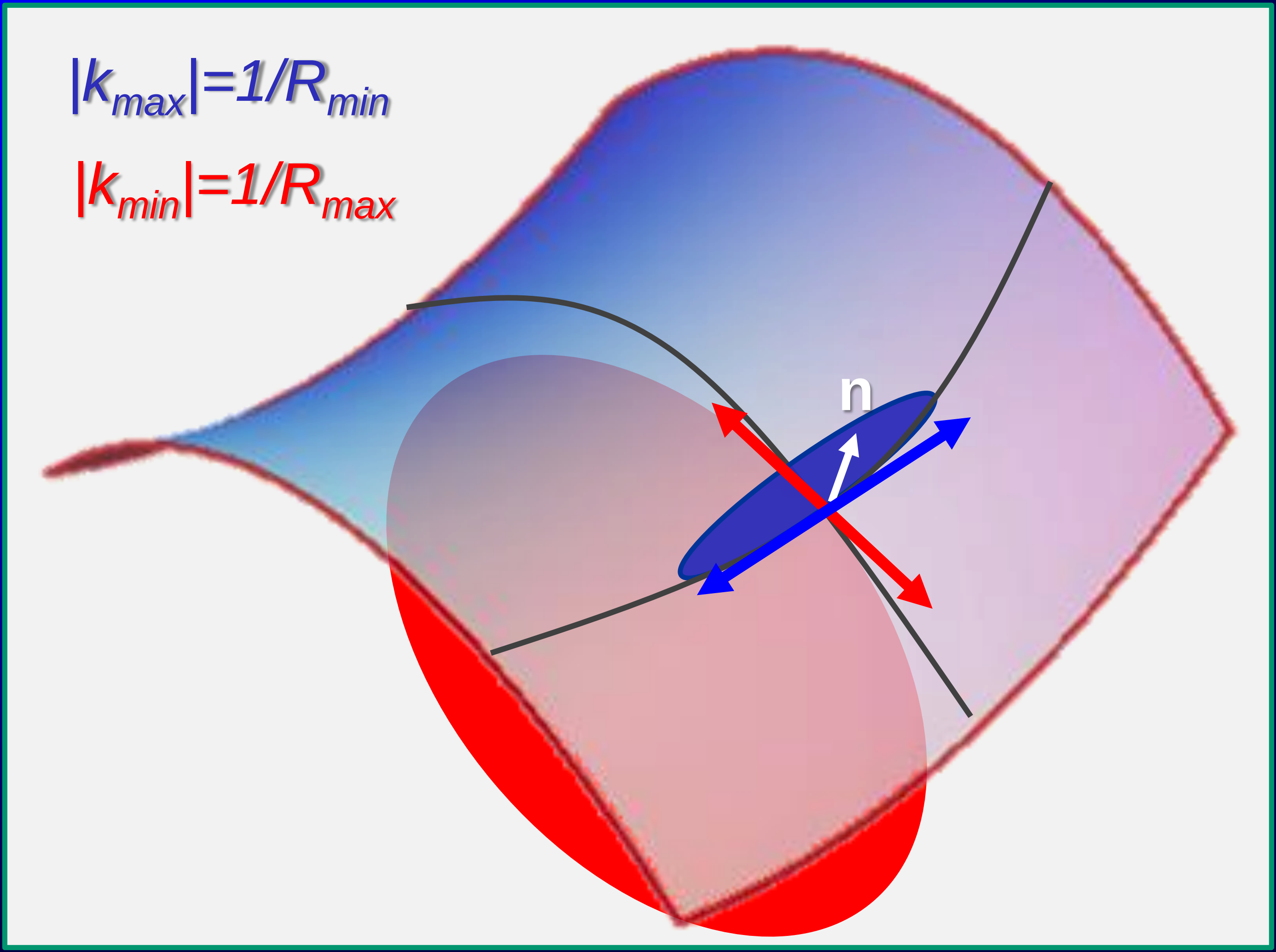

(Mai et al., 2009)

Geometries of some folded surfaces

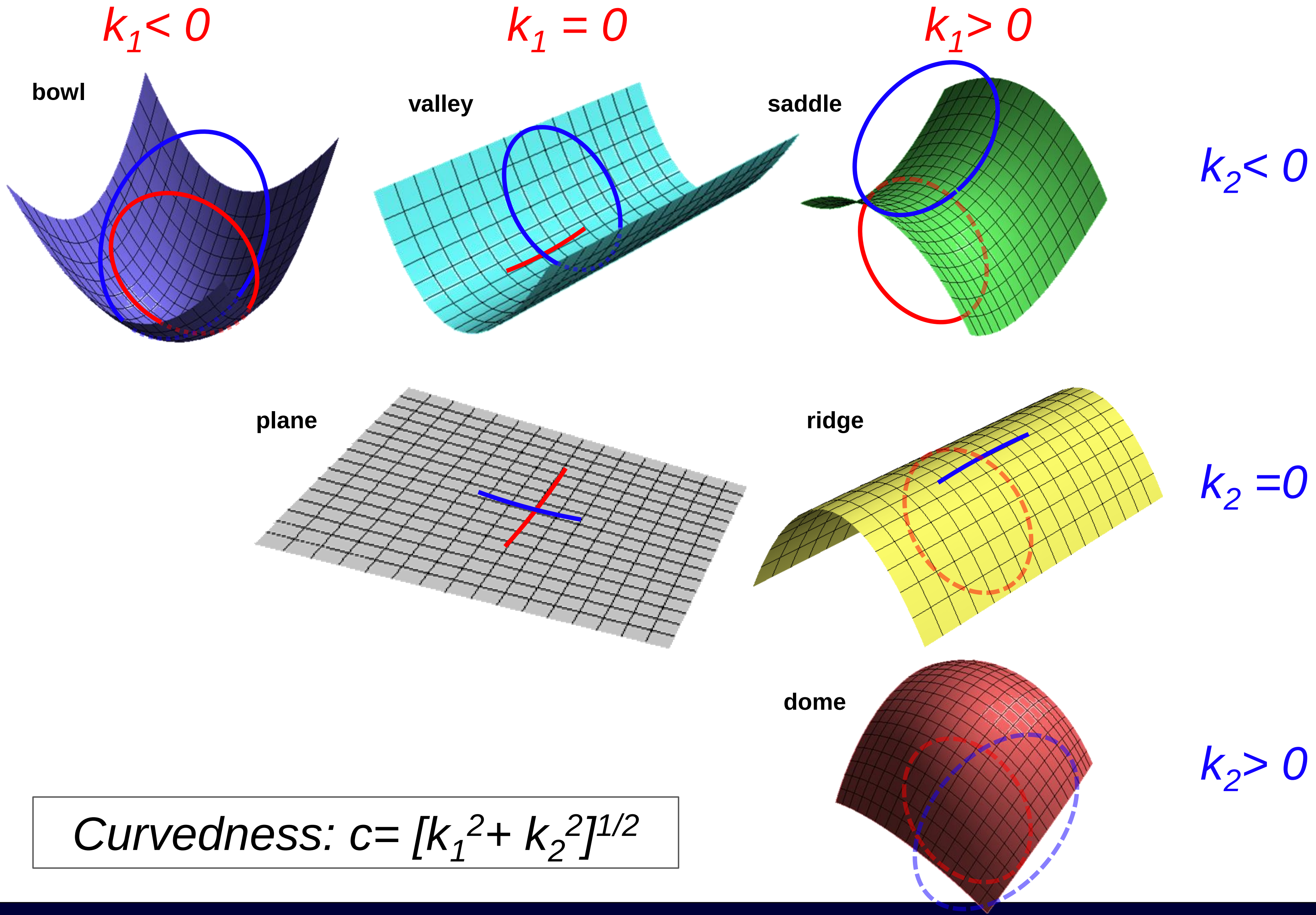

Curvedness: $c = [k_1^2 + k_2^2]^{1/2}$

(courtesy of Ha Mai)

An interactive program showing curvature

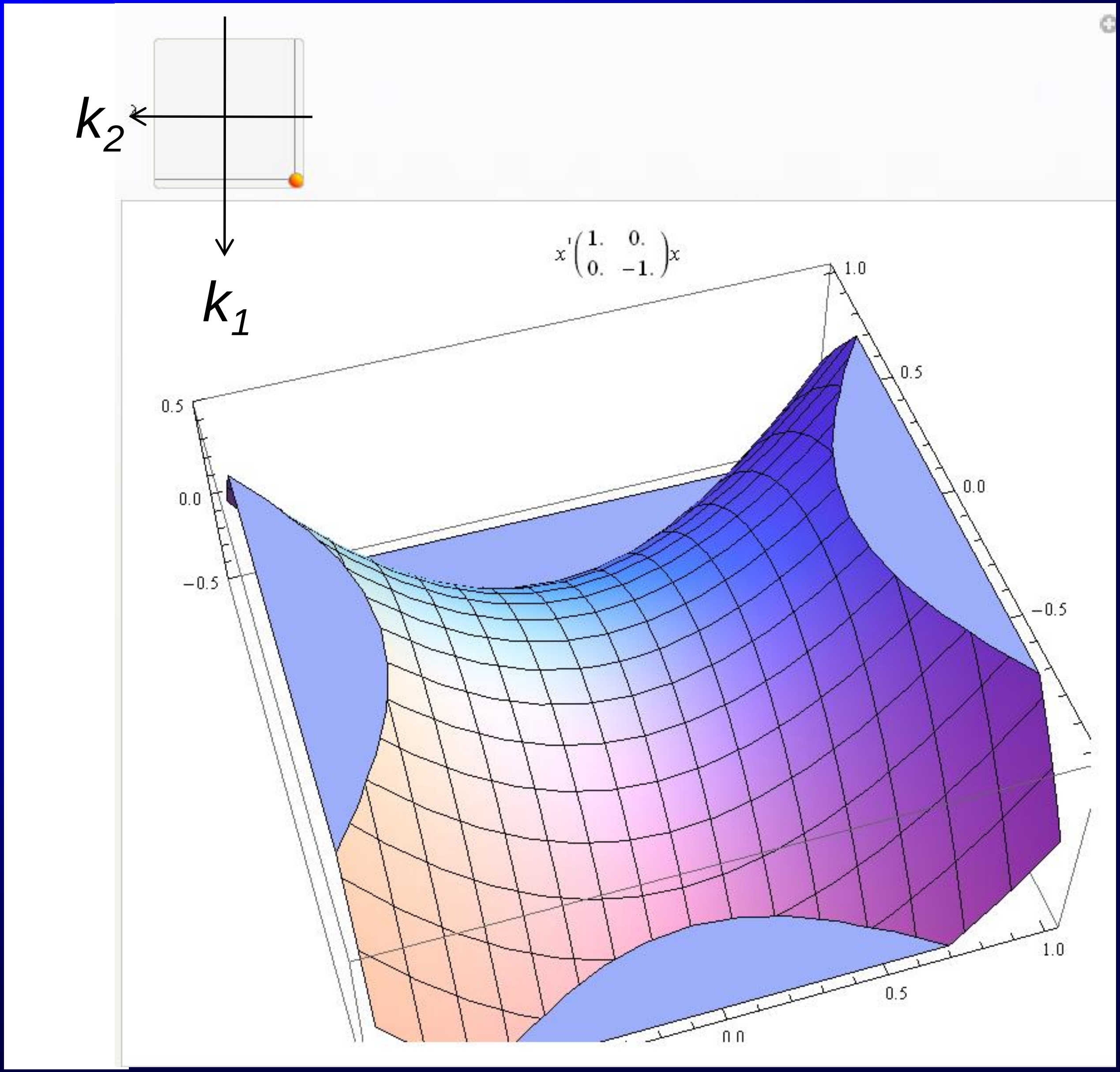

(Wolfram demonstration project)

Curvature of picked horizons

kx-ky transform of time picks

Seismic horizon

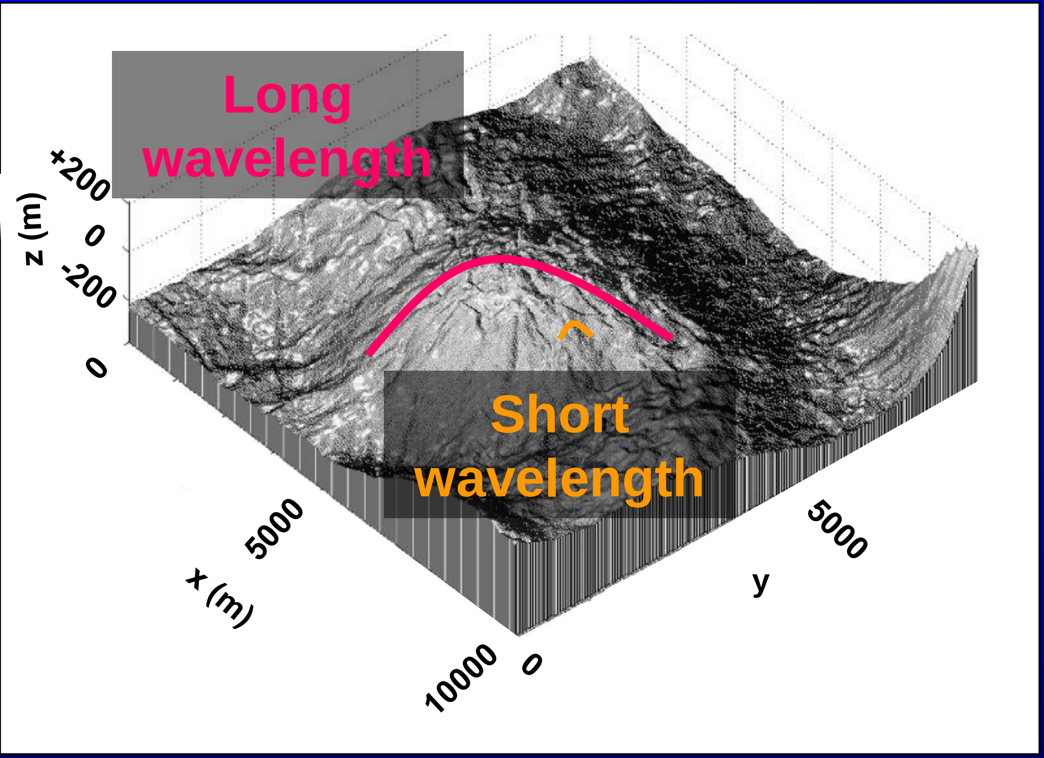

k_x-k_y spectrum

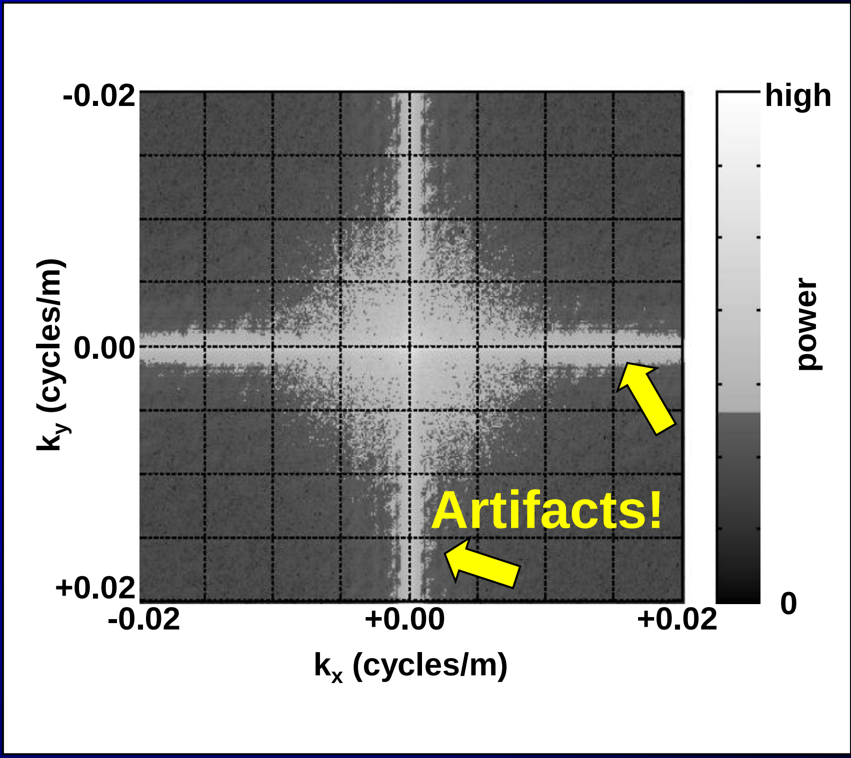

The horizon exhibits different scale structures such as domes and basins on the broad-scale, faults on the intermediate-scale, and smaller scale undulations.

(Bergbauer et al, 2003)

kx-ky transform of time picks after bandpass filter

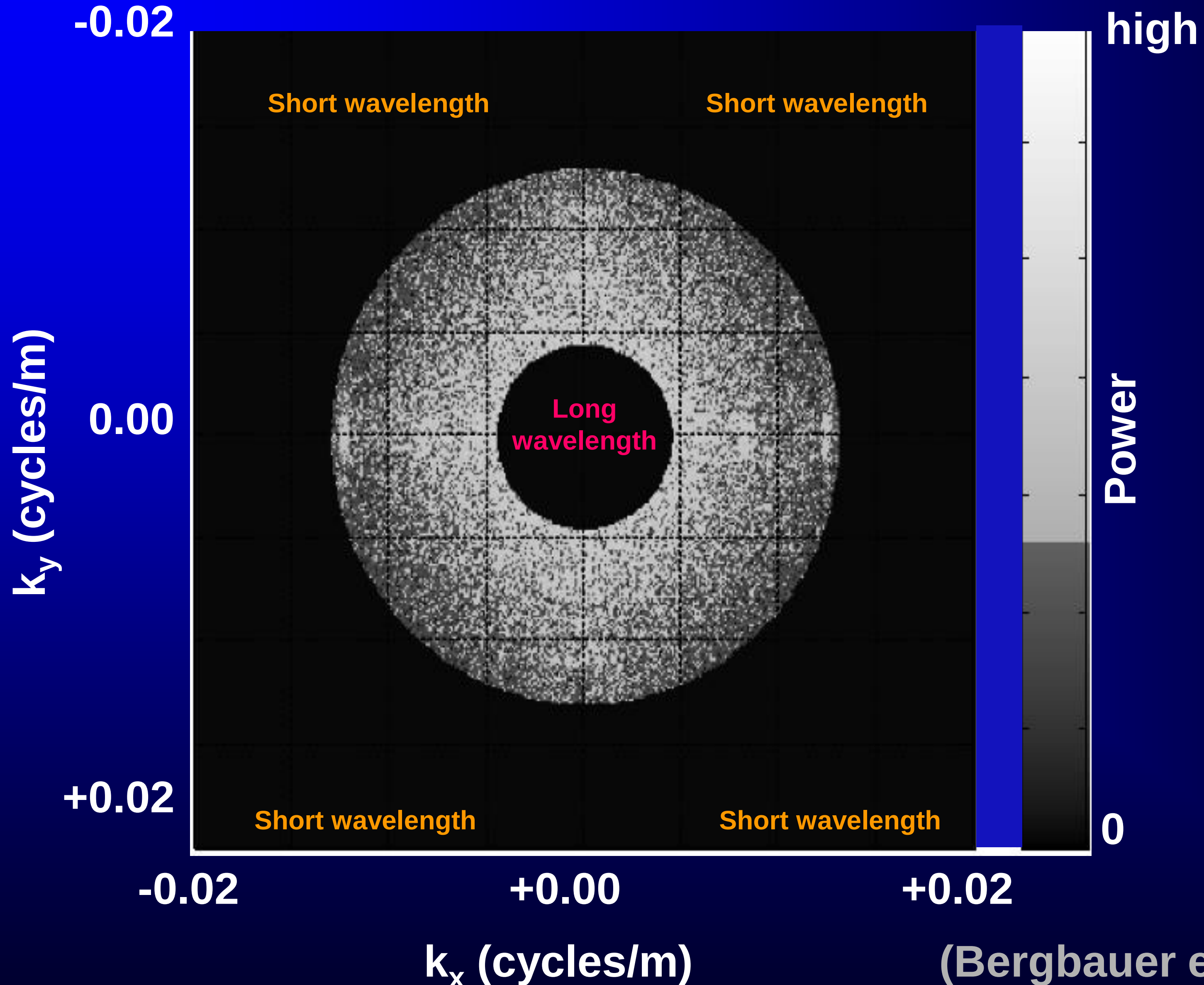

(Bergbauer et al, 2003)

Maximum curvature after k_x-k_y bandpass filter

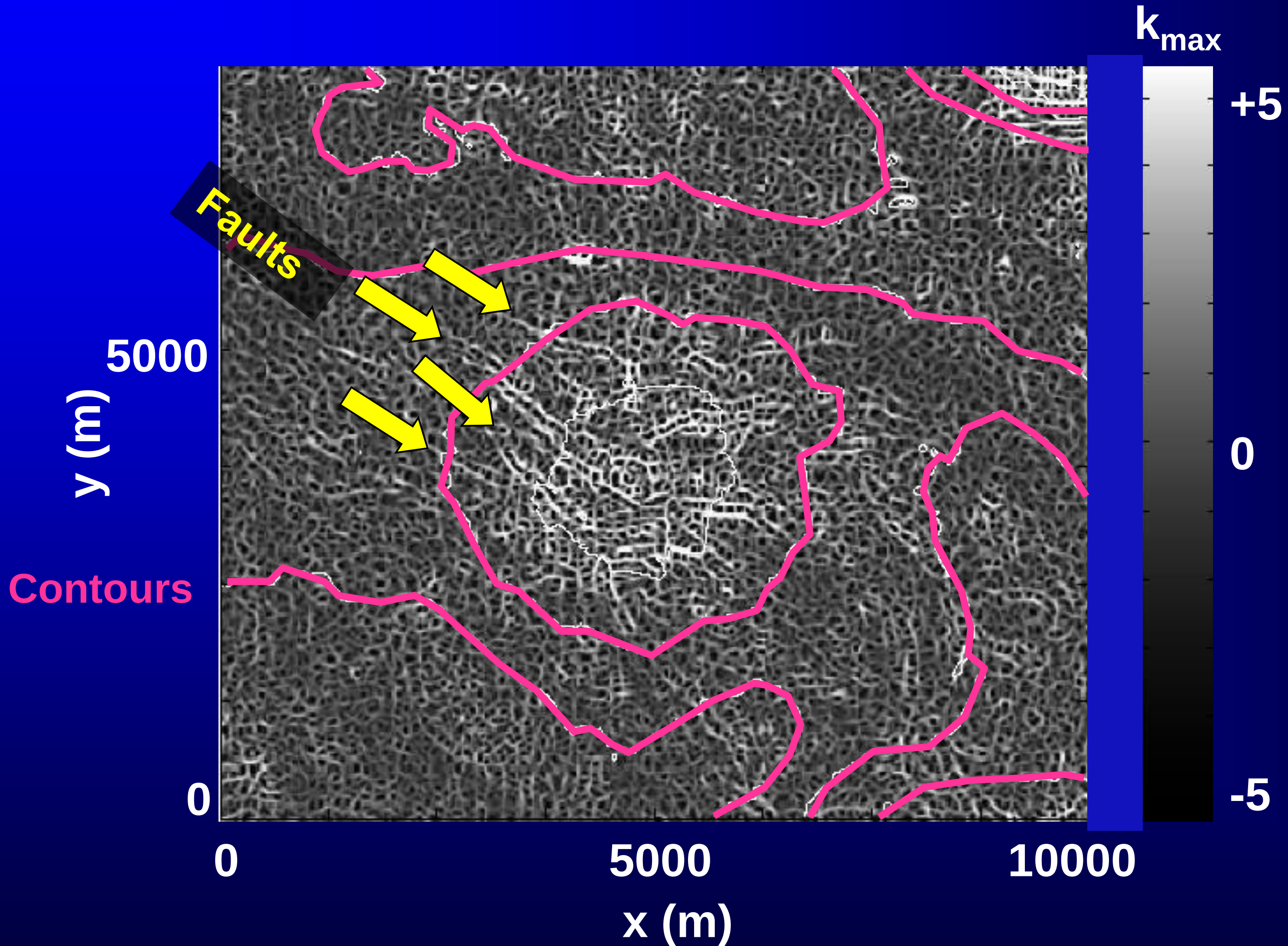

(Bergbauer et al, 2003)

Radius of Curvature

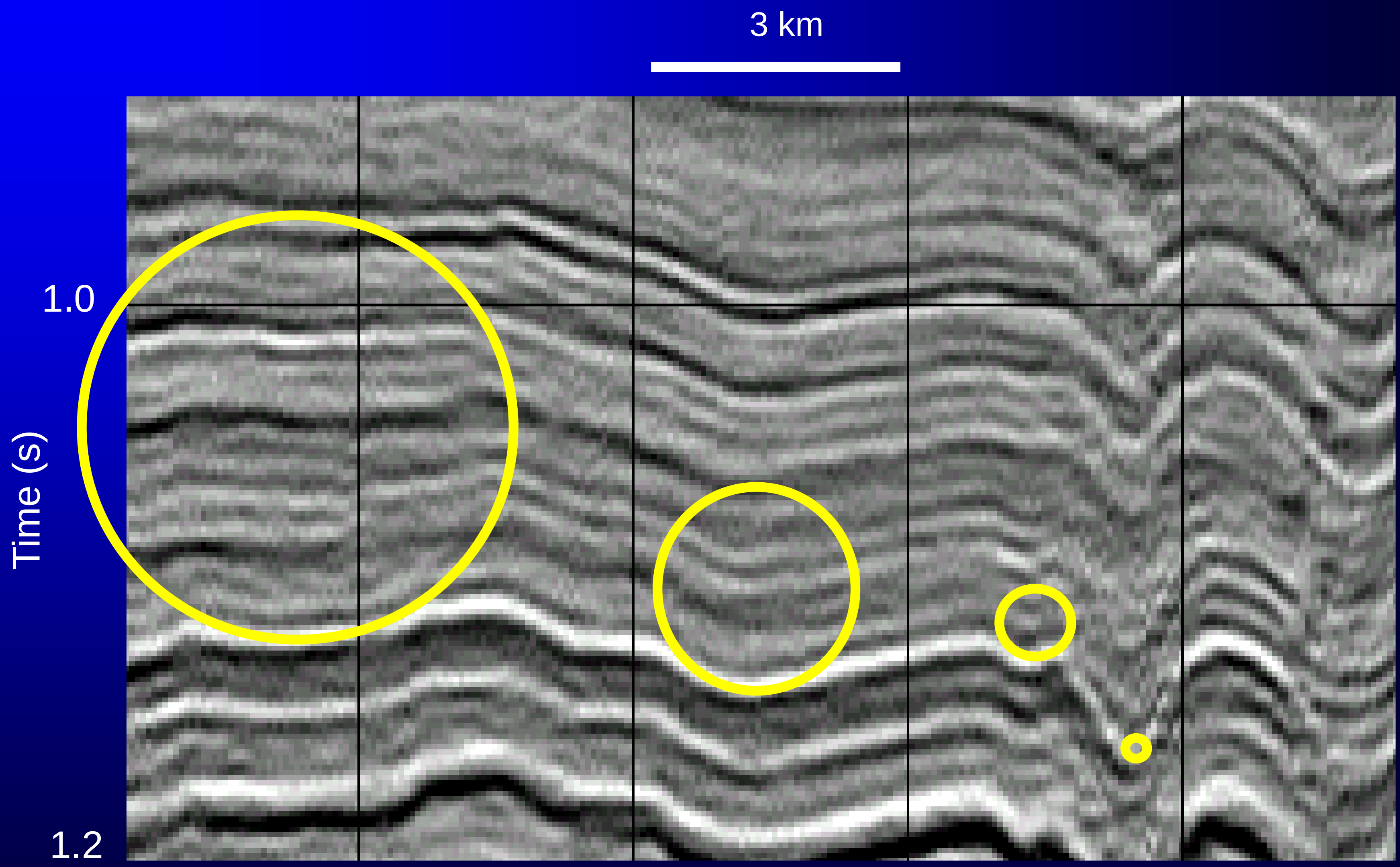

Thermal imagery with sun-shading

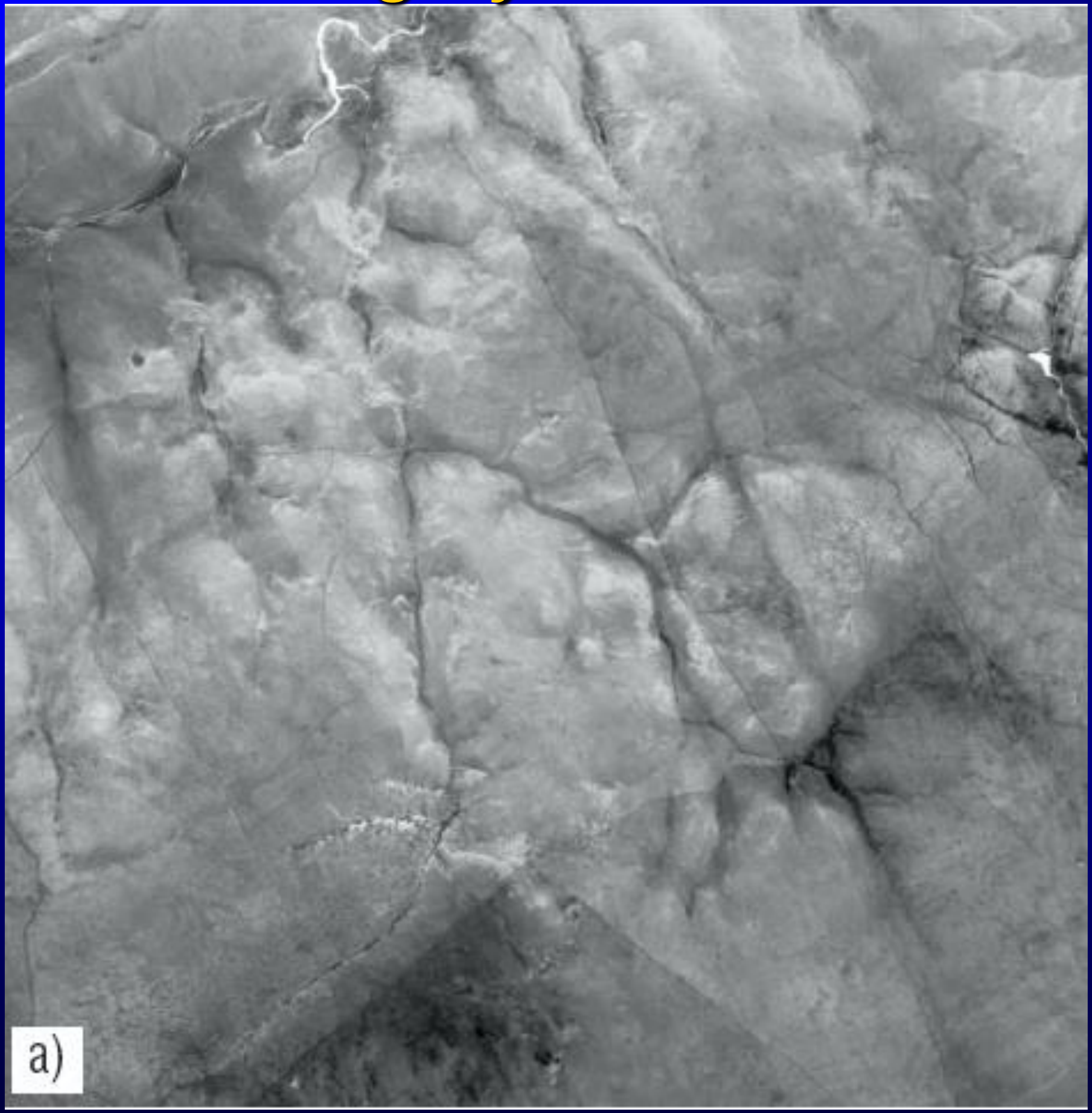

(Cooper and Cowan, 2003)

Fractional derivatives with sun-shading

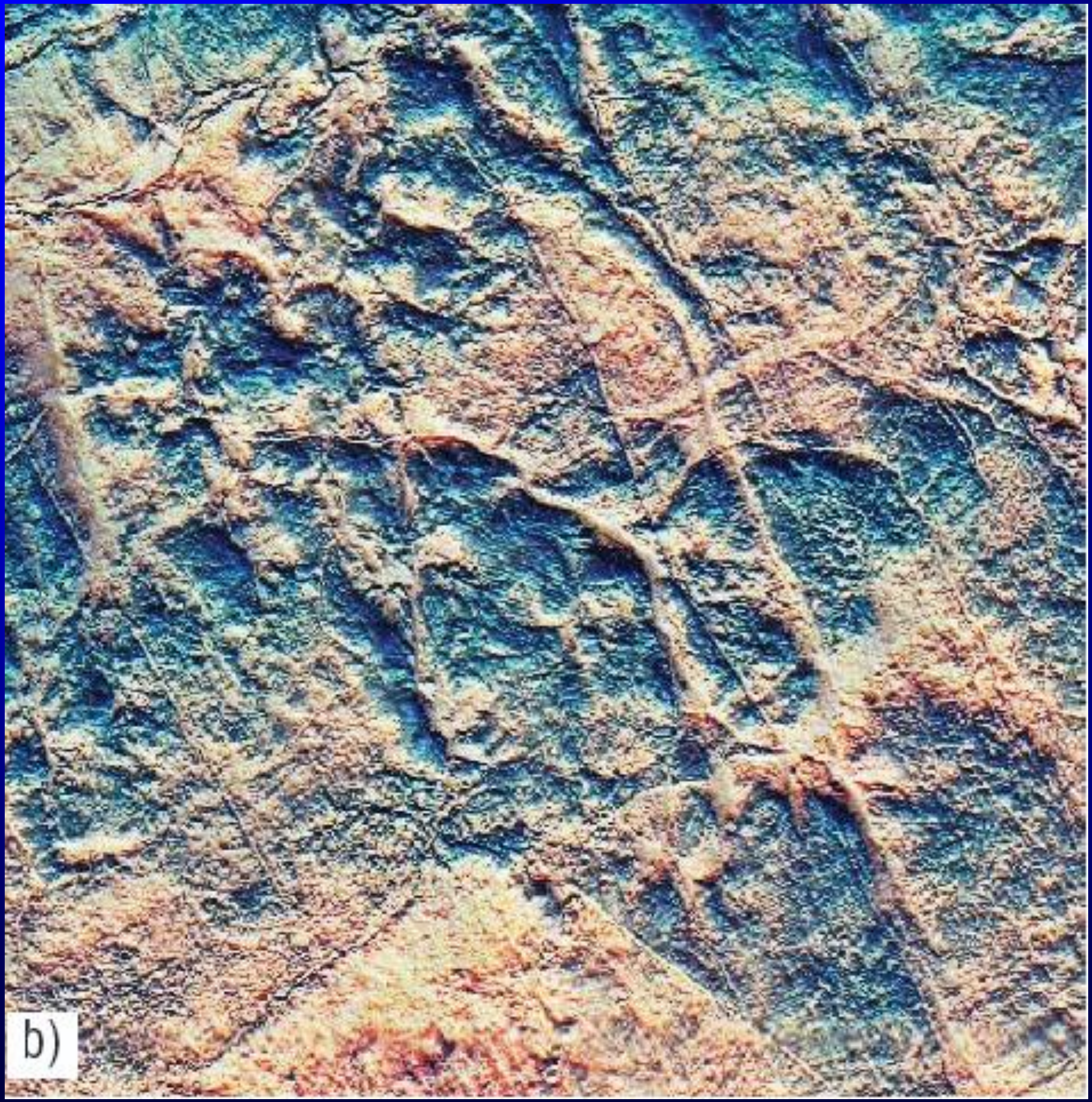

Red=0.75
Green=1.00
Blue=1.25

(Cooper and Cowan, 2003)

2D curvature estimates from inline dip, p:

1st derivative

$$dp/dx = F^{-1}[\, ik_x F(p)\,]$$

fractional derivative
(or 1st derivative followed by a low pass filter)

$$d^{\alpha}p/dx^{\alpha} \approx F^{-1}[i(k_x)^{\alpha} F(p)\,]$$

(al-Dossary and Marfurt, 2006)

Attributes extracted along a geological horizon

Vertical Slice – Fort Worth Basin, USA

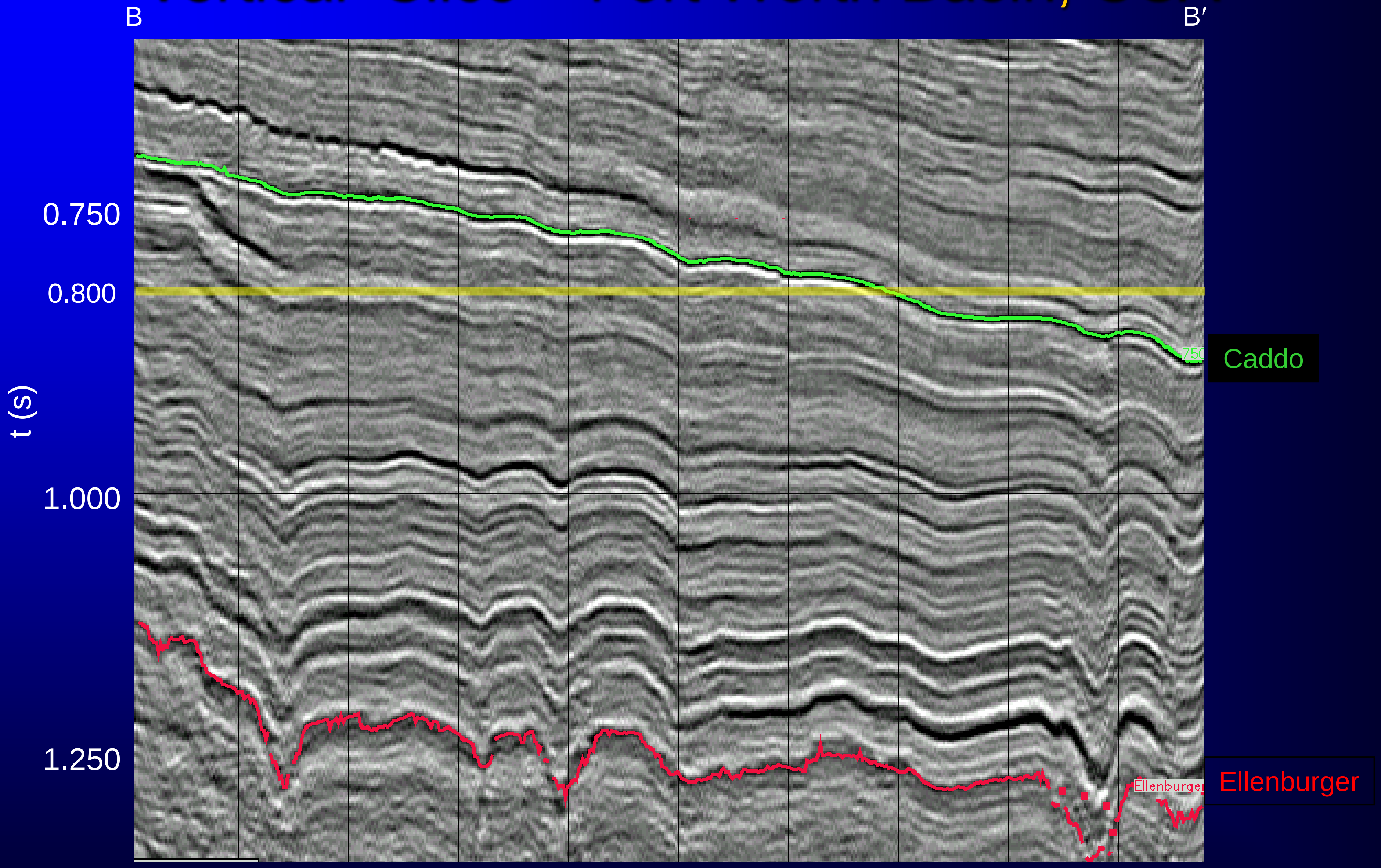

(al-Dossary and Marfurt, 2006)

k_{mean}=1/2(d²T/dx²+d²T/dy²) – Caddo (Horizon pick calculation)

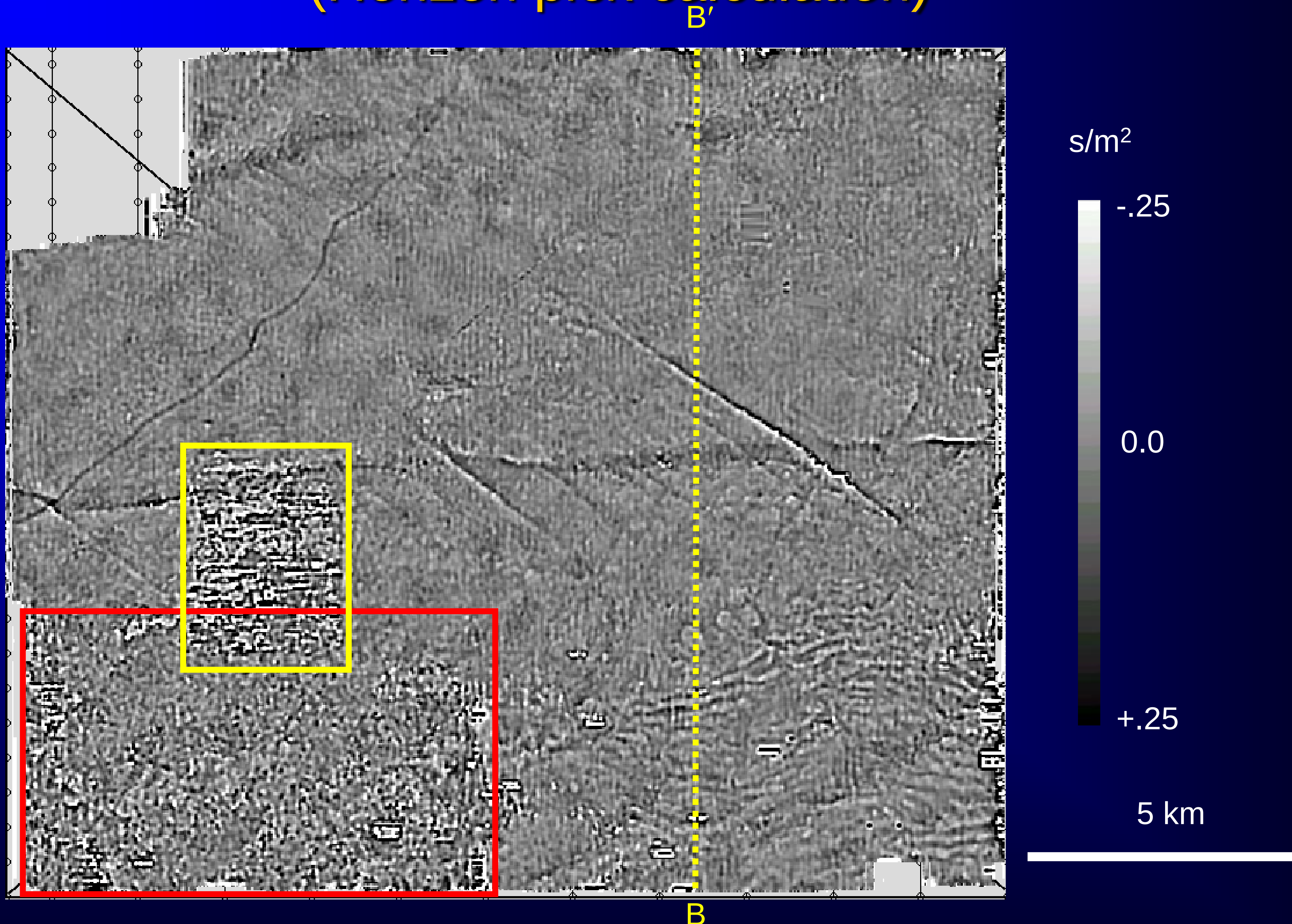

k_{mean} horizon slice – Caddo (volumetric calculation)

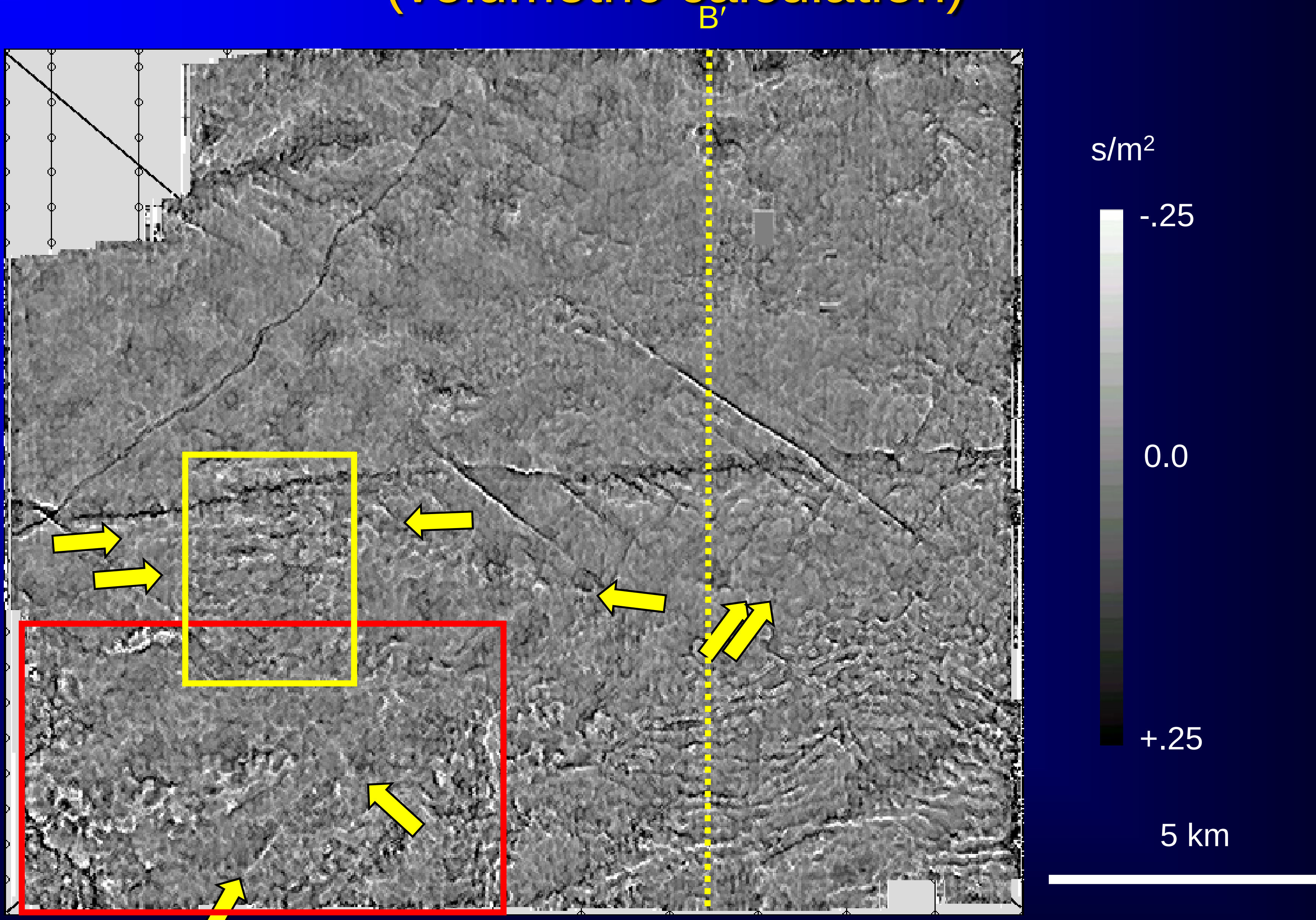

Coherence horizon slice – Caddo

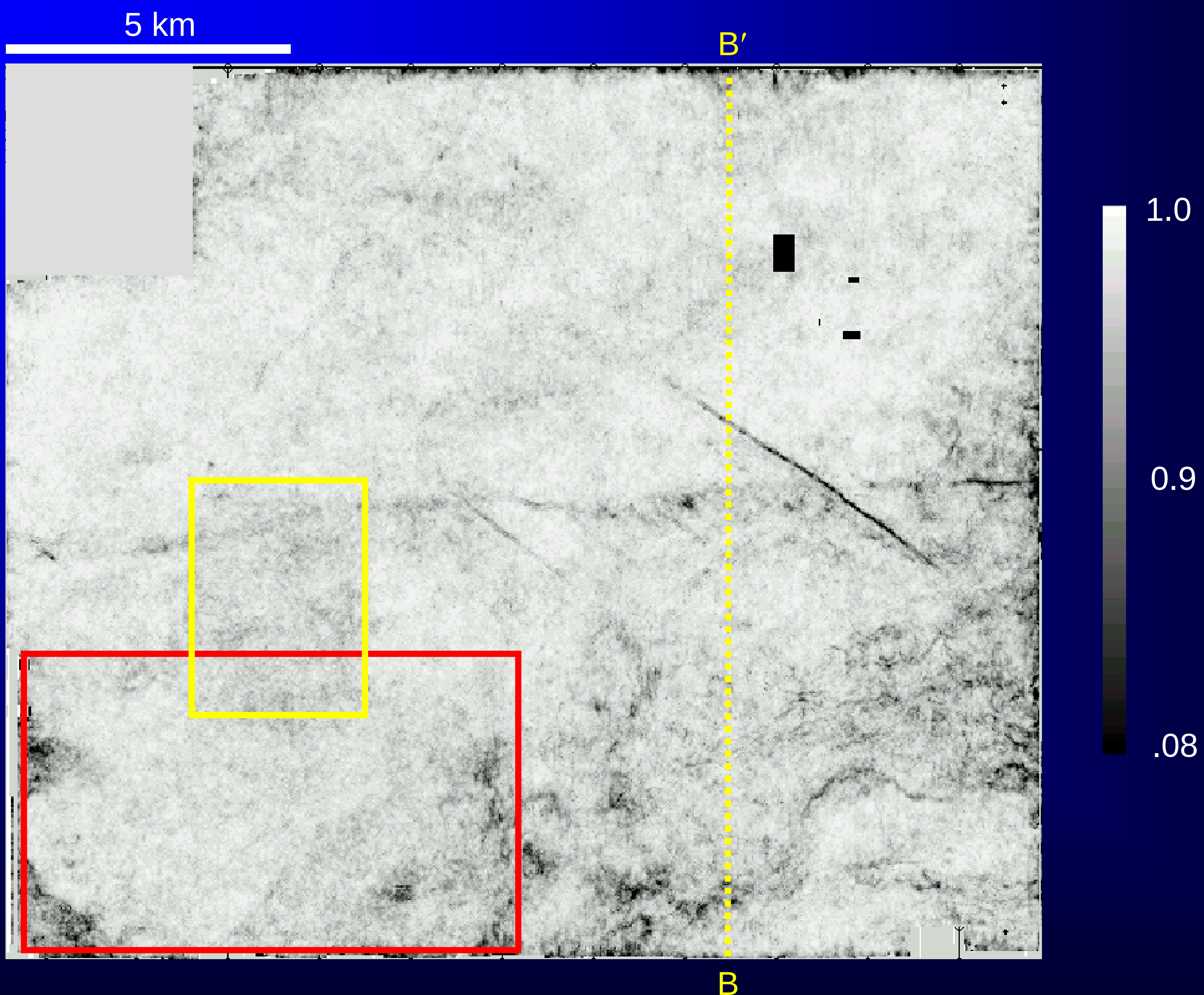

Attributes extracted along time slices

Vertical slice through seismic

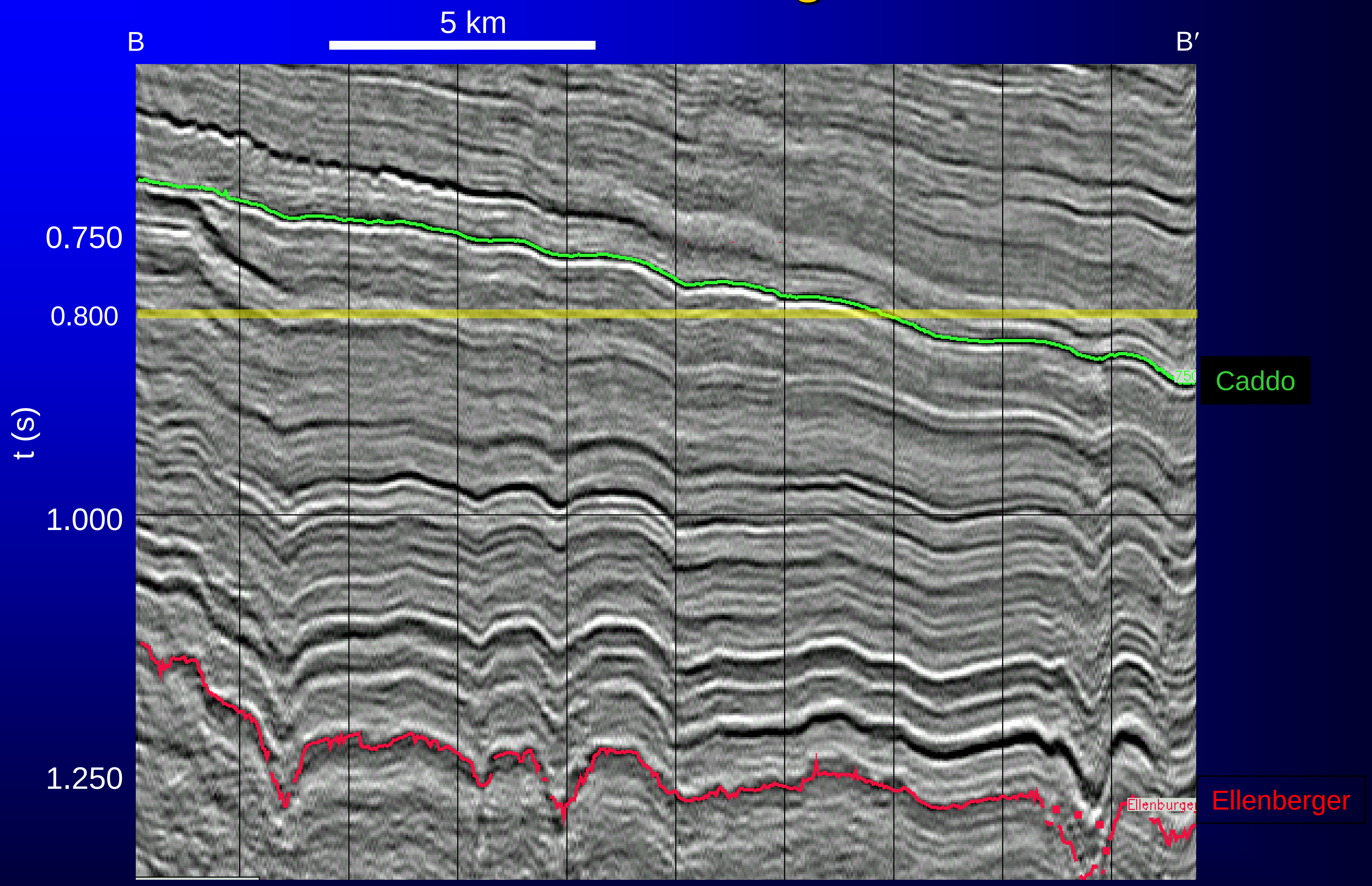

(al-Dossary and Marfurt, 2006)

Time slice through coherence
t=0.8 s

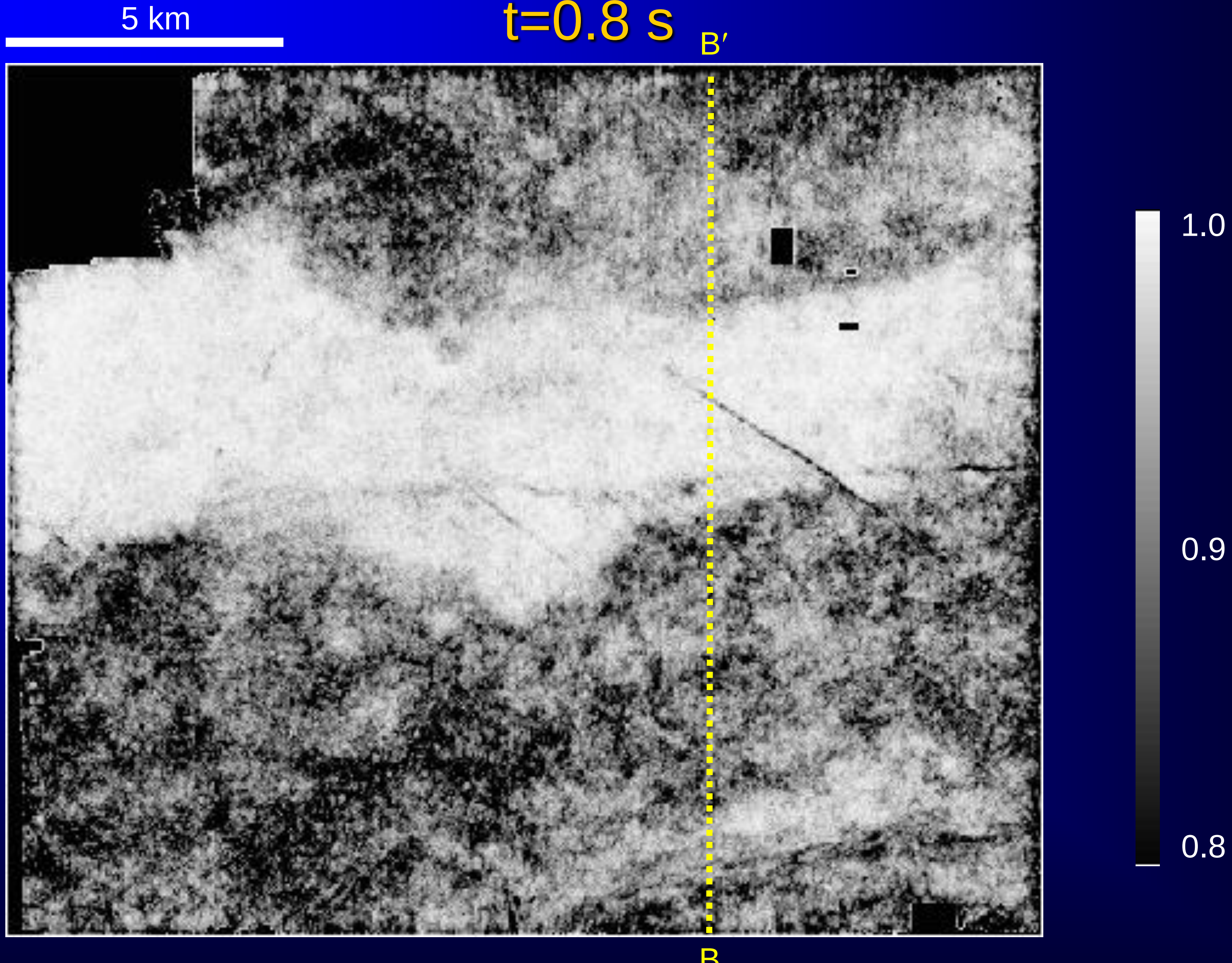

(al-Dossary and Marfurt, 2006)

Most-negative curvature computed at different wavelengths
t=0.8 s

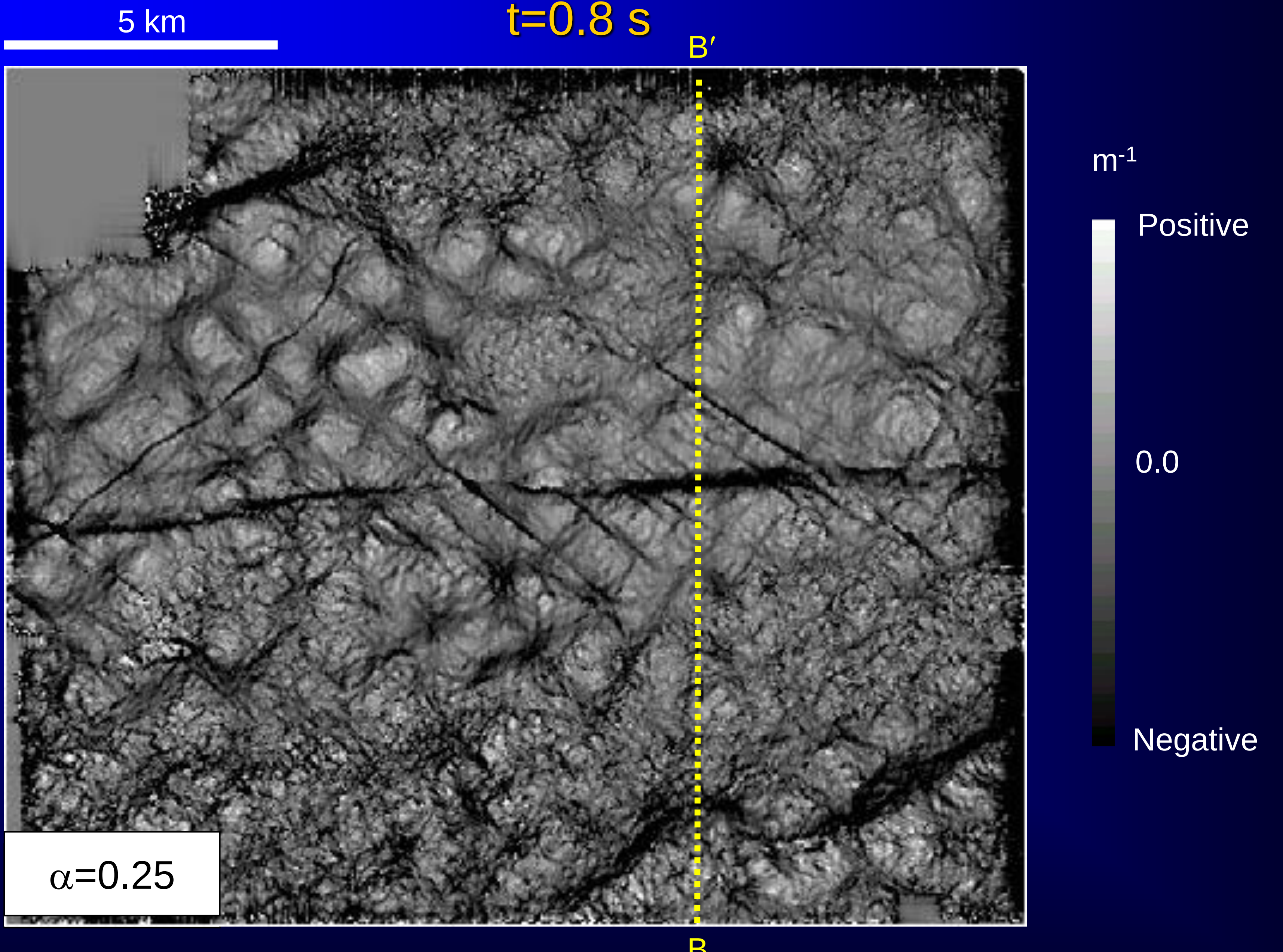

(al-Dossary and Marfurt, 2006)

Coherence
t=0.8 s

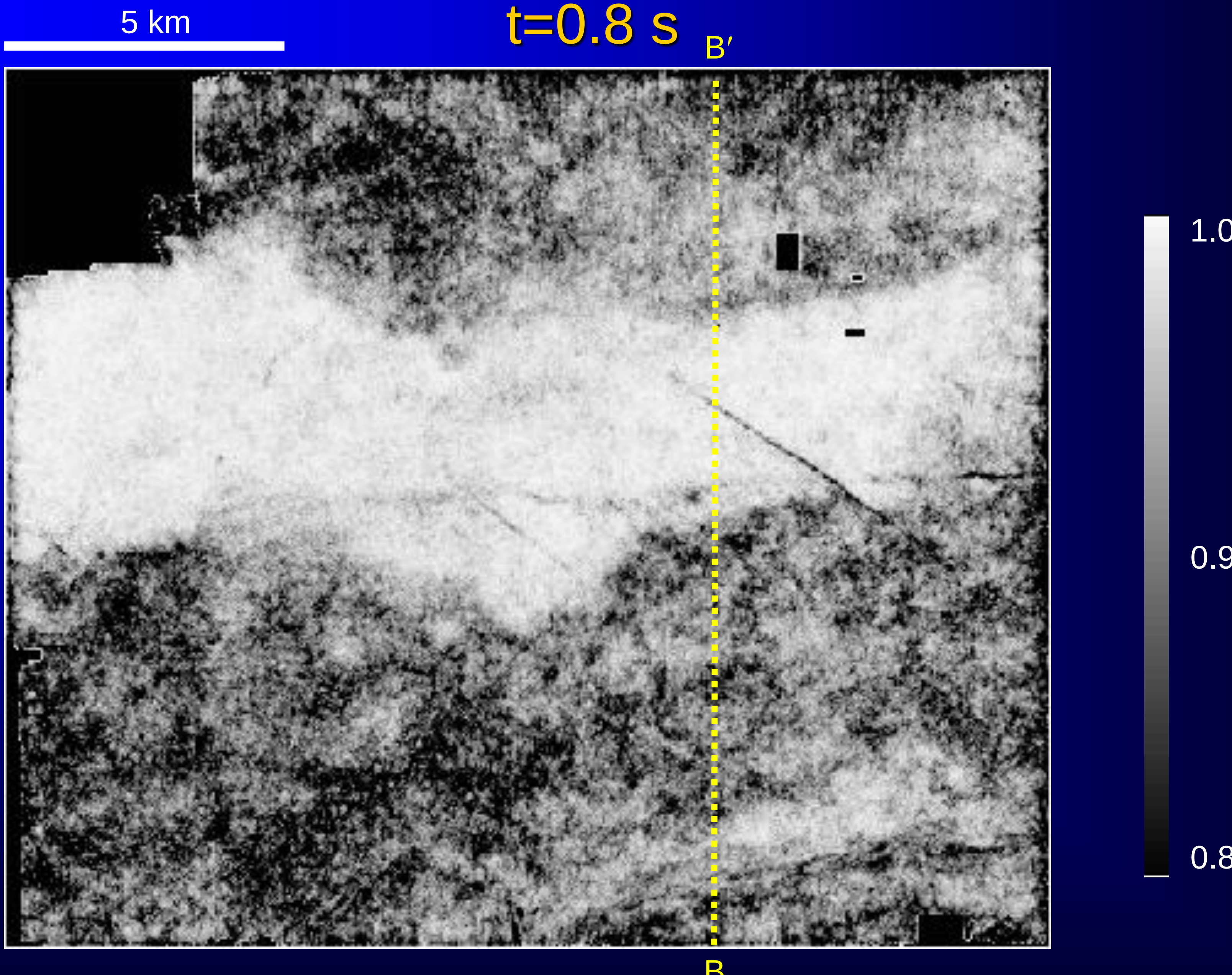

(al-Dossary and Marfurt, 2006)

Coherence

t=1.2 s

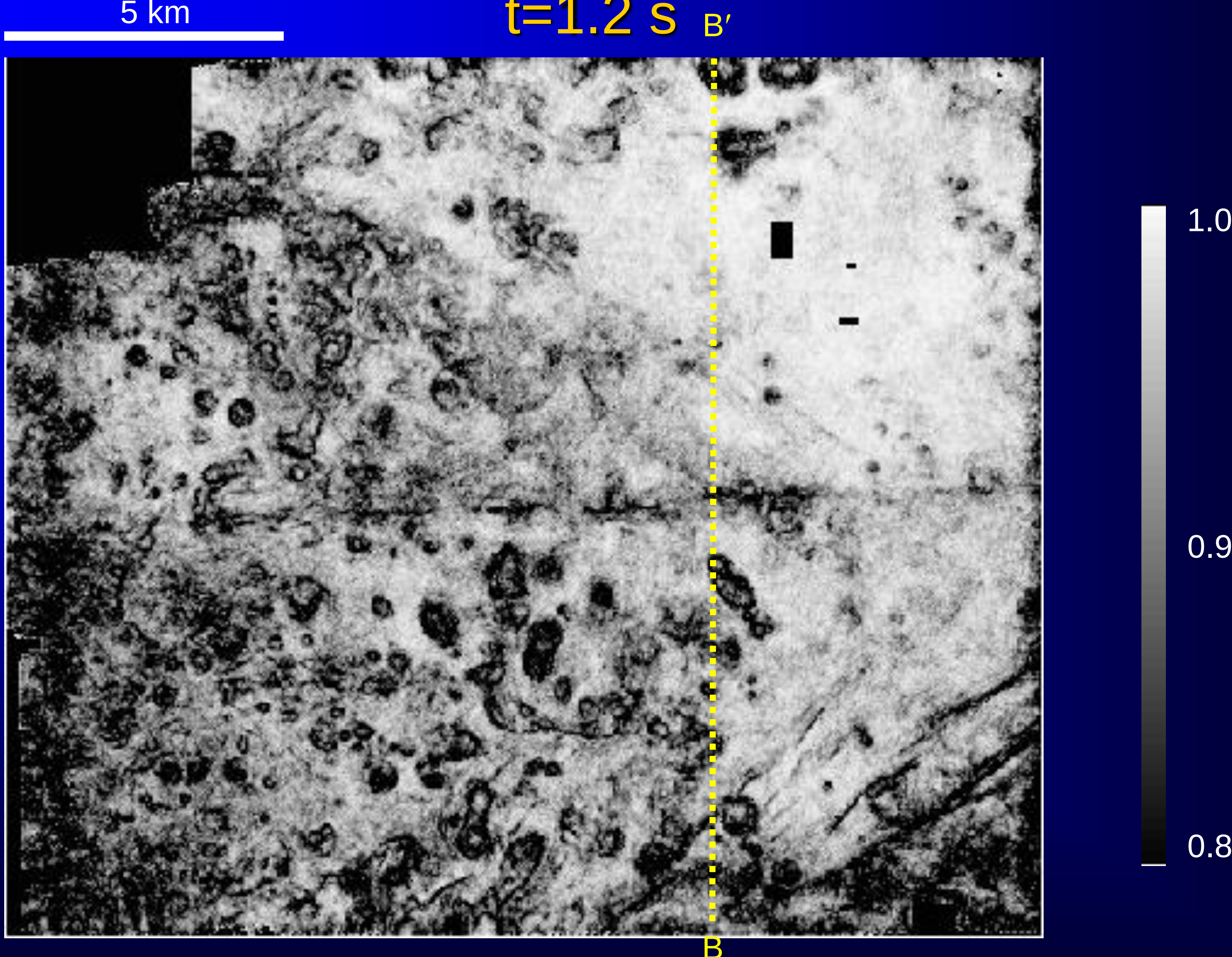

(al-Dossary and Marfurt, 2006)

Most negative curvature (α=0.25)
t=1.2 s

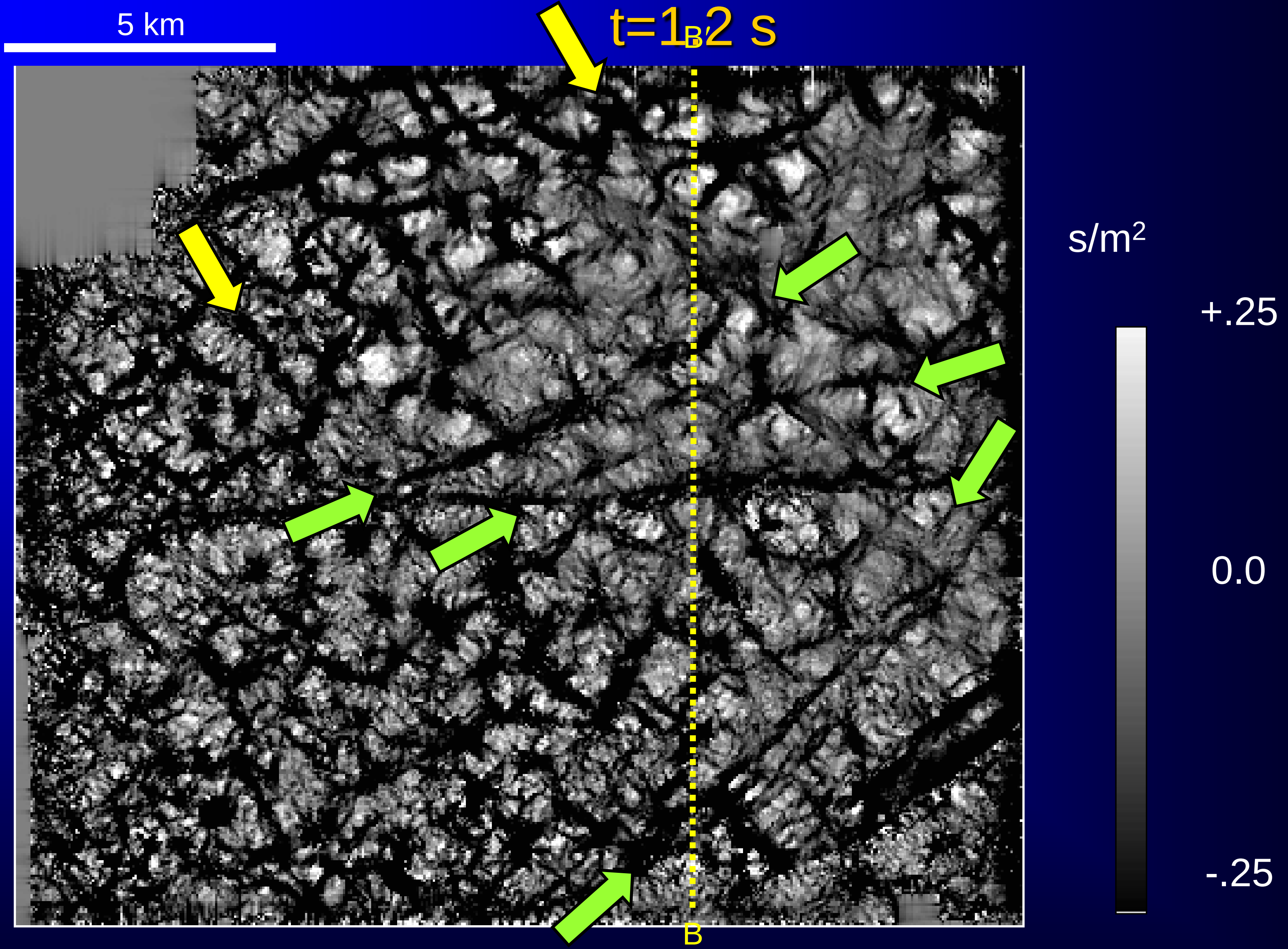

(al-Dossary and Marfurt, 2006)

Filters corresponding to "long-wavelength" and "short-wavelength" curvature computation

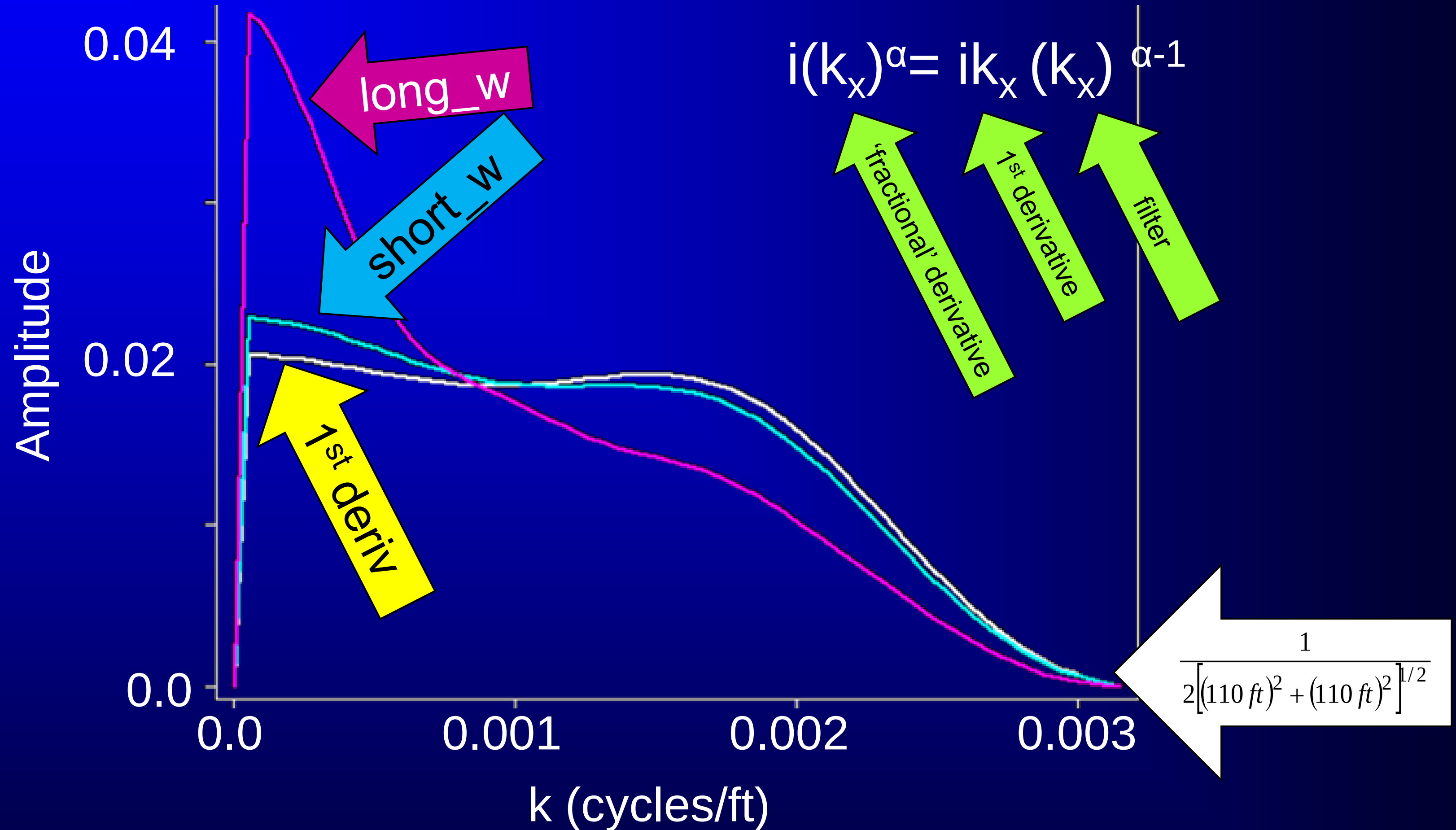

Attributes based on volumetric dip and azimuth

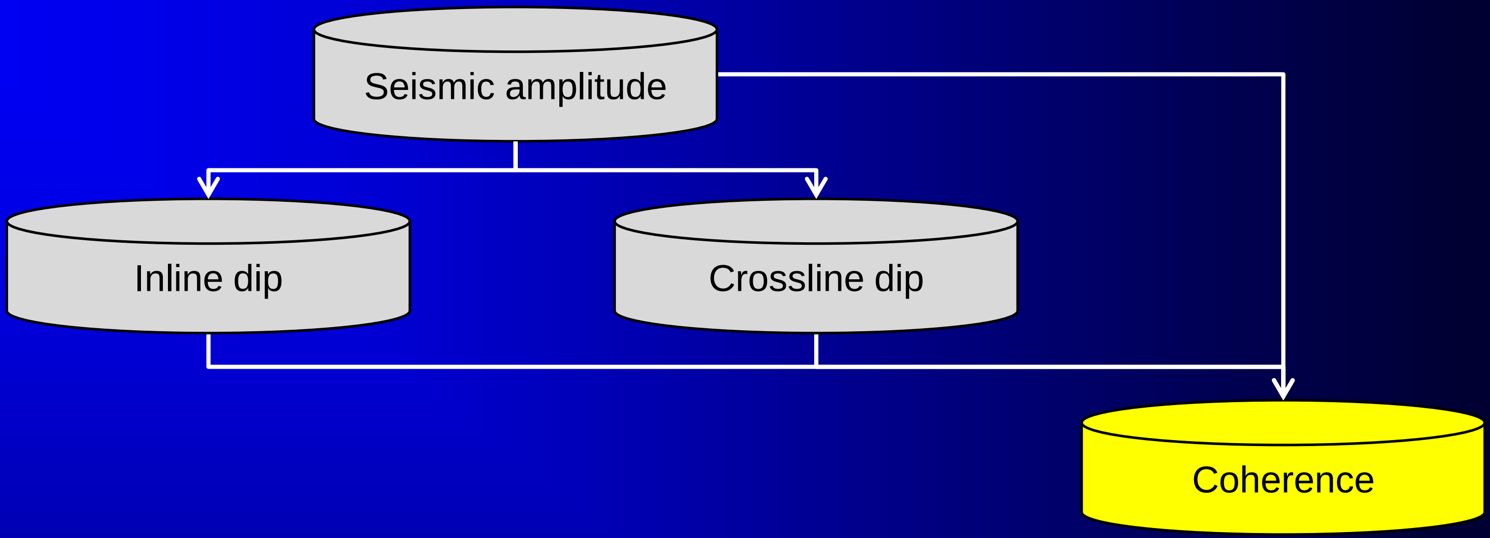

Coherence

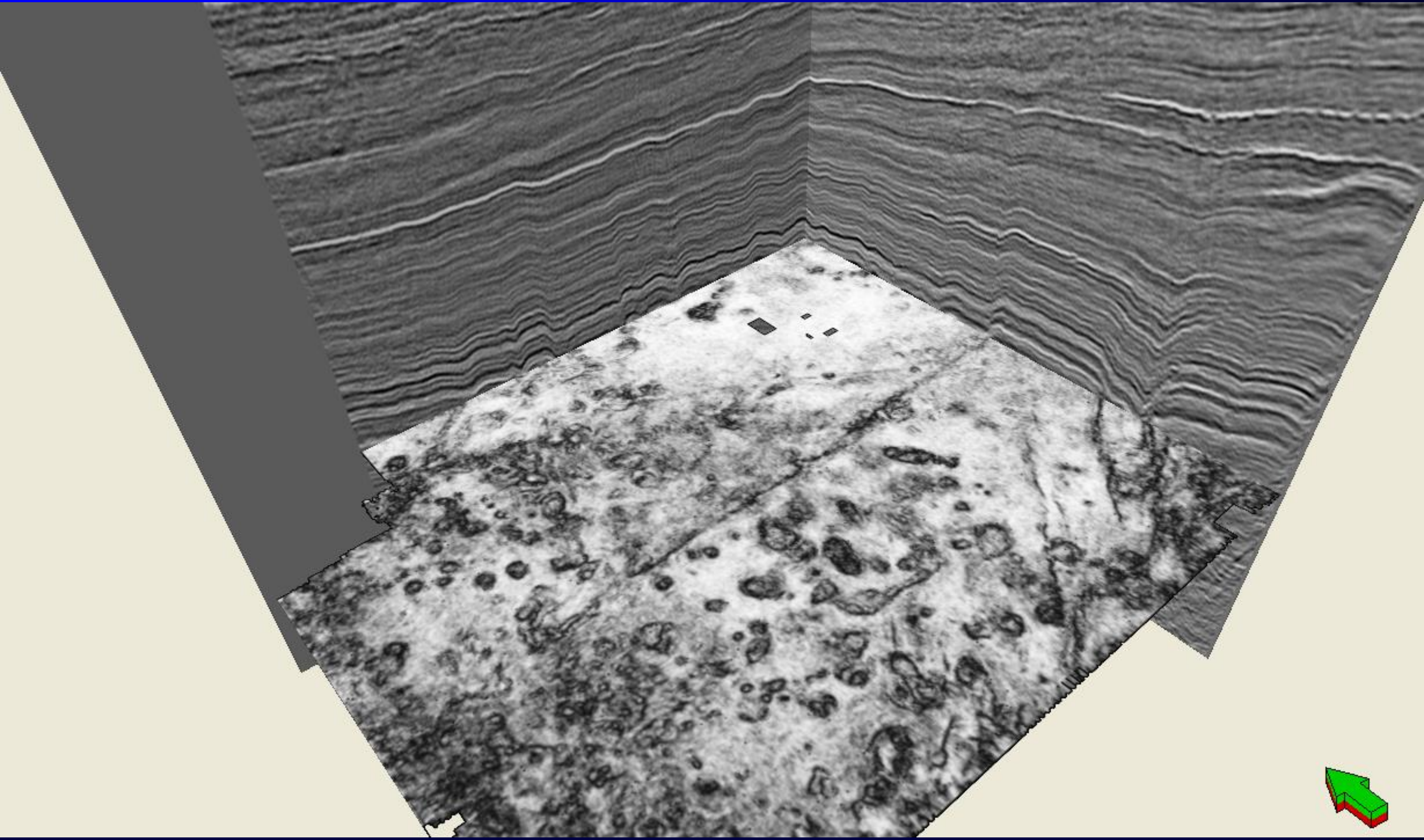

(Seismic data courtesy of Devon Energy)

Attributes based on volumetric dip and azimuth

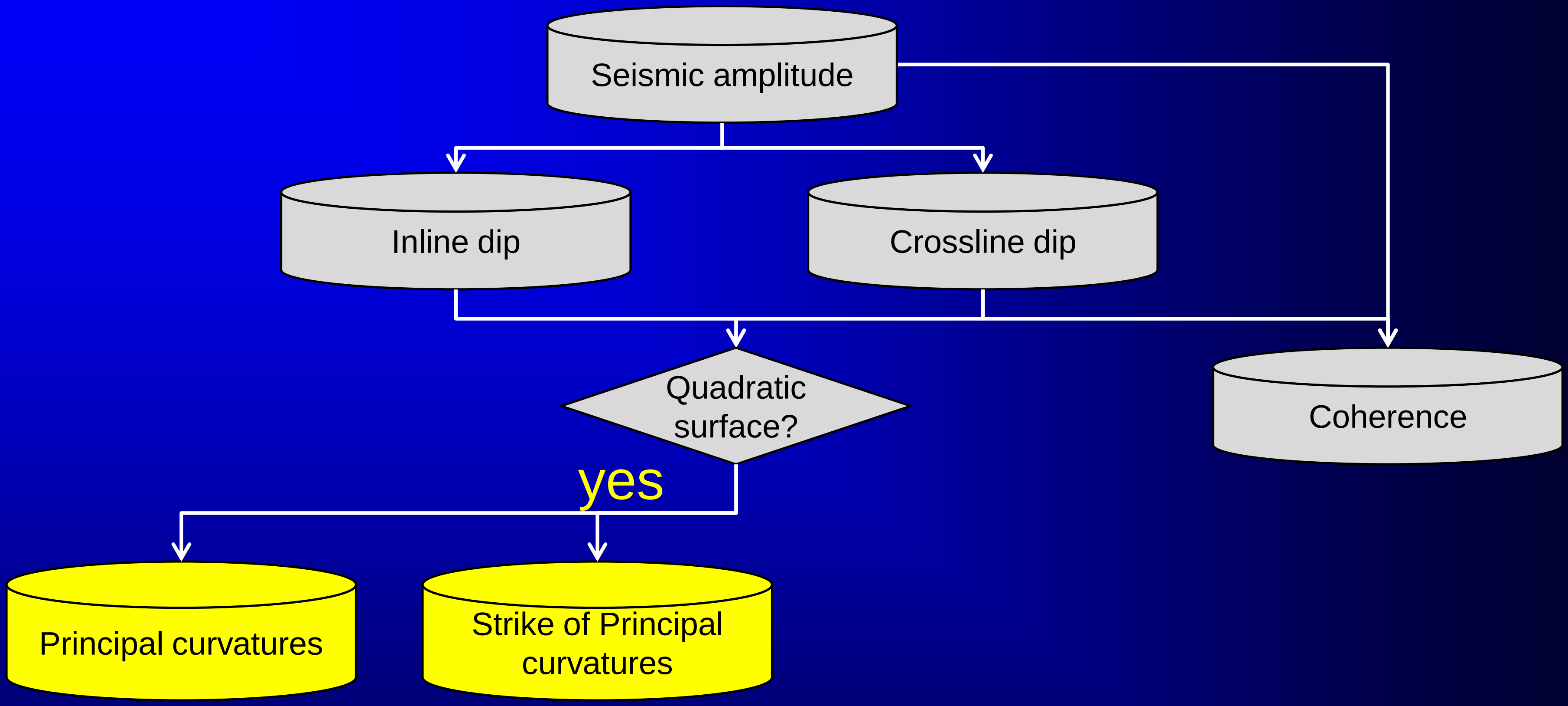

Most negative principal curvature, k_2

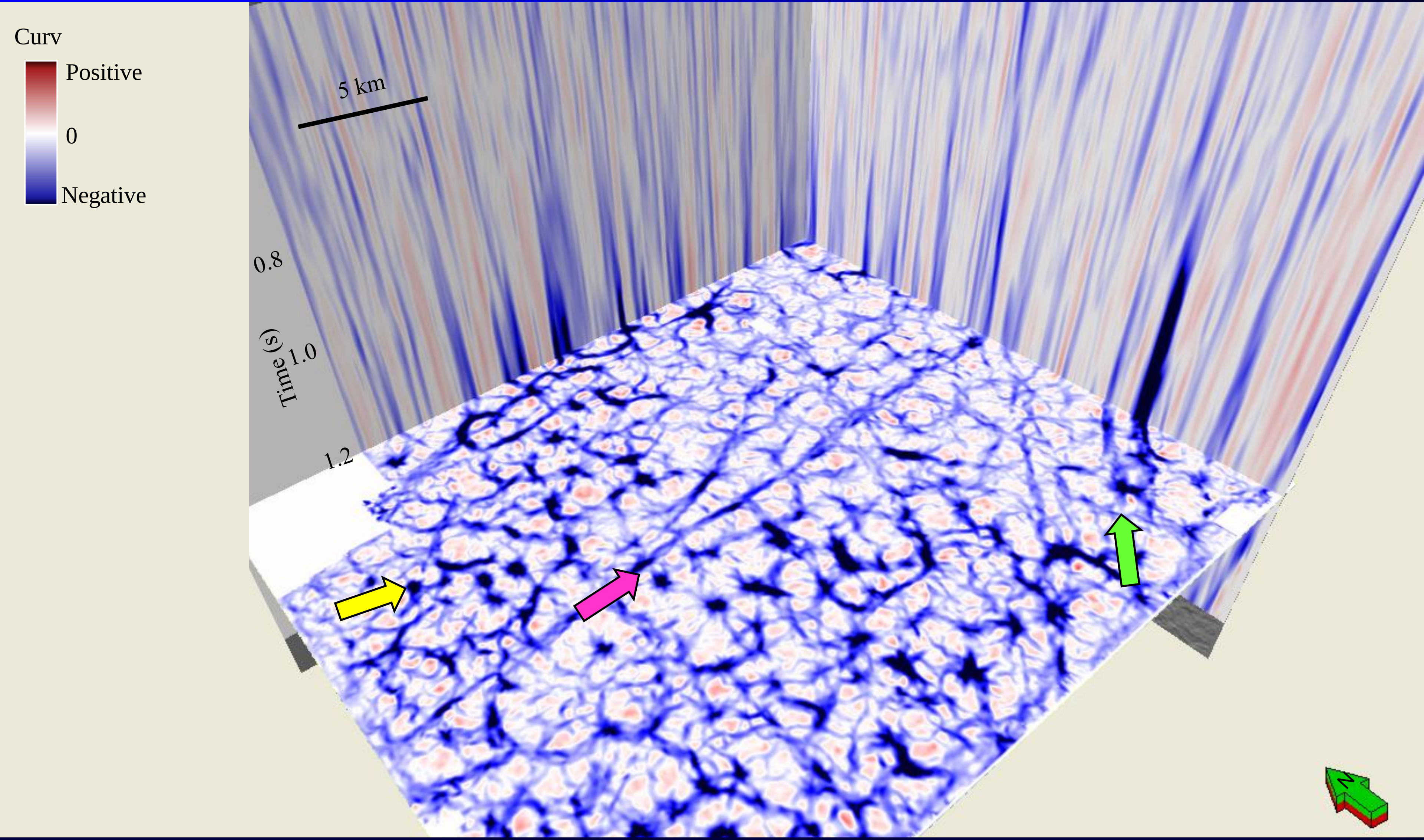

(Seismic data courtesy of Devon Energy)

Most negative principal curvature, k_2, co-rendered with coherence

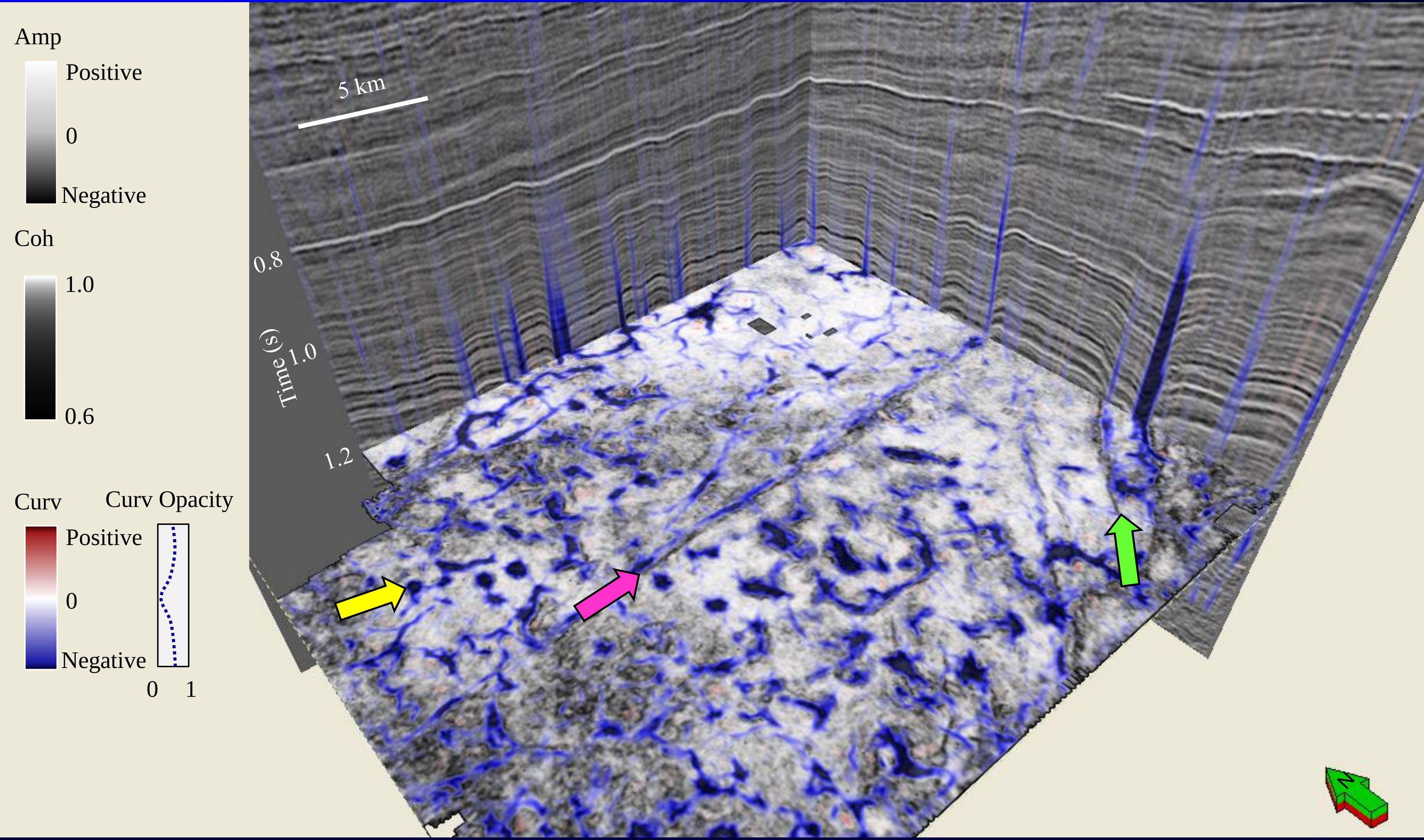

(Seismic data courtesy of Devon Energy)

Most postive principal curvature, k_1

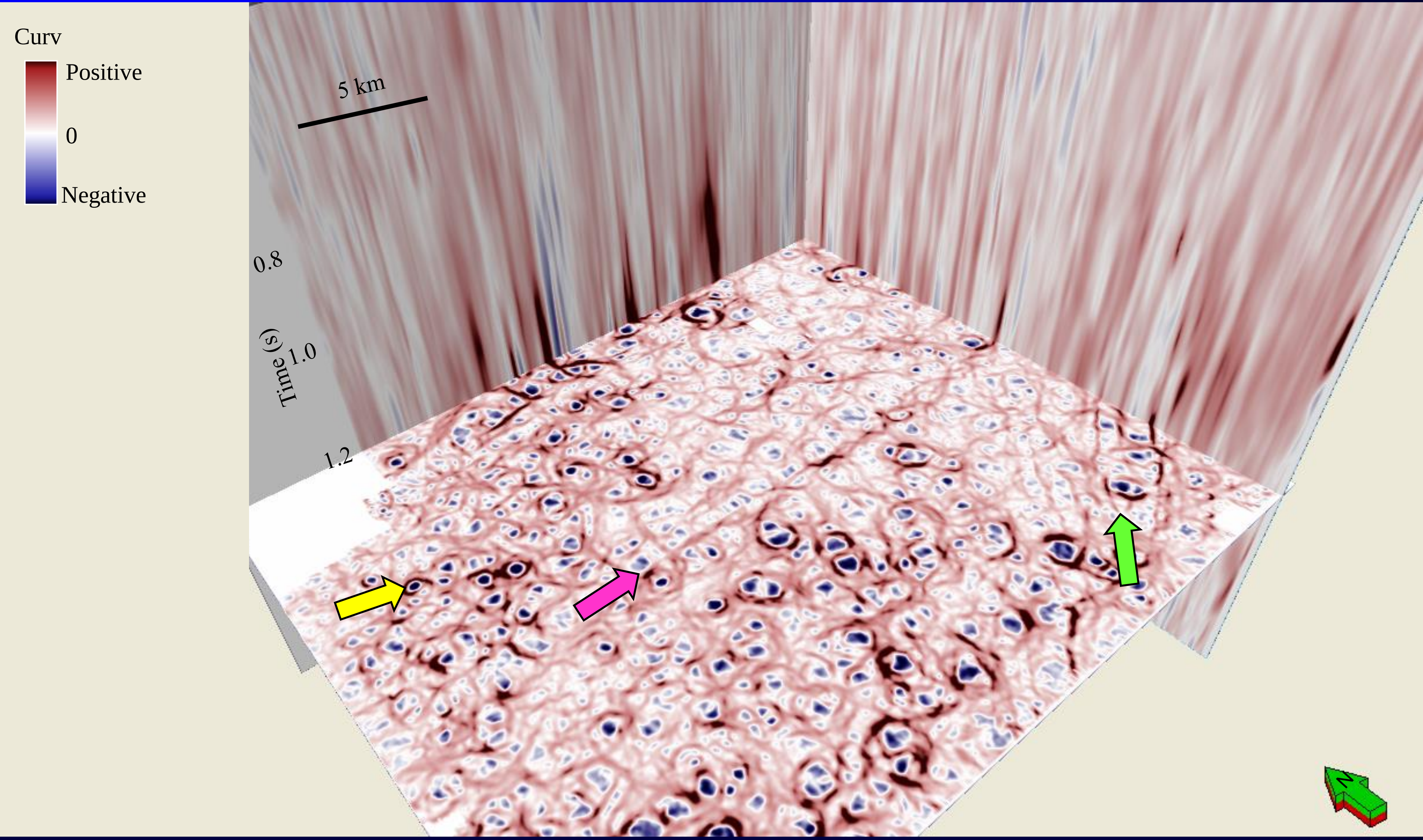

(Seismic data courtesy of Devon Energy)

Most positive principal curvature, k_1, co-rendered with coherence

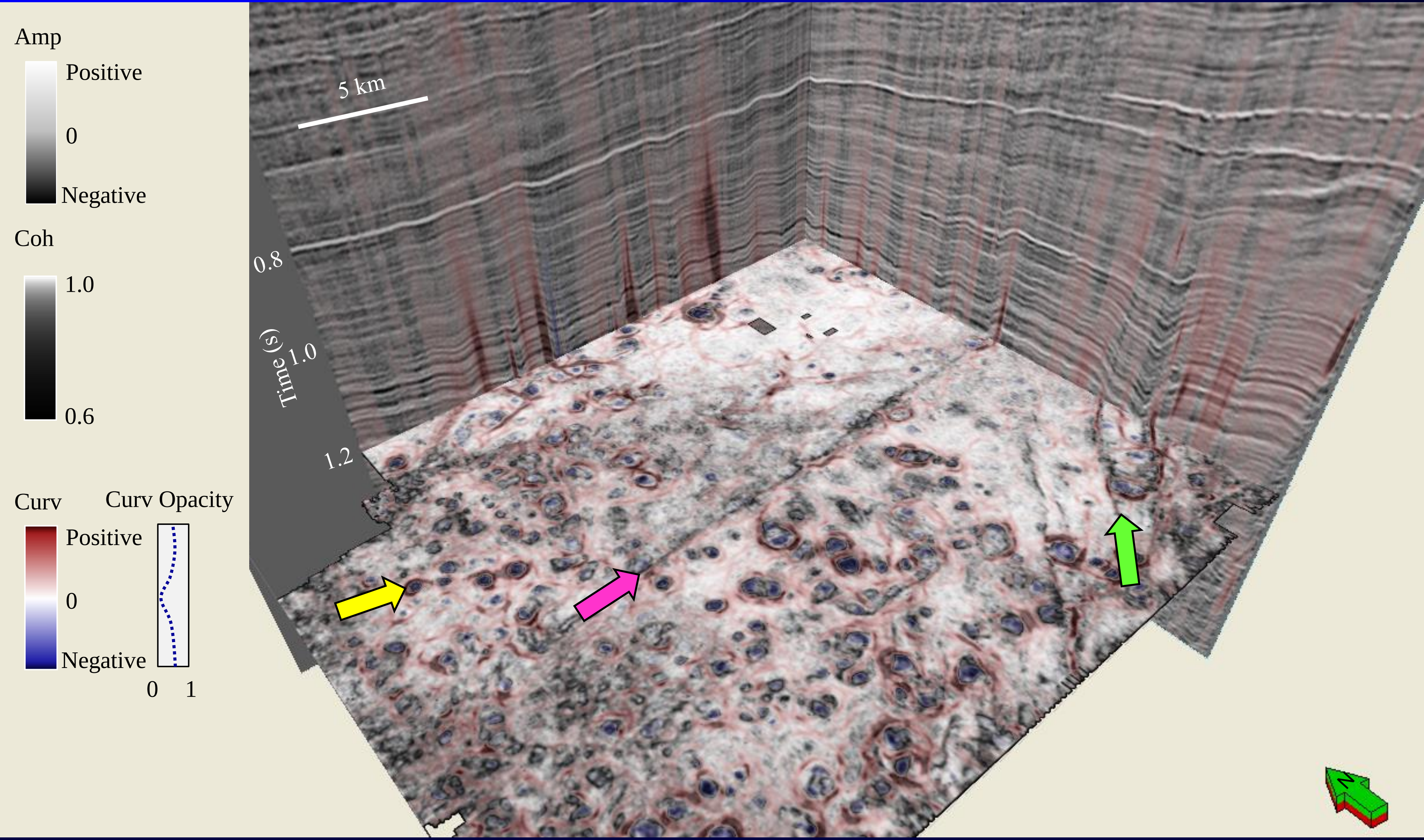

(Seismic data courtesy of Devon Energy)

Both principal curvatures, k_1 and k_2, co-rendered with coherence

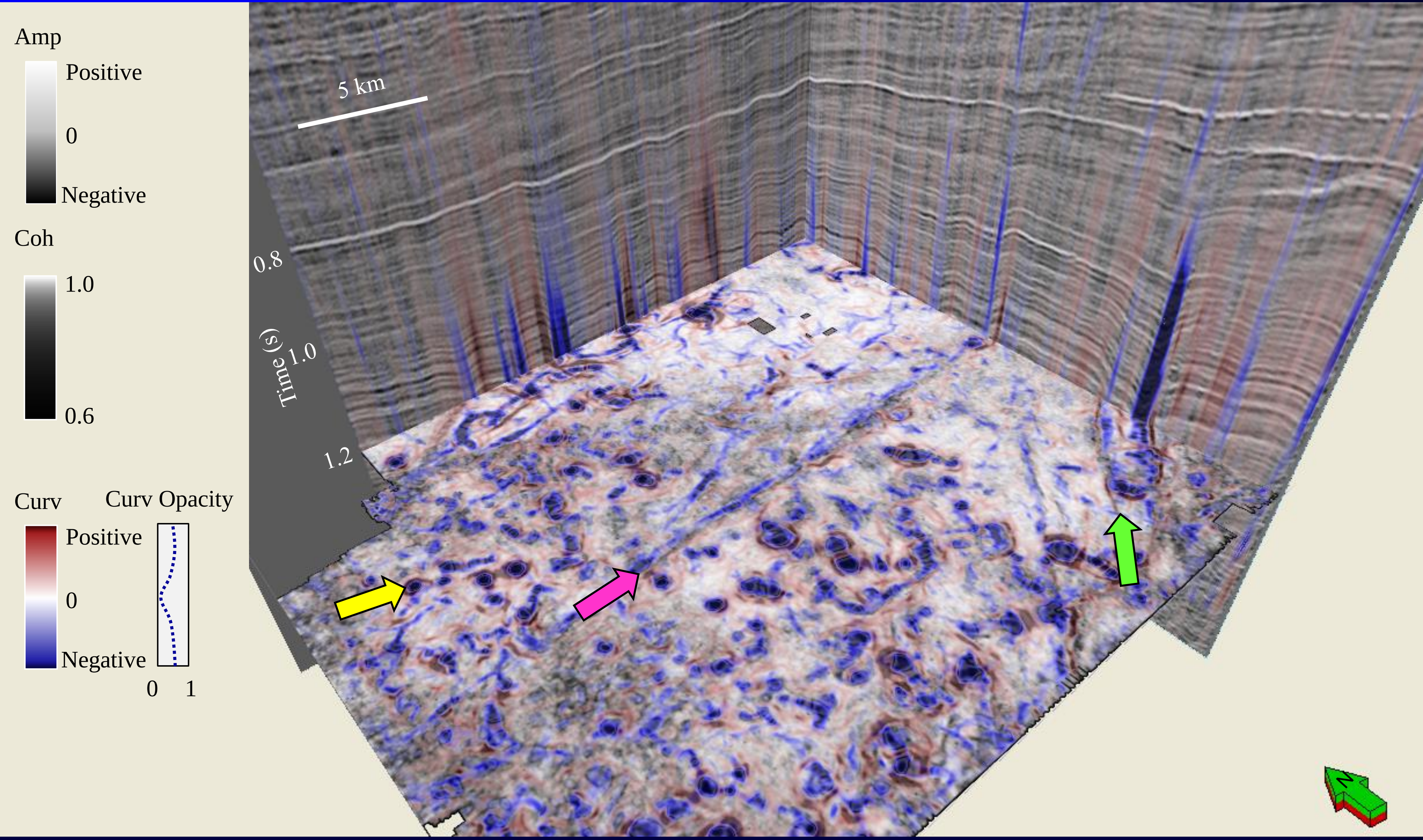

(Seismic data courtesy of Devon Energy)

Reflector Shape

Attributes based on volumetric dip and azimuth

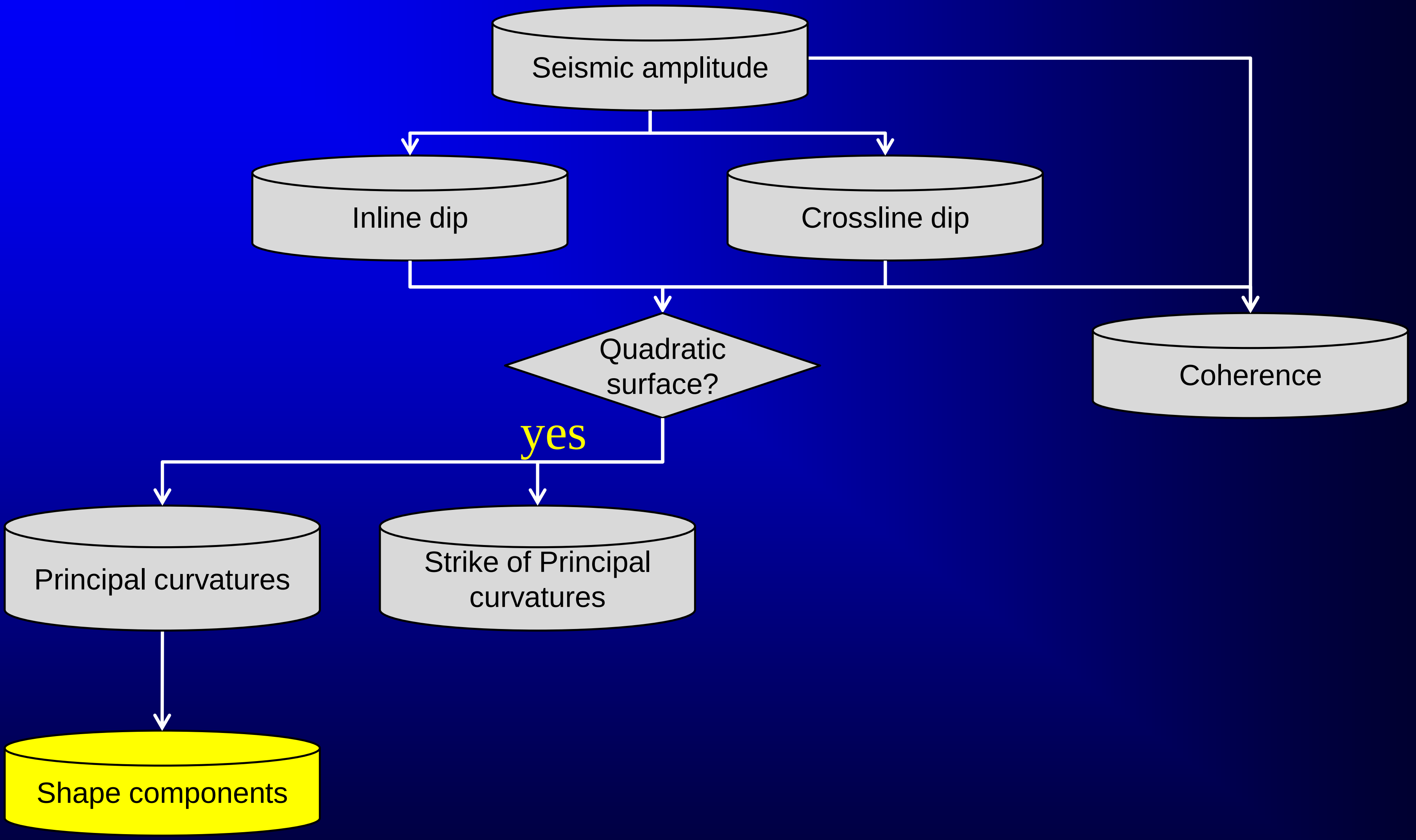

The shape index, s:

$$s = -\frac{2}{\pi}\,\mathbf{ATAN}\left(\frac{k_2 + k_1}{k_2 - k_1}\right)$$

$$k_1 \geq k_2$$

Principal curvatures

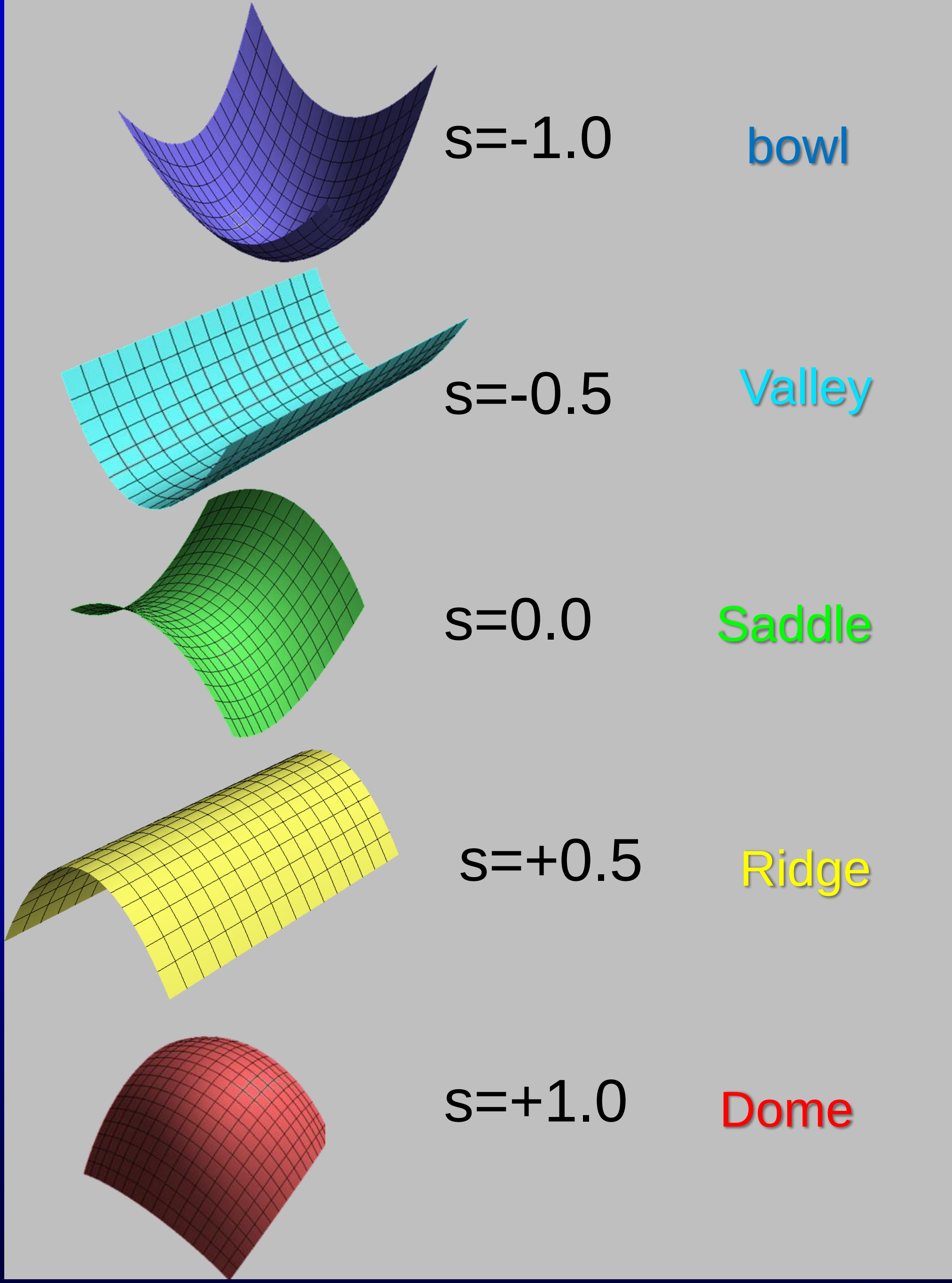

(Courtesy of Ha Mai)

Shape index and biometric identification

photographic image

distance scan

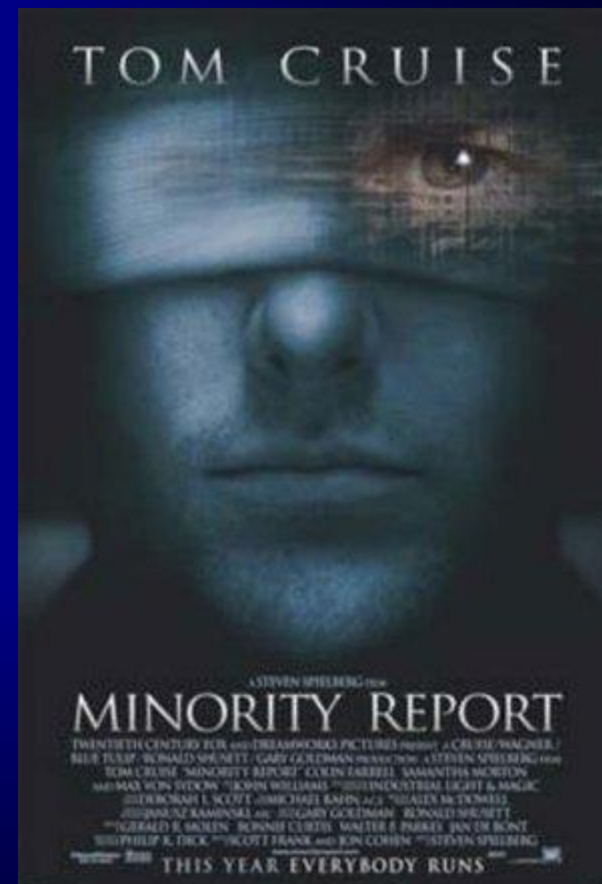

Shape indices

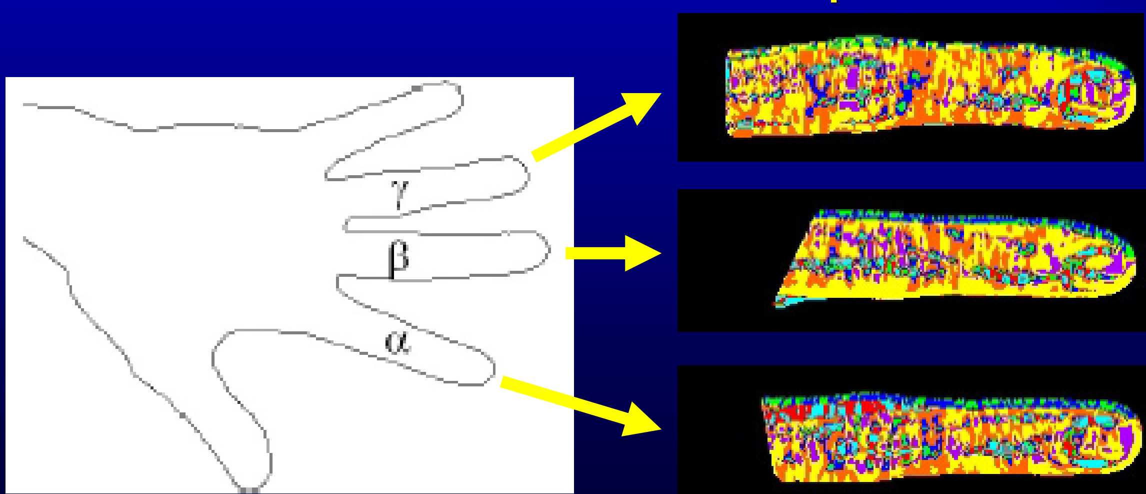

(Woodward and Flynn, 2004)

Shape index modulated by curvedness

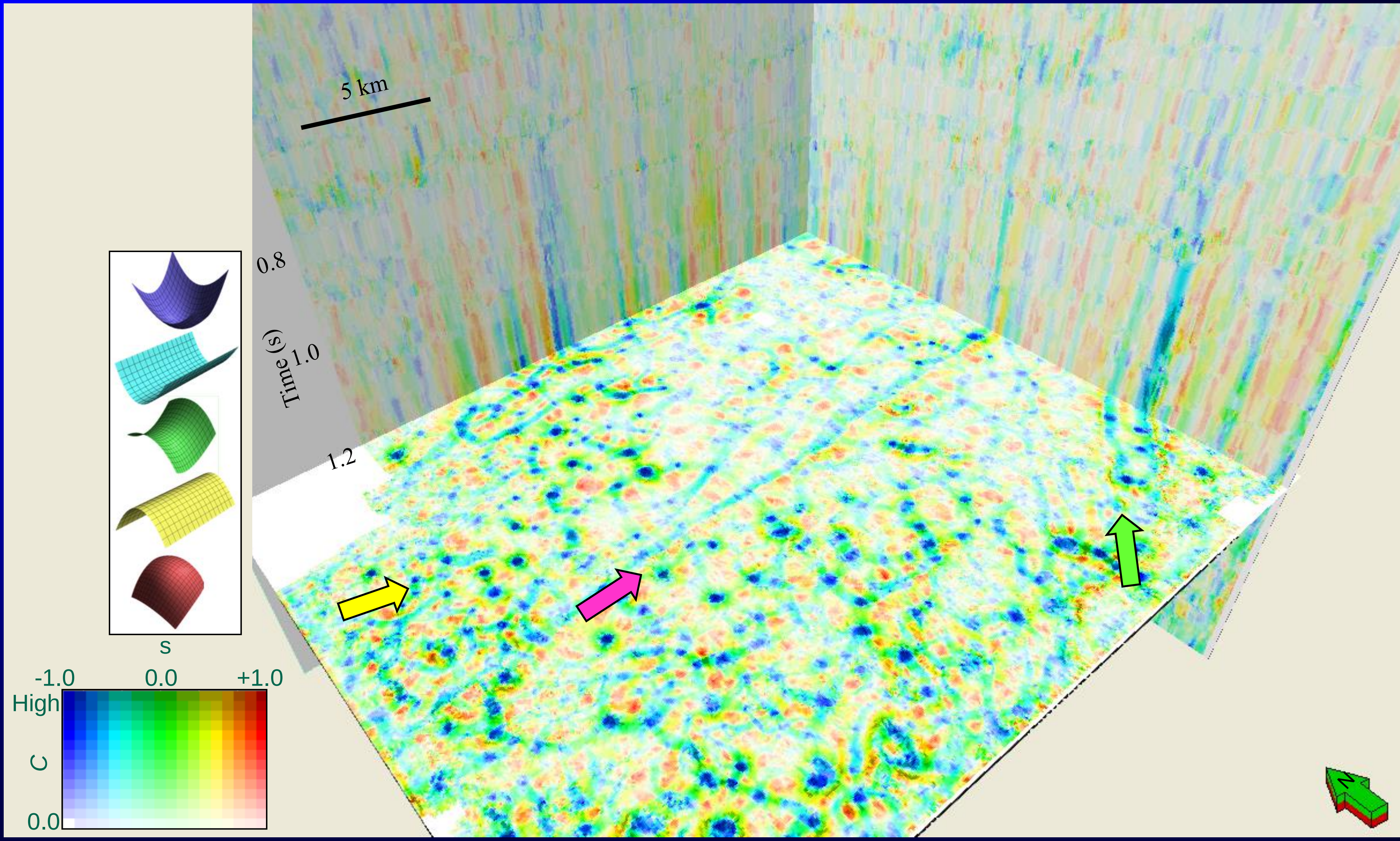

(Seismic data courtesy of Devon Energy)

Shape index modulated by curvedness, co-rendered with coherence

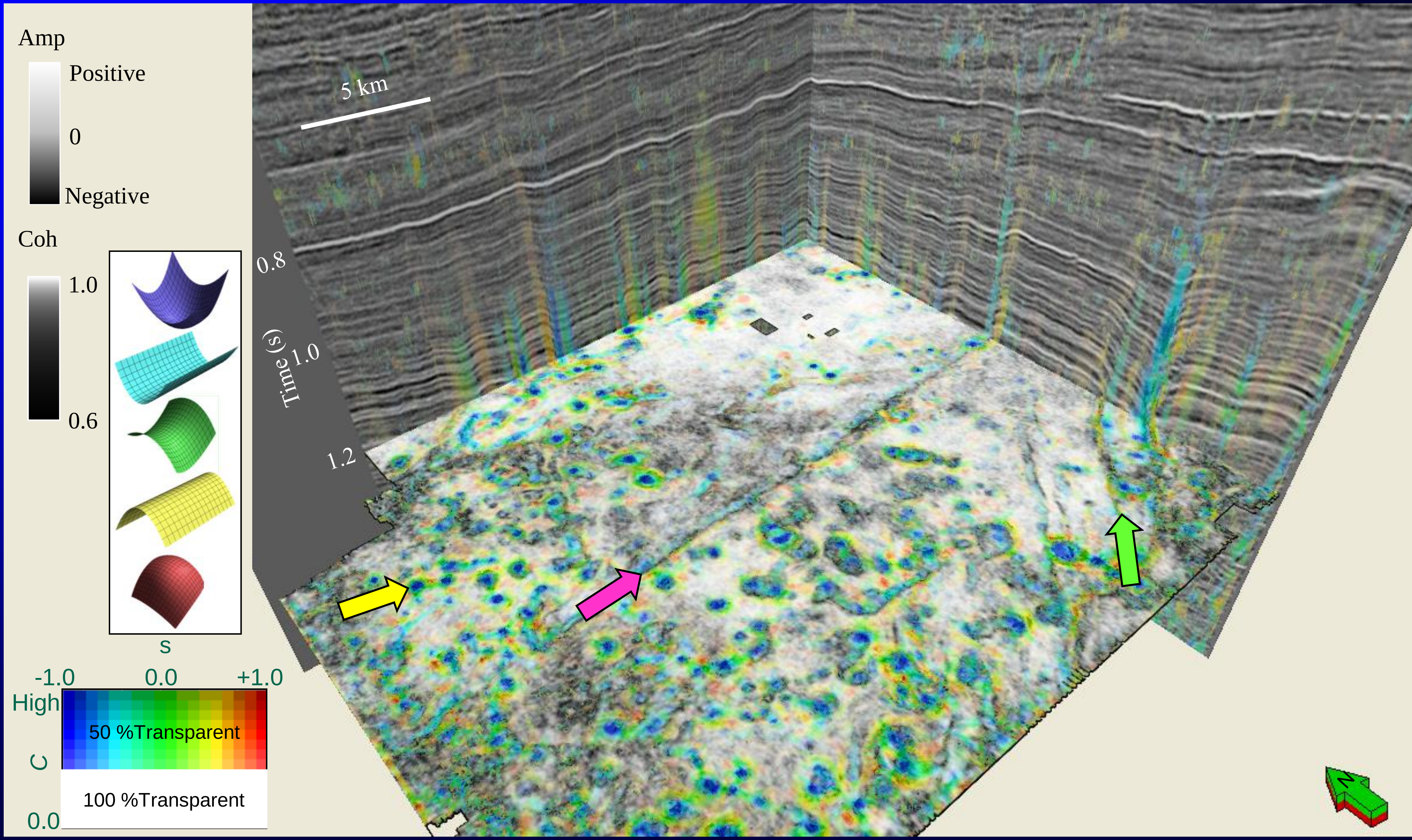

(Seismic data courtesy of Devon Energy)

Filter to enhance bowl-shaped features

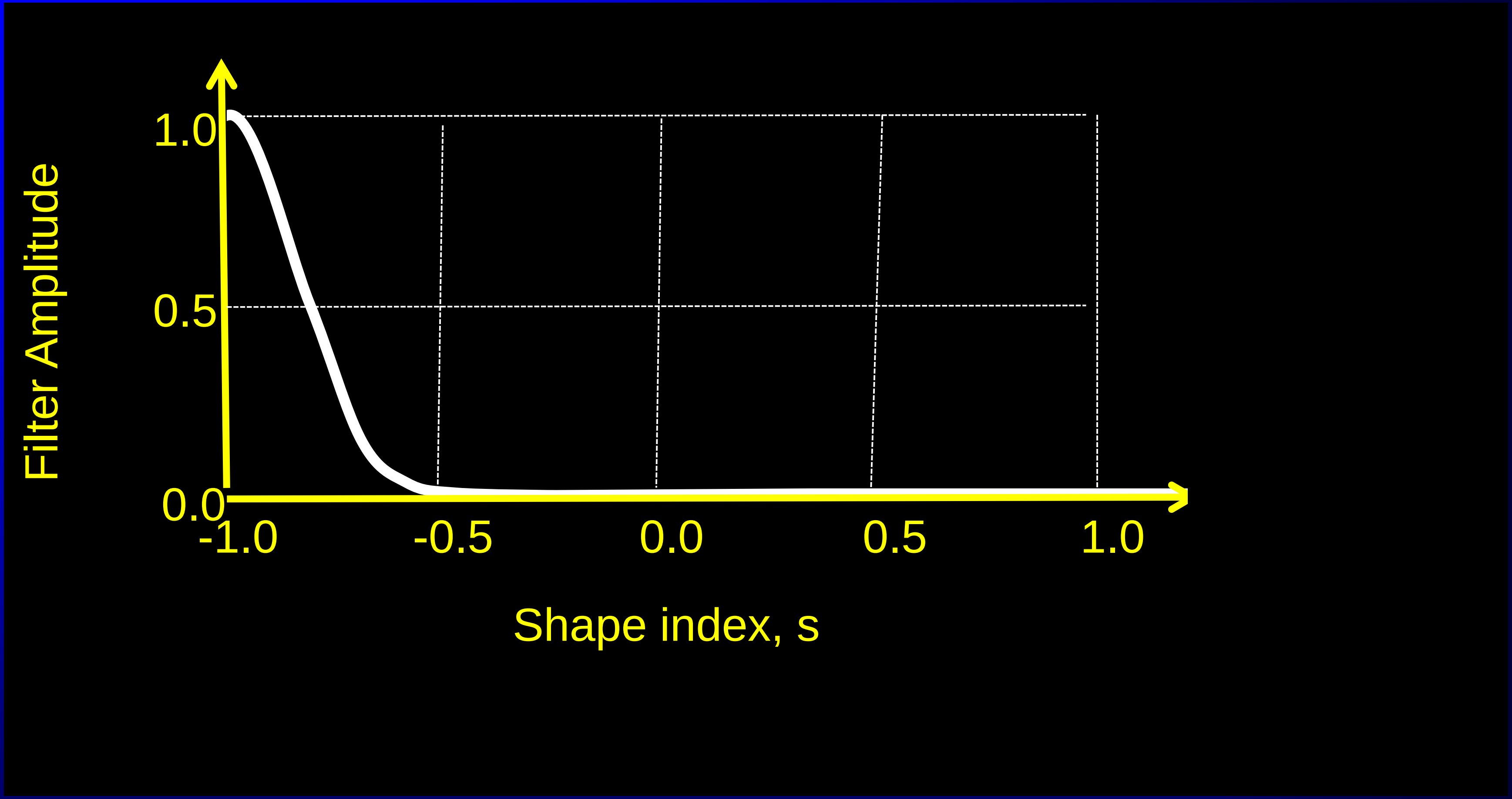

Bowl component co-rendered with coherence

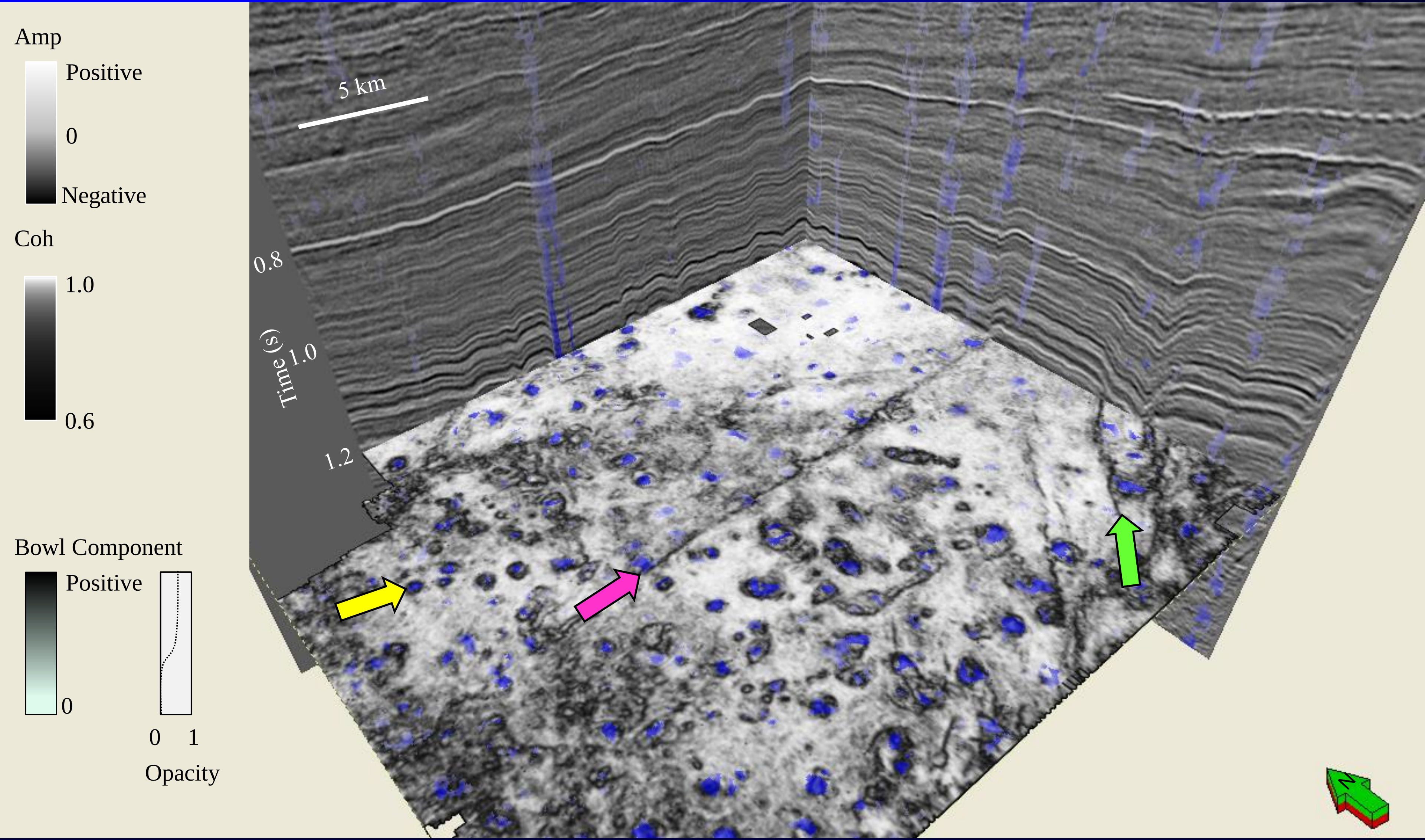

(Seismic data courtesy of Devon Energy)

Correlation of bowl shape component with collapse features

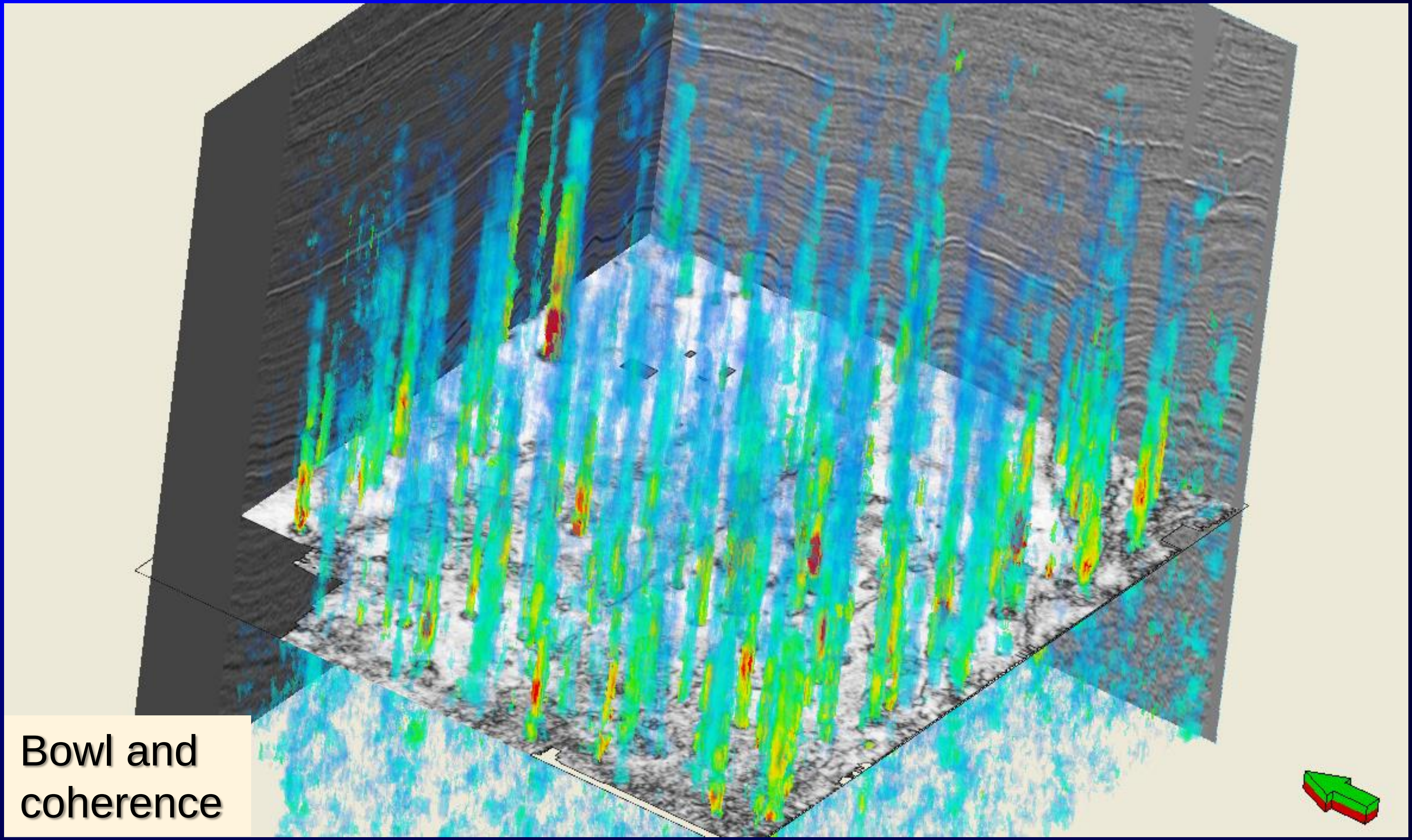

(data courtesy of Devon Energy)

Correlation of bowl shape component with collapse features

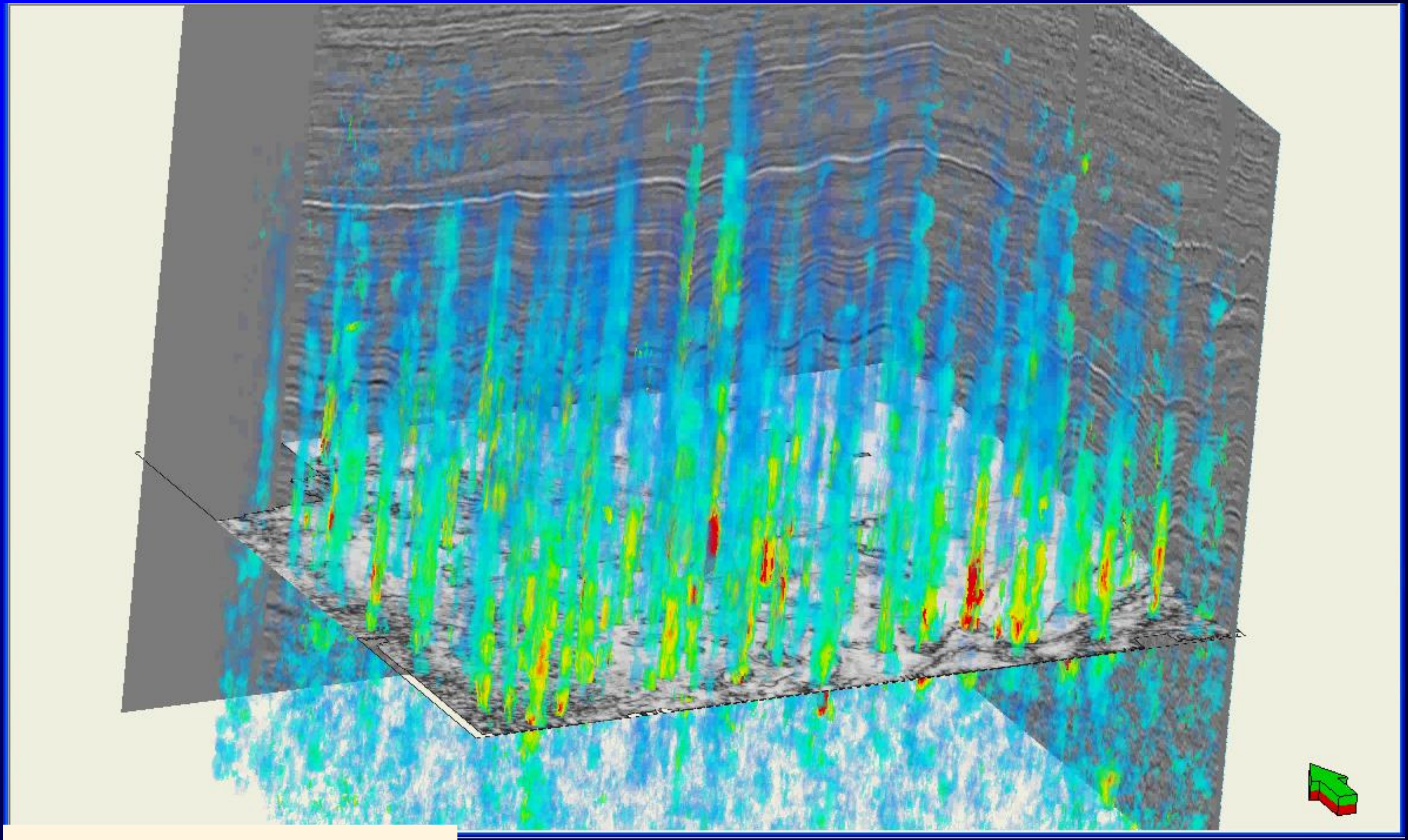

Bowl and coherence

(data courtesy of Devon Energy)

Structural Lineaments

Attributes based on volumetric dip and azimuth

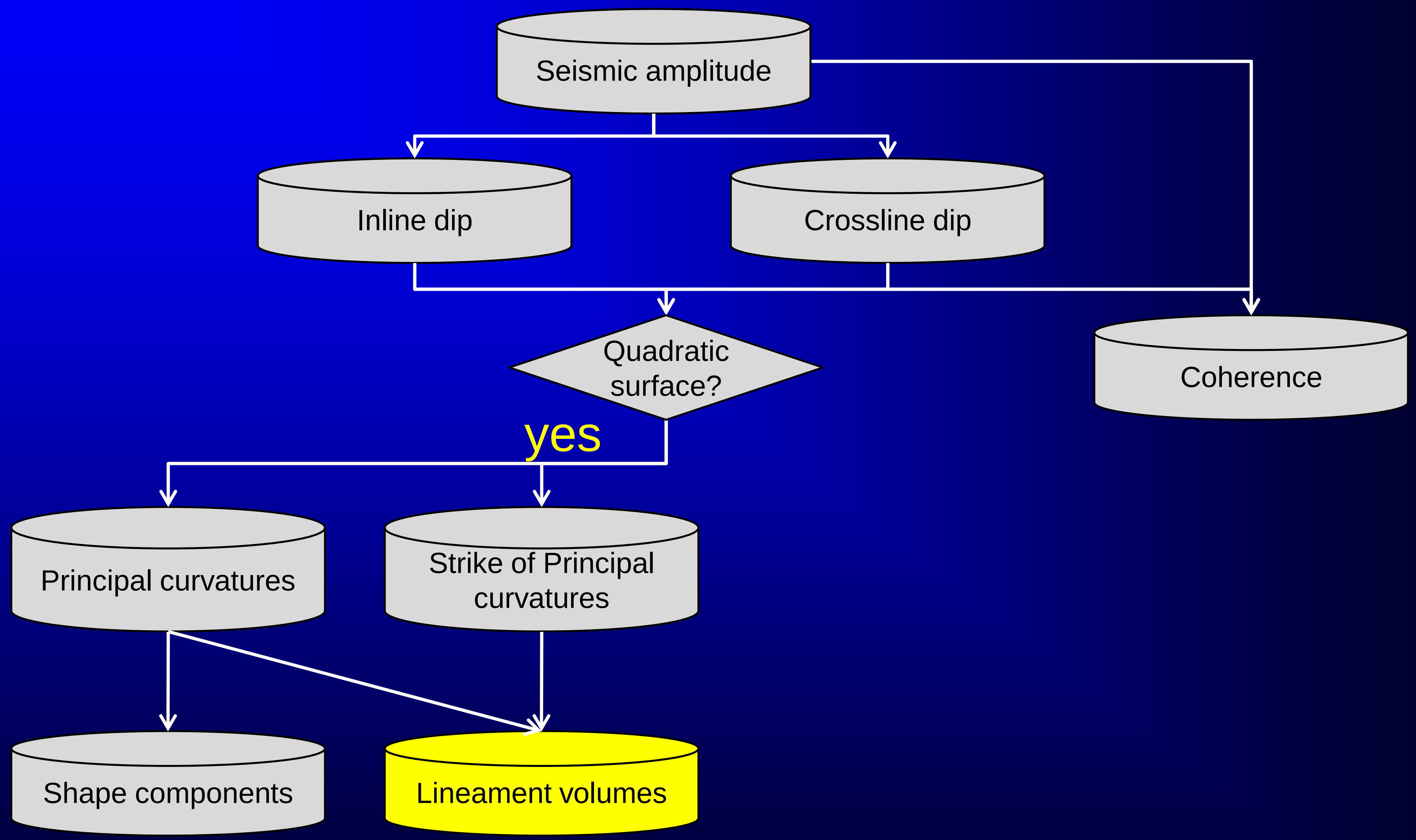

Orientation of lineaments

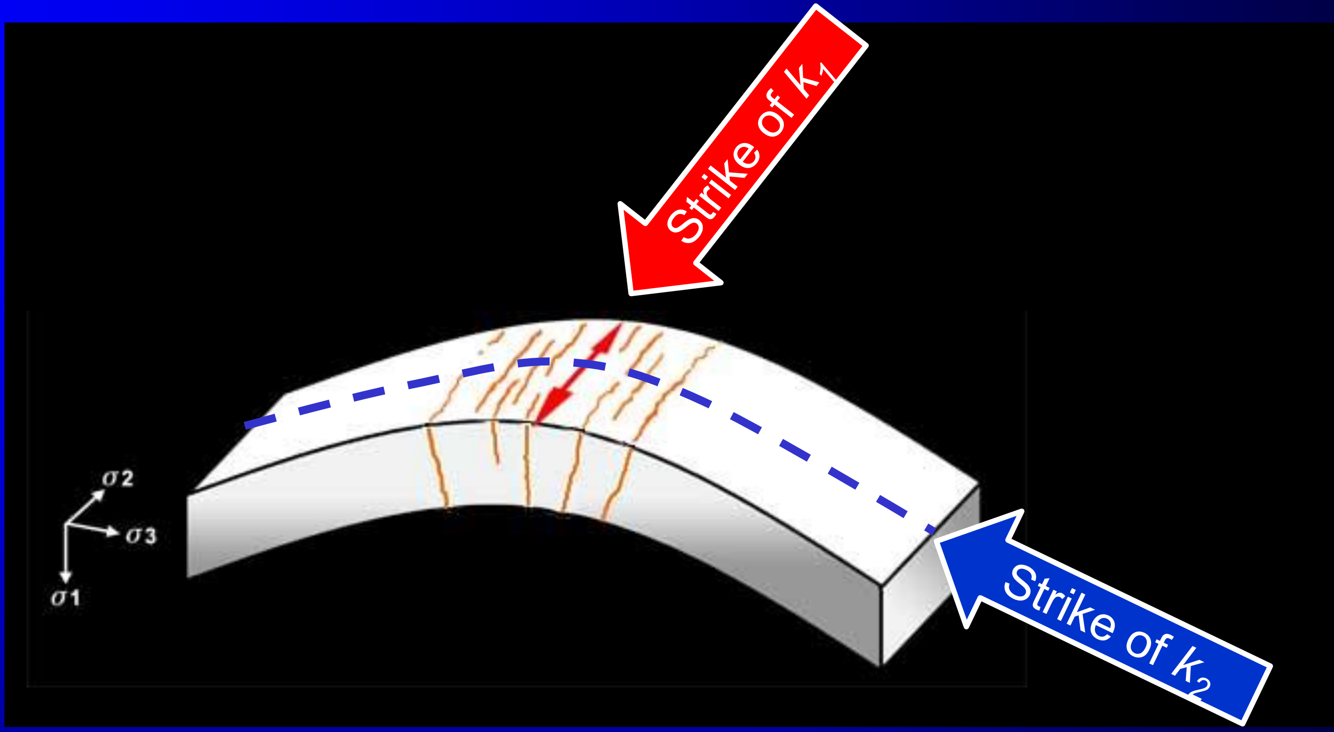

Fractures are often stronger near the fold axis (sometimes parallel, often at an angle associated with Mohr's circle), and hence to the strike of the curvature anomalies

(Chopra and Marfurt, 2011)

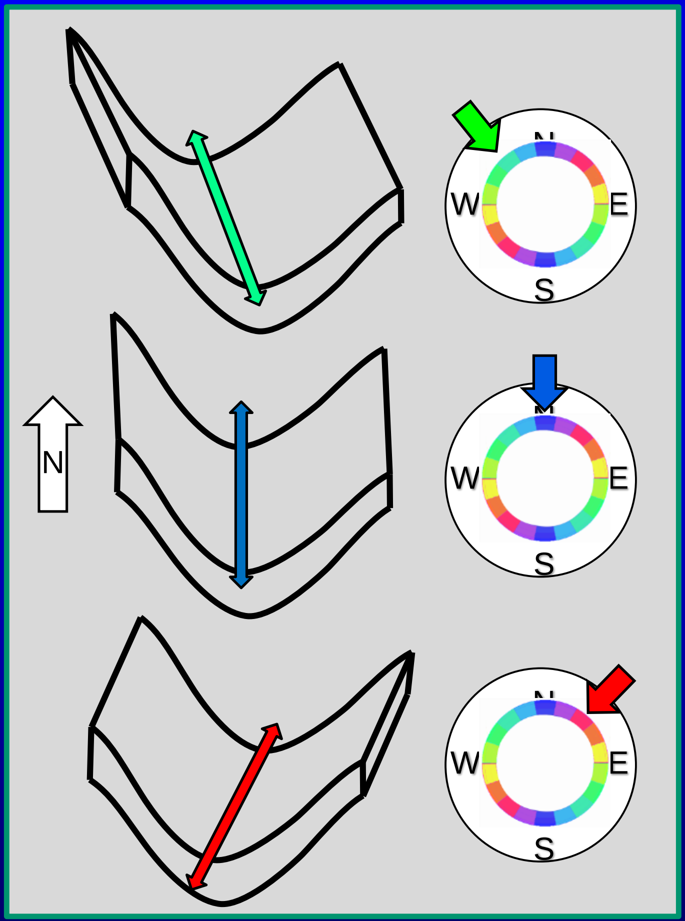

N
W
E
S
N

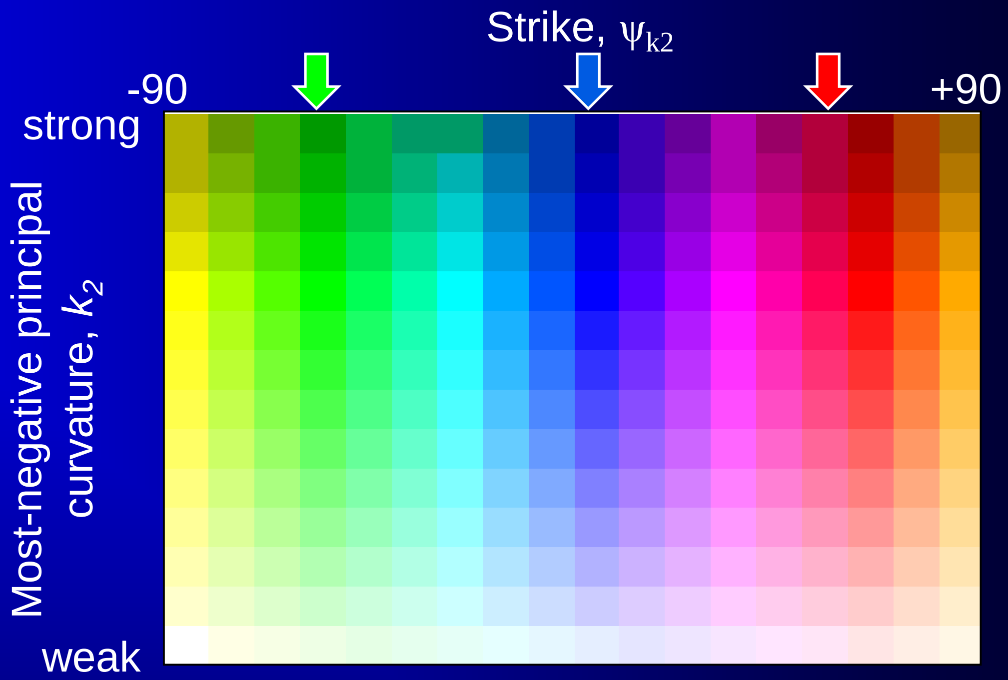

Strike, ψk2
-90
+90
strong
weak
Most-negative principal curvature, k2

Strike modulated by most-negative principal curvature

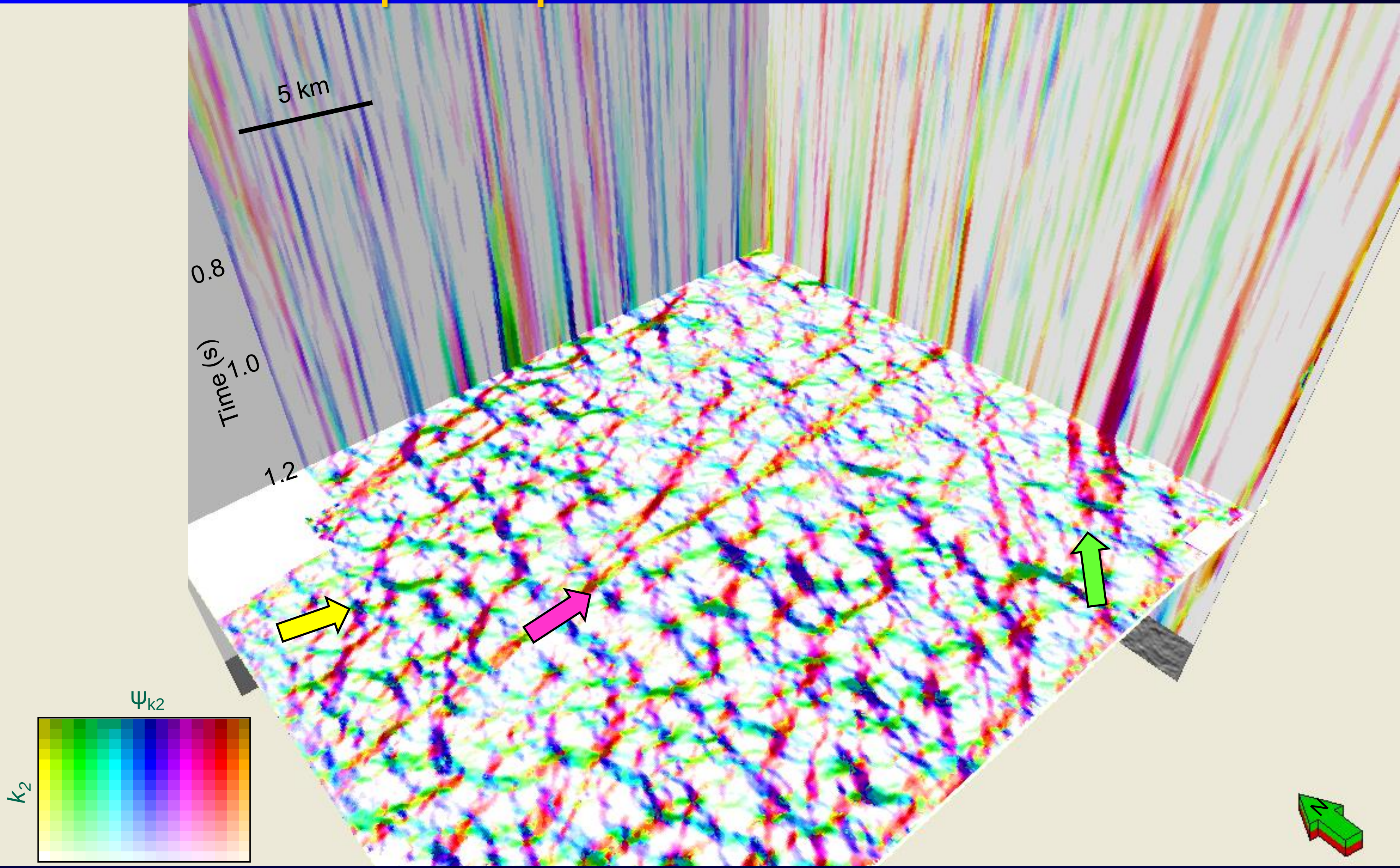

(Seismic data courtesy of Devon Energy)

Strike modulated by most-negative principal curvature, co-rendered with coherence

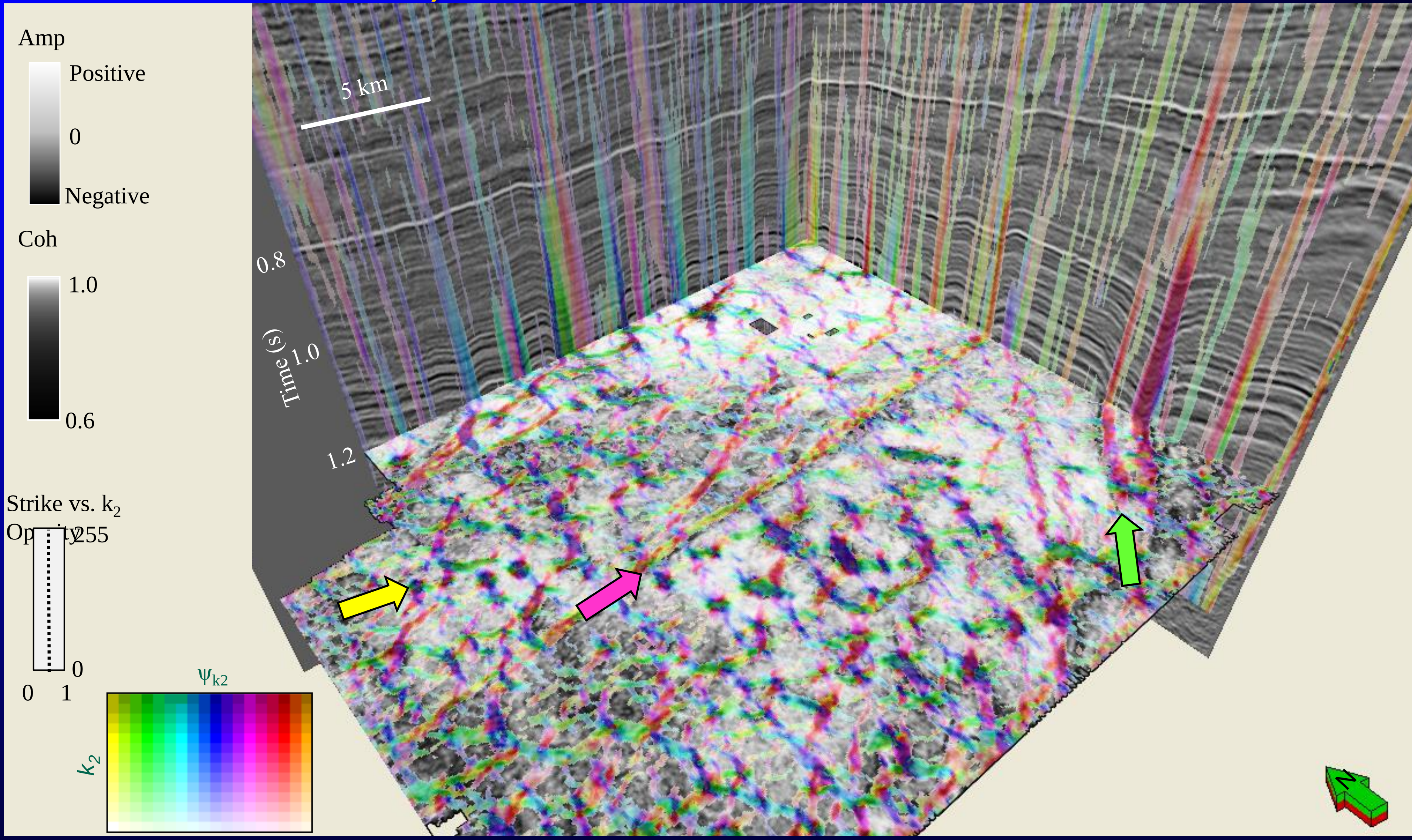

(Seismic data courtesy of Devon Energy)

Volume visualization of structural lineaments

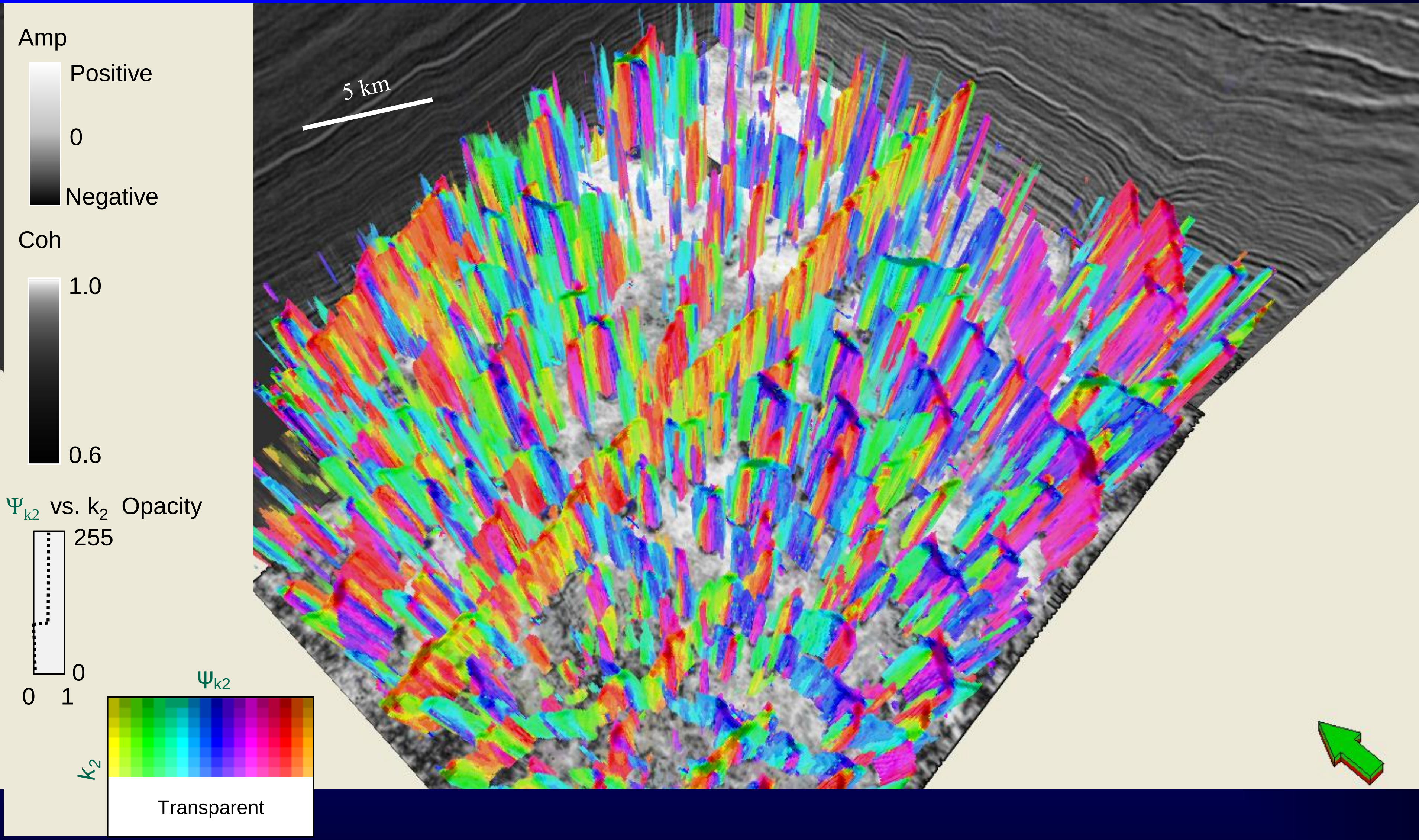

(Seismic data courtesy of Devon Energy)

Generating rose diagrams

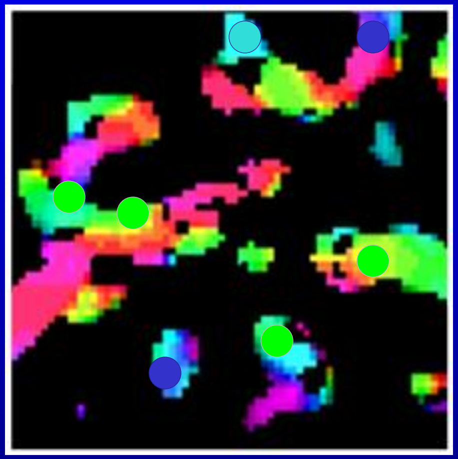

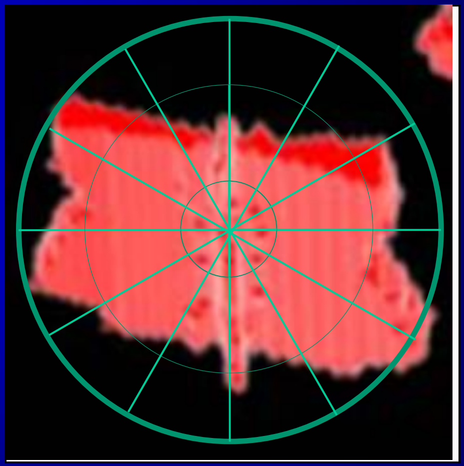

Structural lineaments displayed as roses

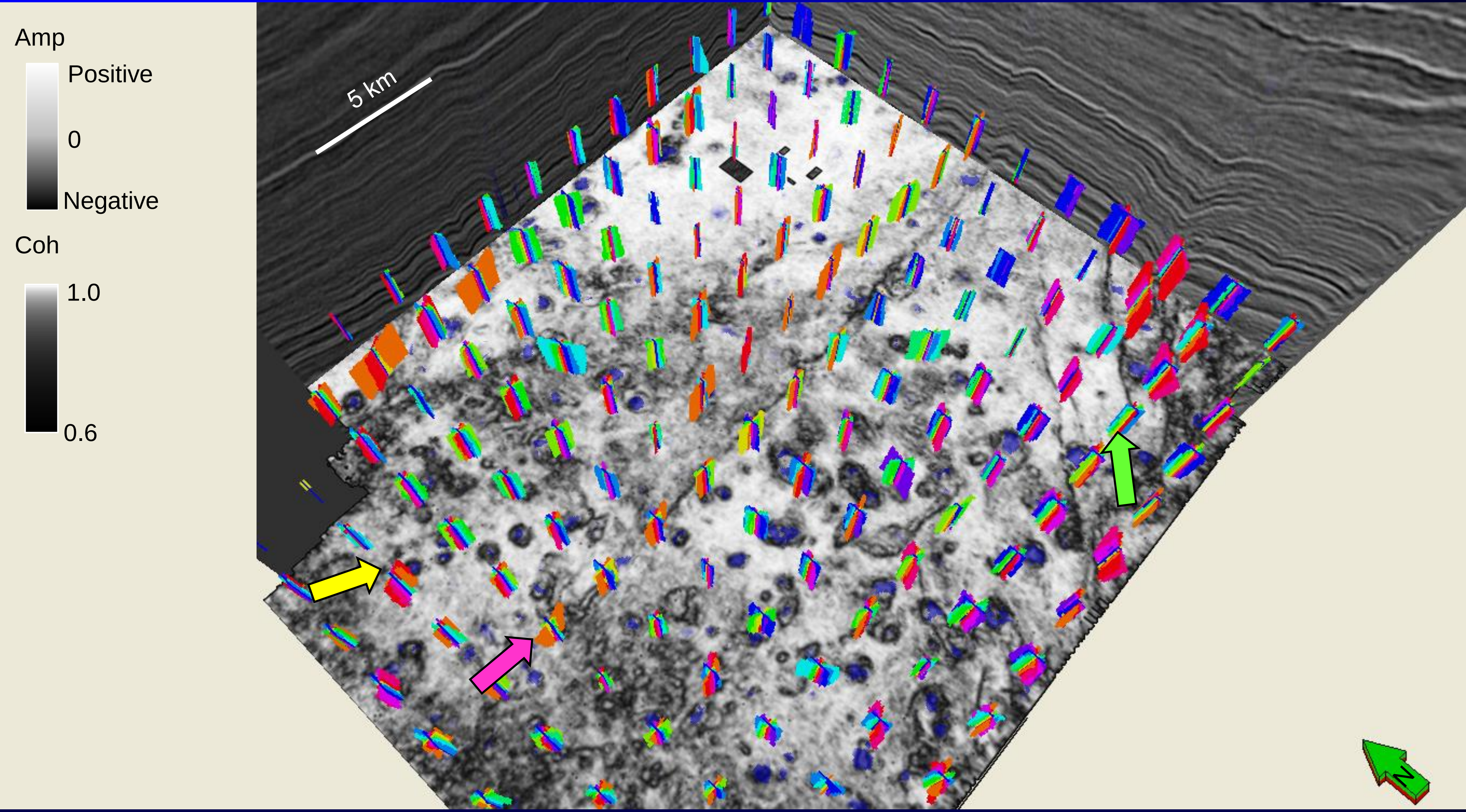

(Seismic data courtesy of Devon Energy)

Reflector Convergence

Volumetric mapping of angular unconformities

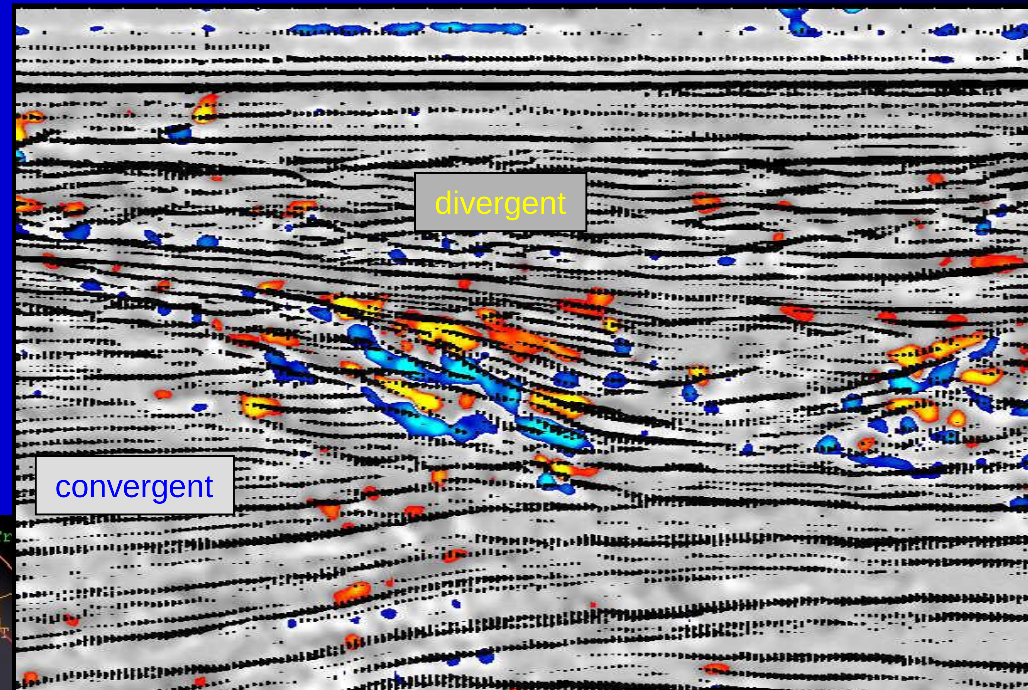

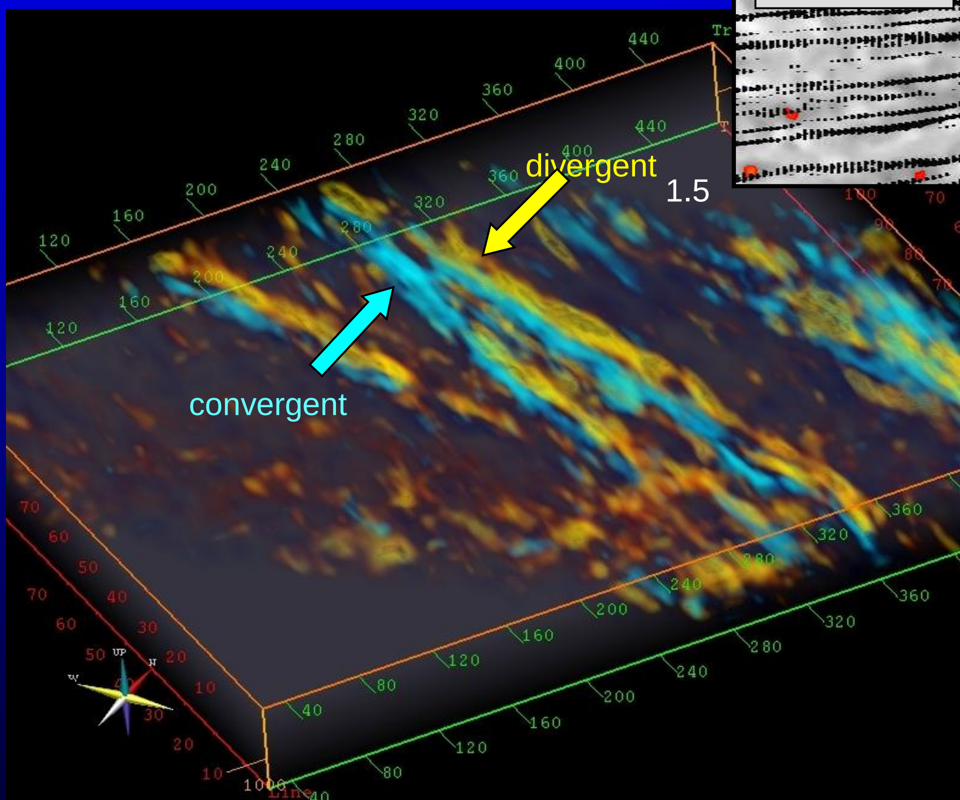

(Barnes, 2002)

Computing the normal from apparent dip components

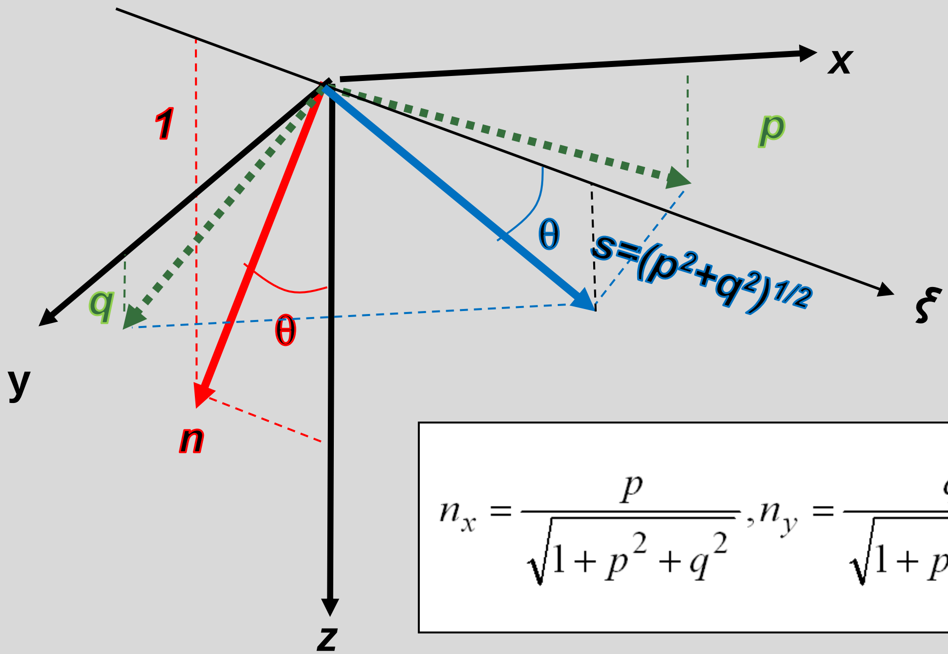

$$n_x = \frac{p}{\sqrt{1+p^2+q^2}}, n_y = \frac{q}{\sqrt{1+p^2+q^2}}, n_z = \frac{1}{\sqrt{1+p^2+q^2}},$$

$$\boldsymbol{\psi} = \nabla \times \mathbf{n} = \hat{\mathbf{x}}\left(\frac{\partial n_y}{\partial z} - \frac{\partial n_z}{\partial y}\right) + \hat{\mathbf{y}}\left(\frac{\partial n_z}{\partial x} - \frac{\partial n_x}{\partial z}\right) + \hat{\mathbf{z}}\left(\frac{\partial n_x}{\partial y} - \frac{\partial n_y}{\partial x}\right),$$

Arithmetic for mapping angular unconformities

$$\mathbf{c} = \mathbf{n} \times \boldsymbol{\psi} = \hat{\mathbf{x}}\left[n_y \left(\frac{\partial n_x}{\partial y} - \frac{\partial n_y}{\partial x} \right) - n_z \left(\frac{\partial n_y}{\partial z} - \frac{\partial n_z}{\partial y} \right) \right]$$

$$+ \hat{\mathbf{y}}\left[n_z \left(\frac{\partial n_y}{\partial z} - \frac{\partial n_z}{\partial y} \right) - n_x \left(\frac{\partial n_x}{\partial y} - \frac{\partial n_y}{\partial x} \right) \right]$$

$$+ \hat{\mathbf{z}}\left[n_x \left(\frac{\partial n_z}{\partial x} - \frac{\partial n_x}{\partial z} \right) - n_y \left(\frac{\partial n_y}{\partial z} - \frac{\partial n_z}{\partial y} \right) \right]$$

Rotation about the each axis (reflector convergence)

(Marfurt and Rich, 2010)

Attributes based on volumetric dip and azimuth

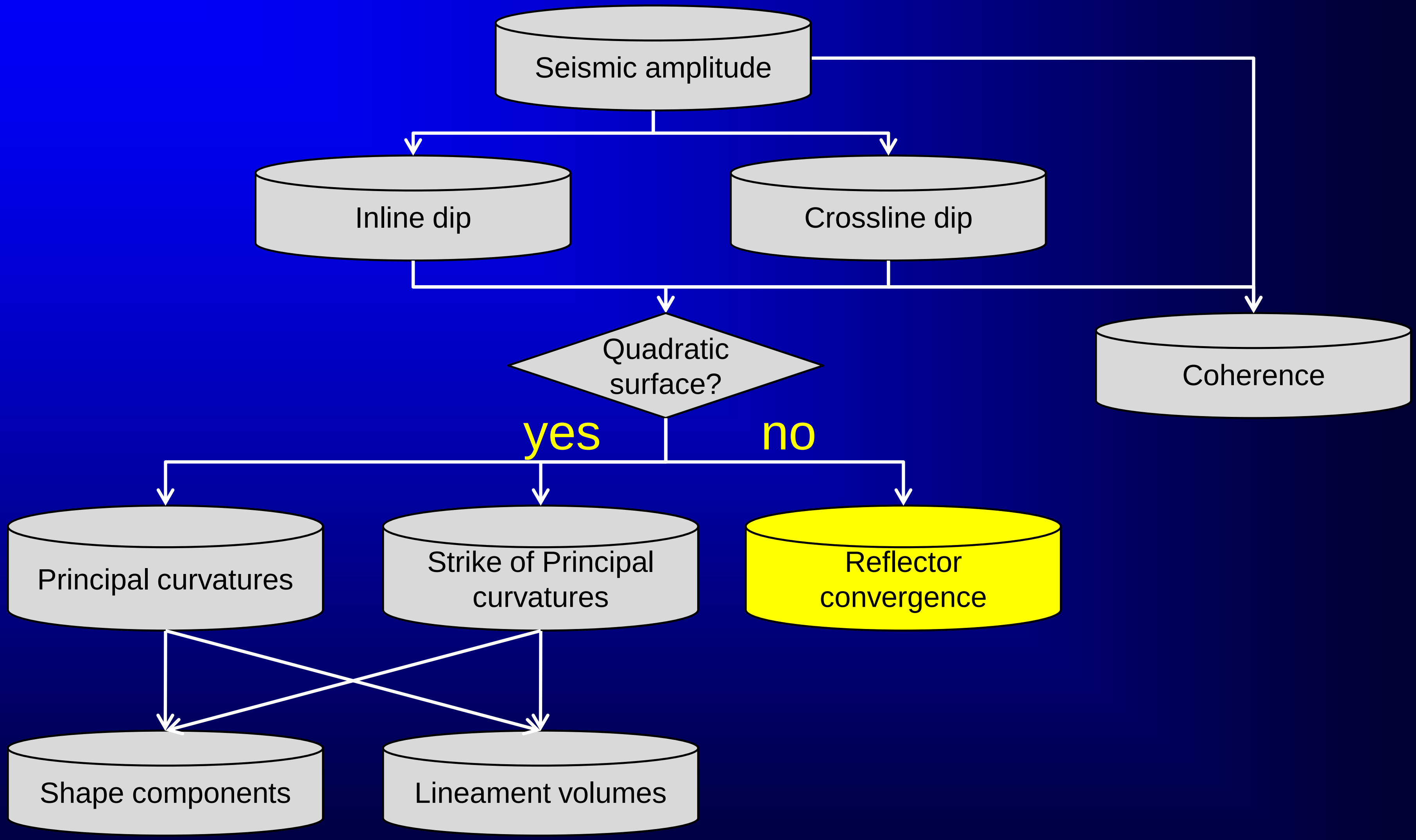

Reflector convergence co-rendered with coherence

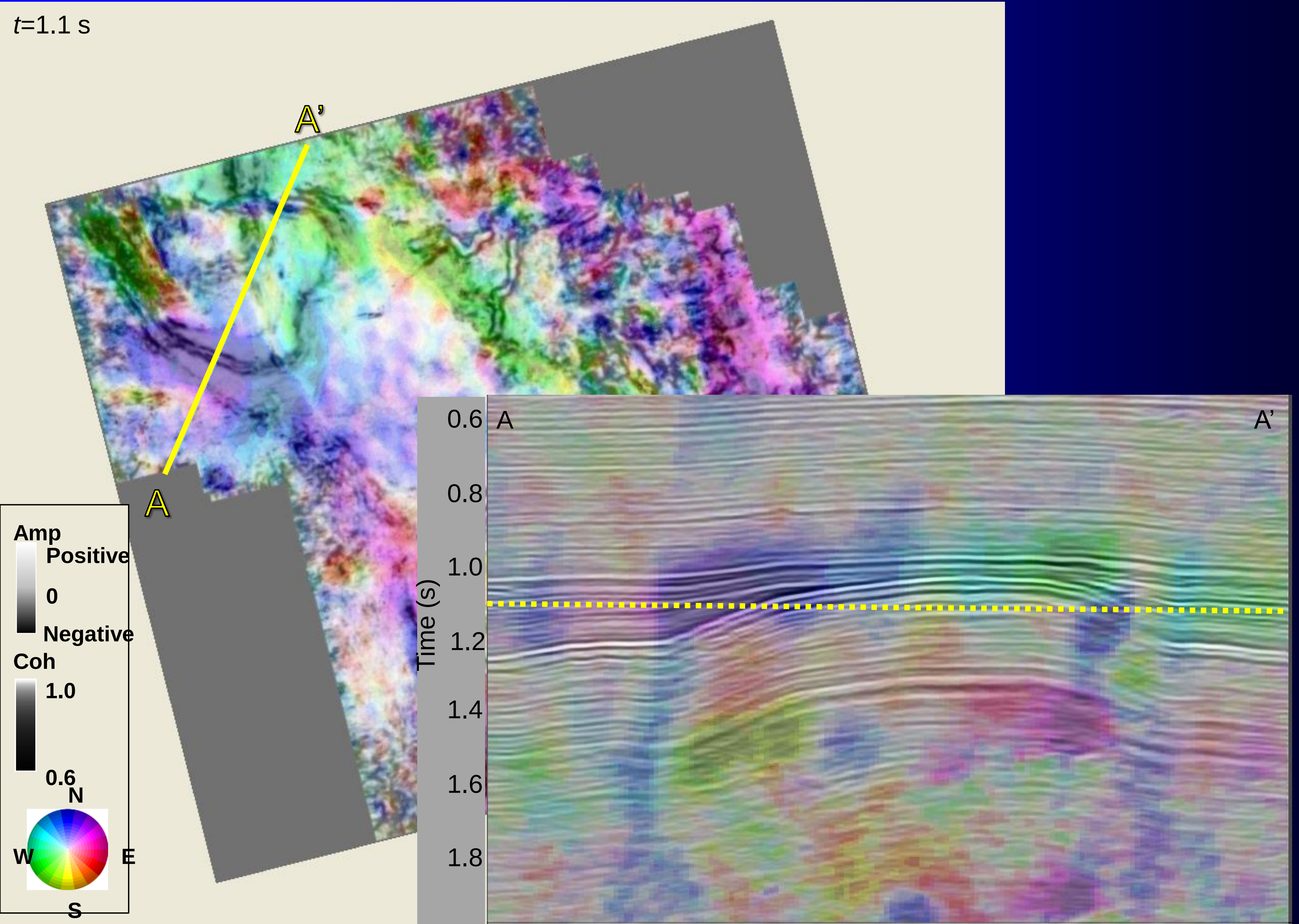

Reflector convergence co-rendered with coherence

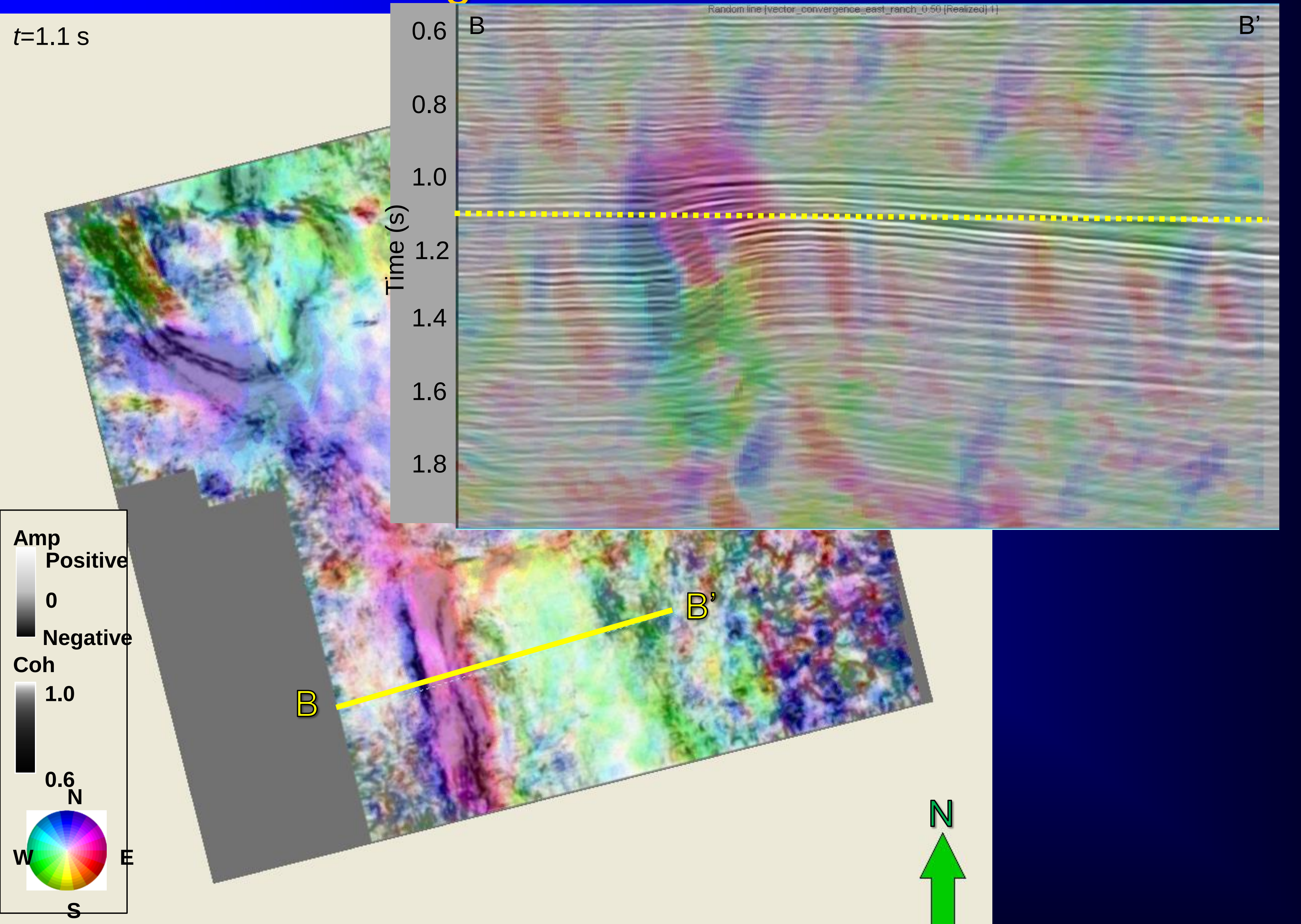

Reflector convergence co-rendered with coherence

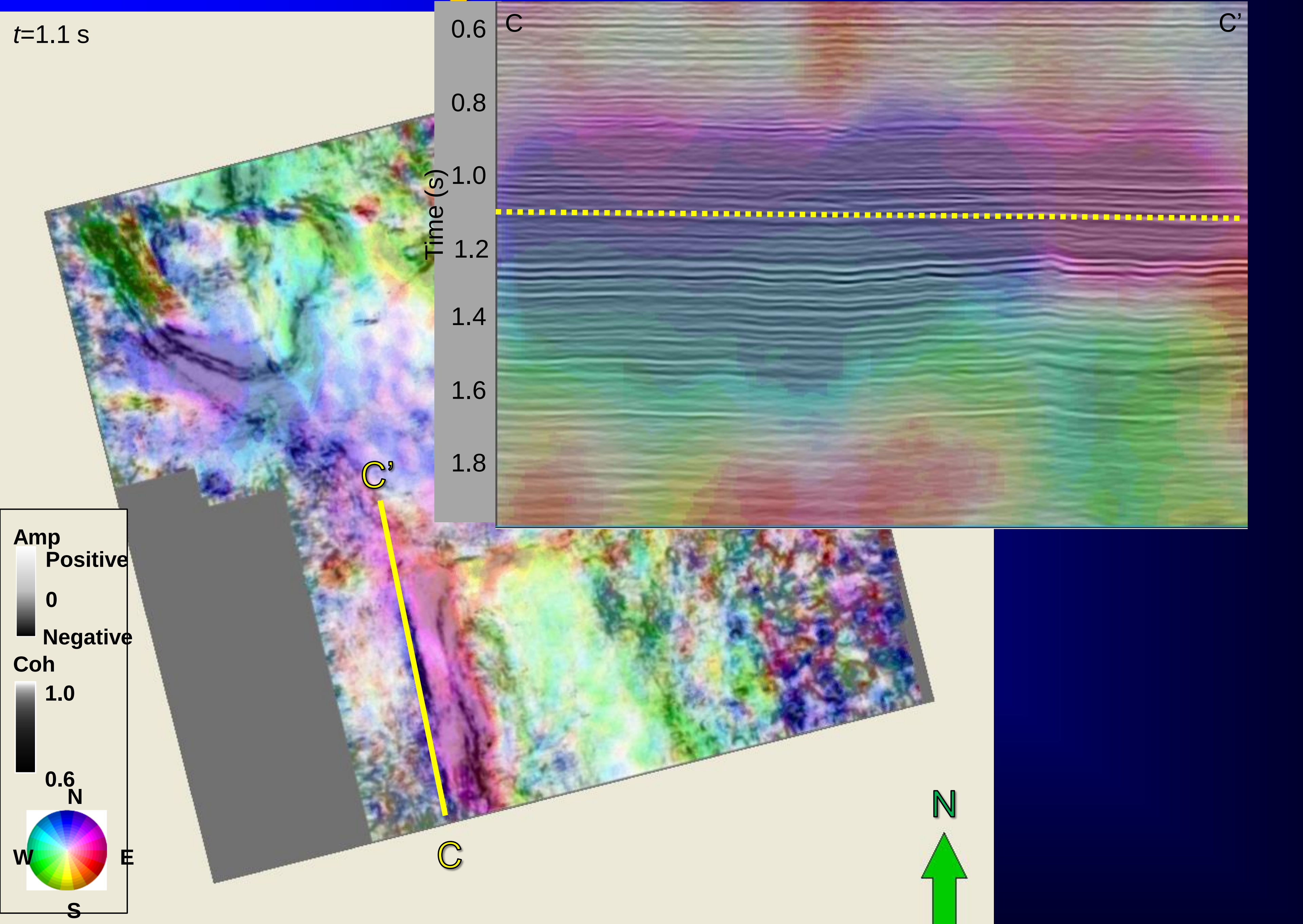

Reflector convergence co-rendered with coherence

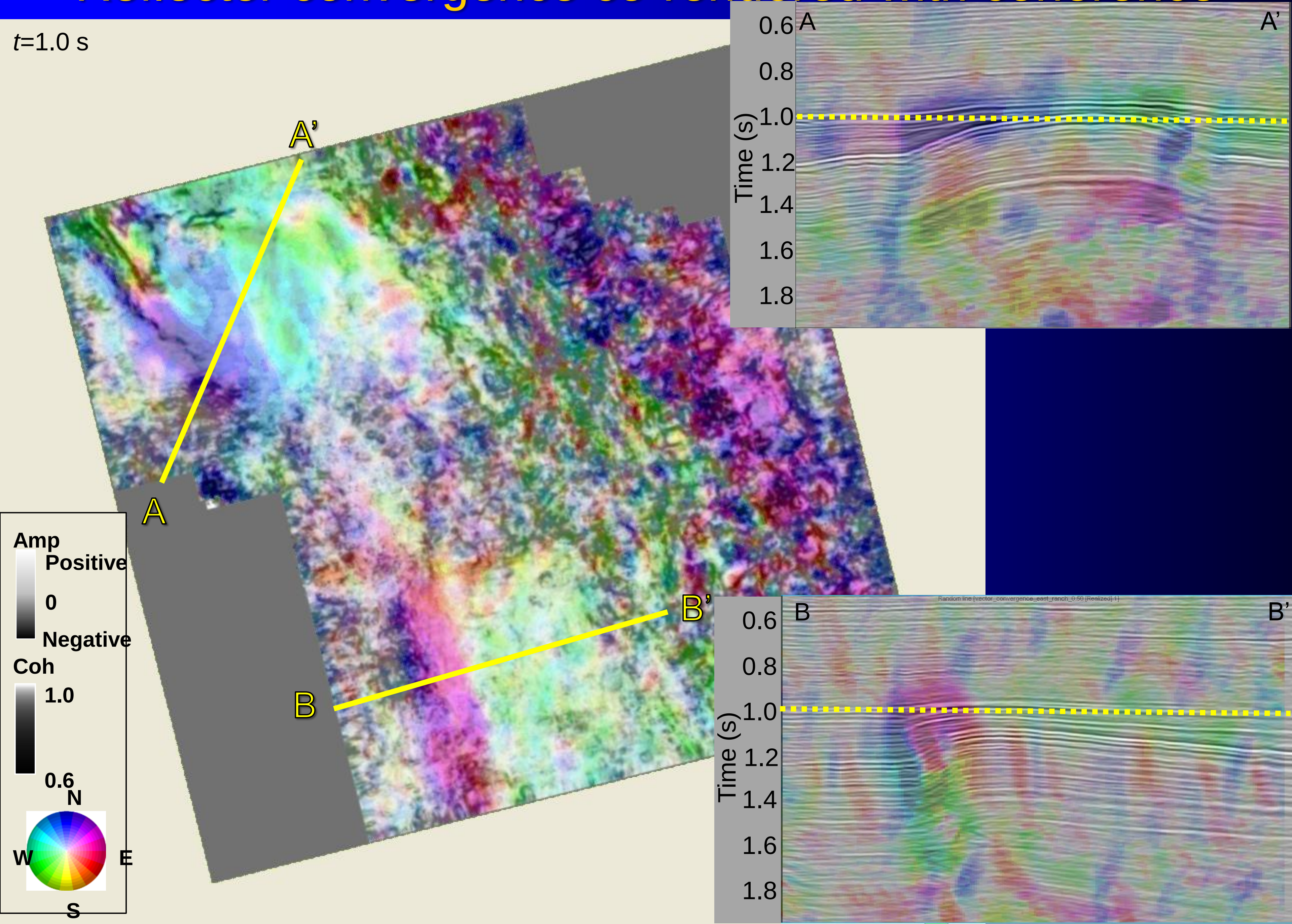

Reflector convergence co-rendered with coherence

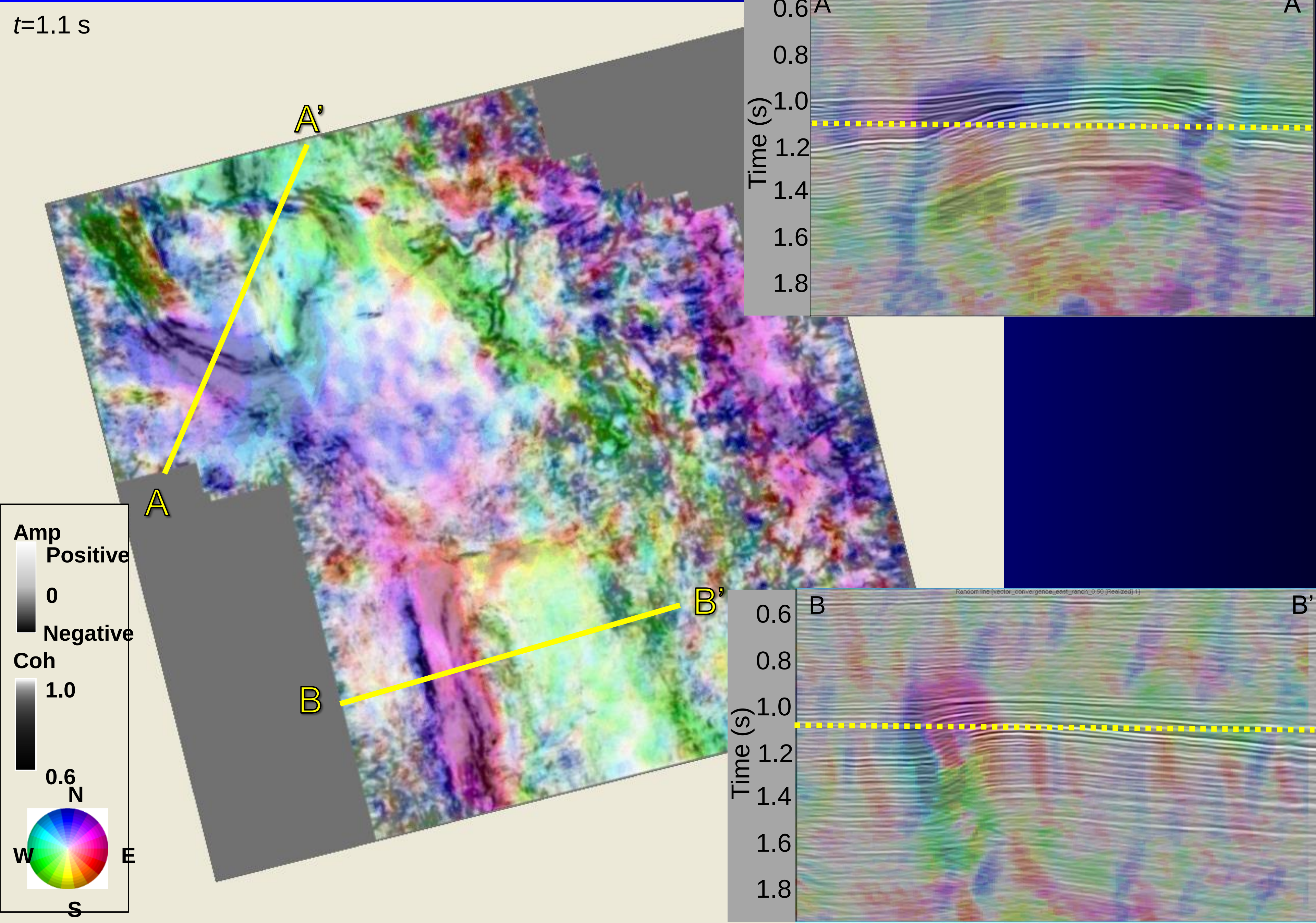

Reflector convergence co-rendered with coherence

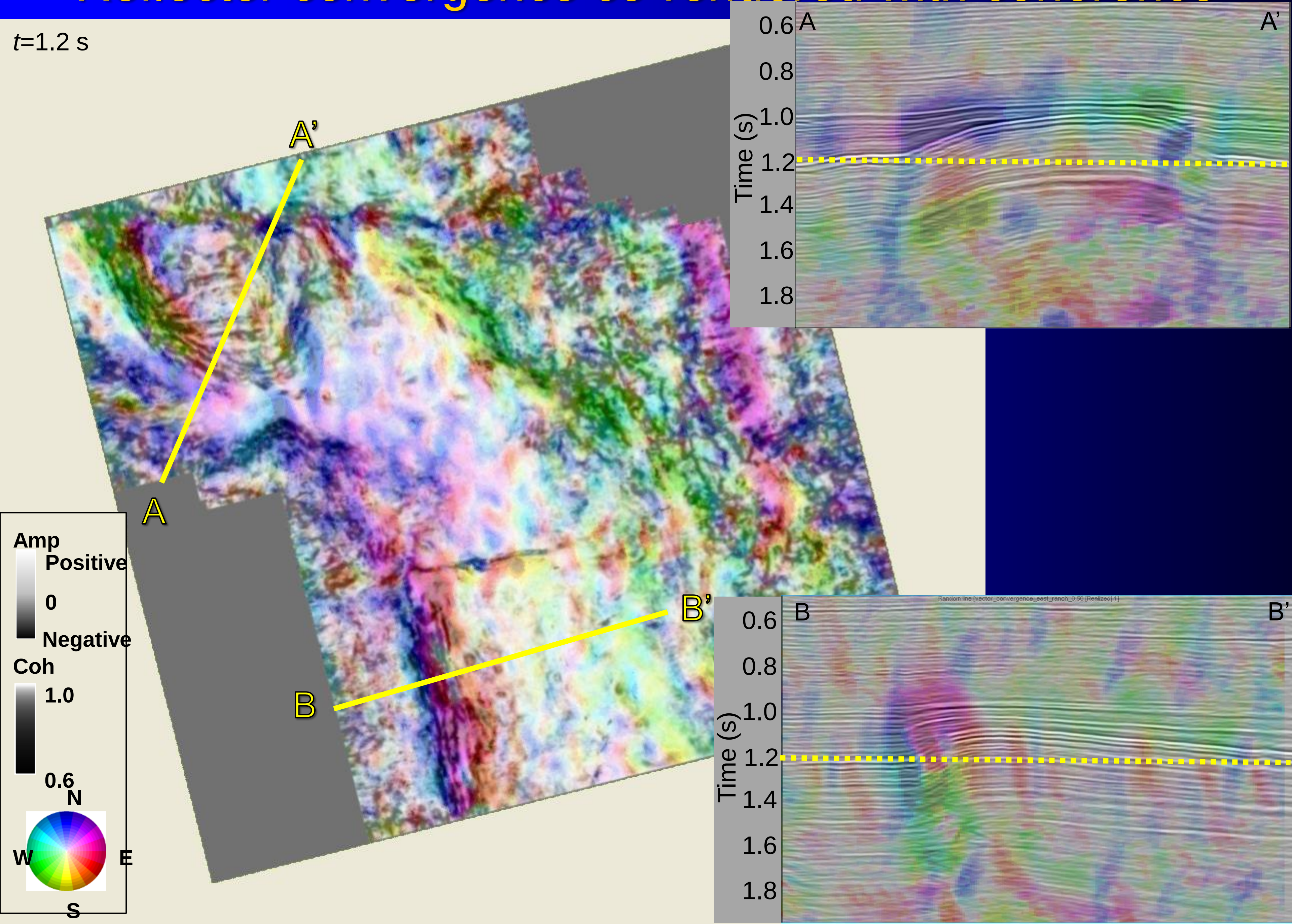

Reflector convergence co-rendered with coherence

t=1.3 s

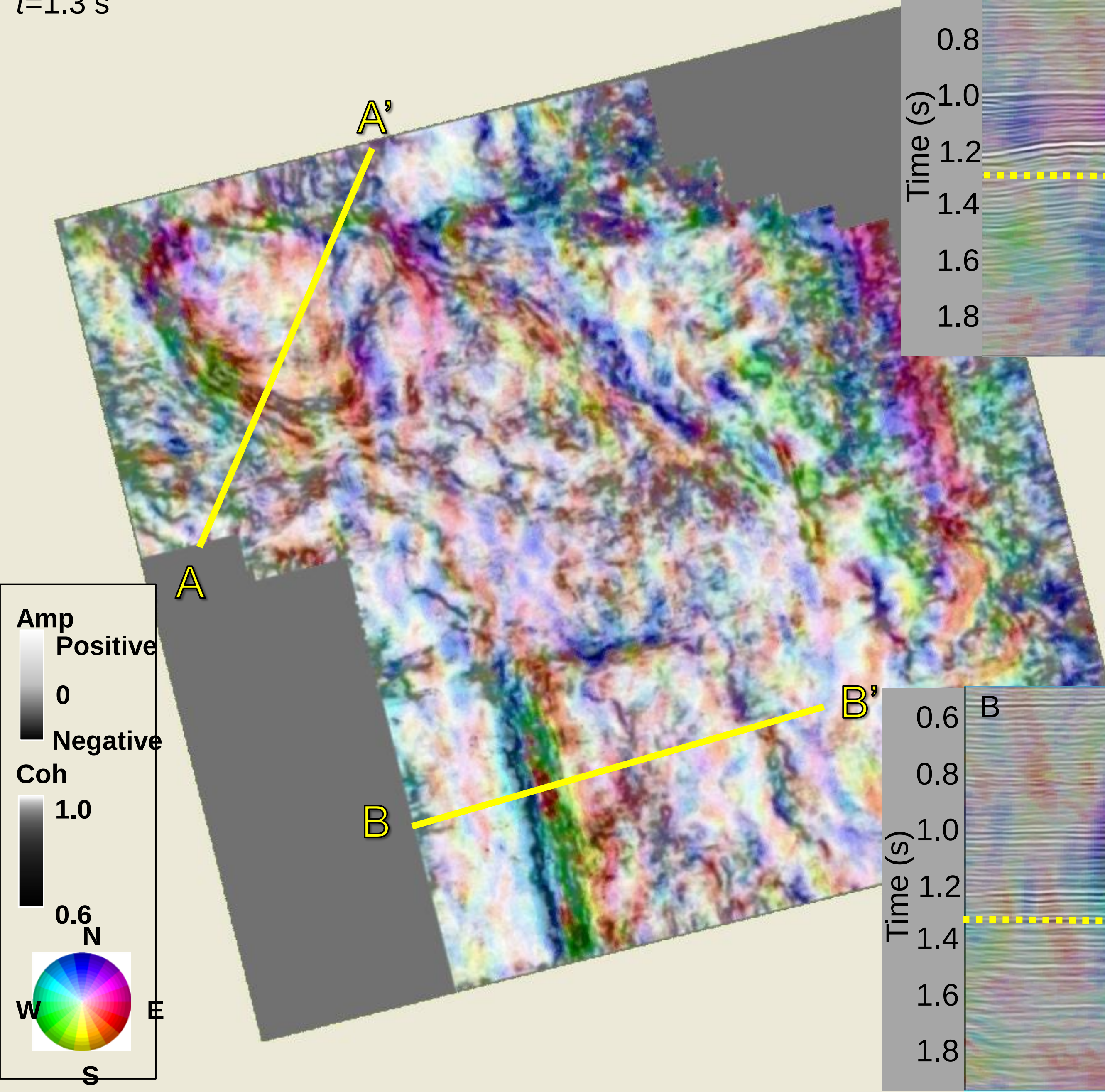

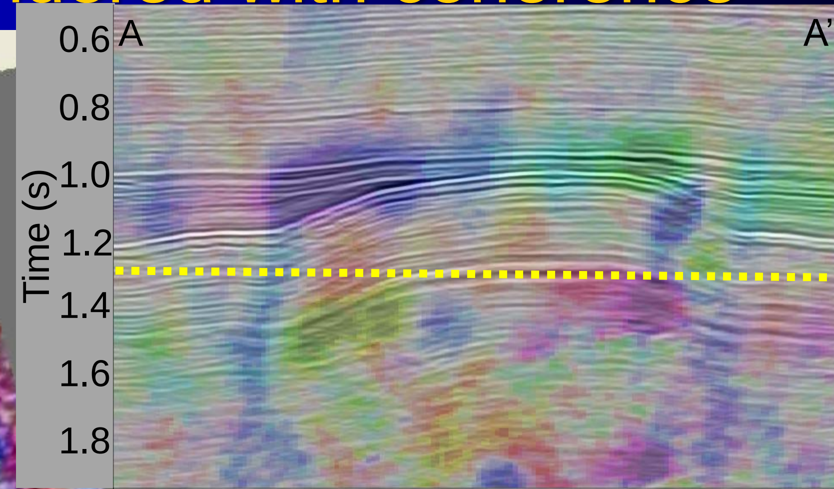

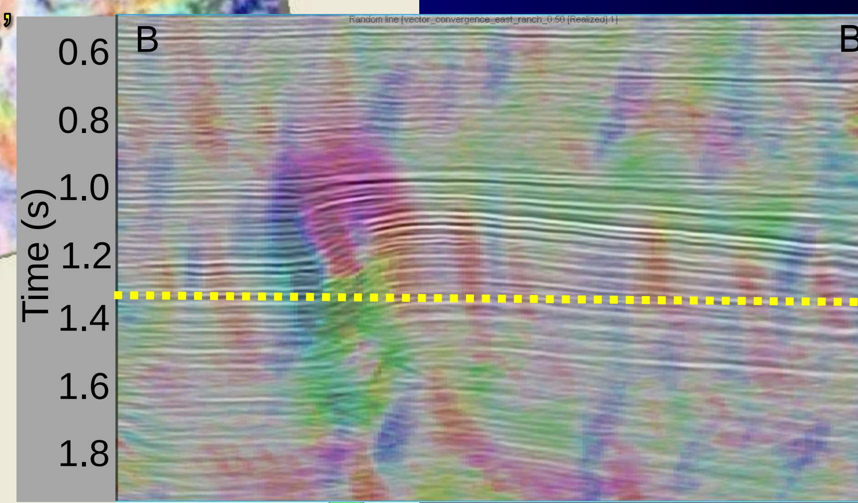

Rotation about the normal to the reflector

$$r = \mathbf{n} \bullet \boldsymbol{\psi} = n_x \left(\frac{\partial n_y}{\partial z} - \frac{\partial n_z}{\partial y} \right) + n_y \left(\frac{\partial n_z}{\partial x} - \frac{\partial n_x}{\partial z} \right) + n_z \left(\frac{\partial n_x}{\partial y} - \frac{\partial n_y}{\partial x} \right)$$

(Marfurt and Rich, 2010)

Reflector rotation co-rendered with coherence

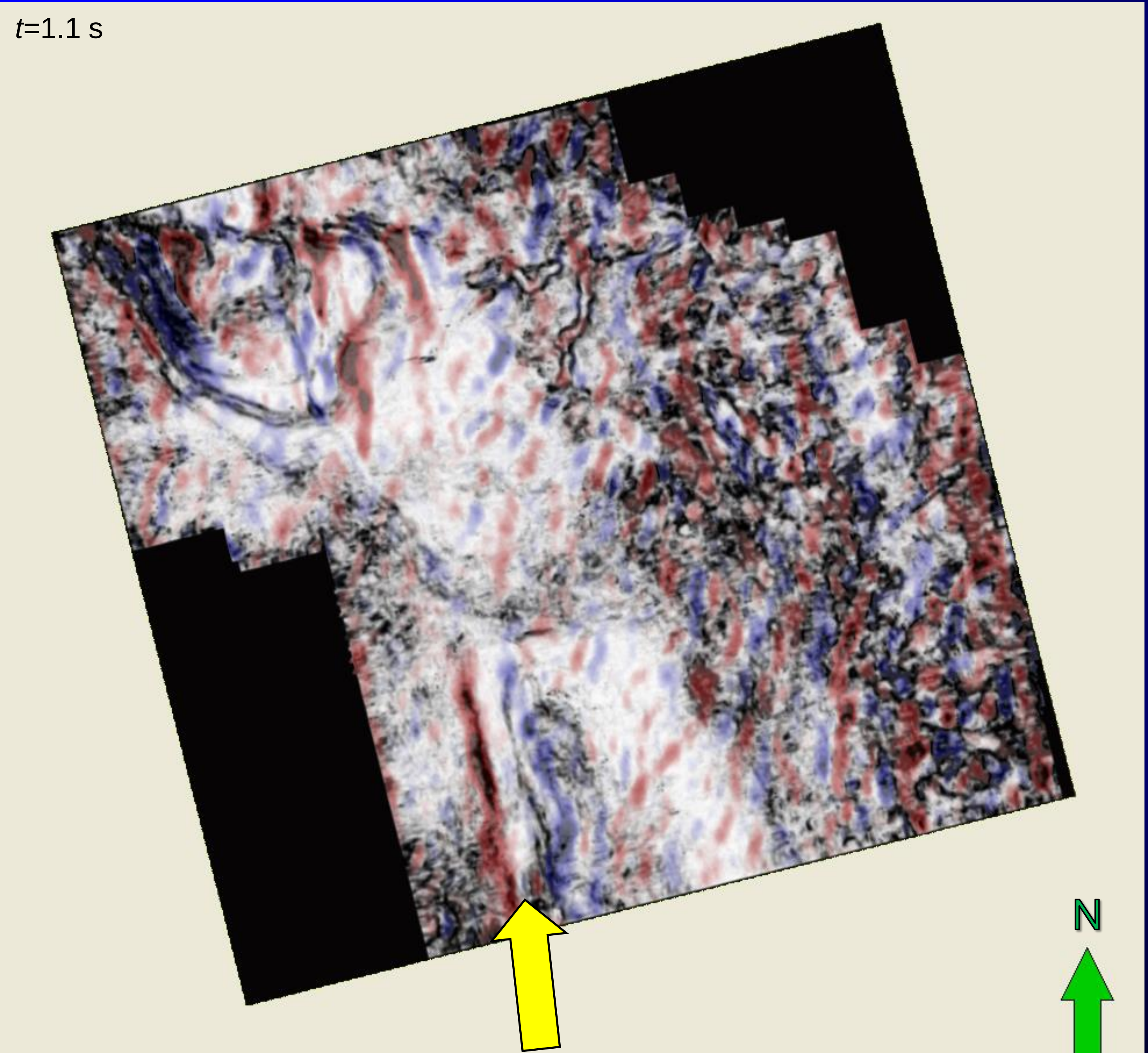

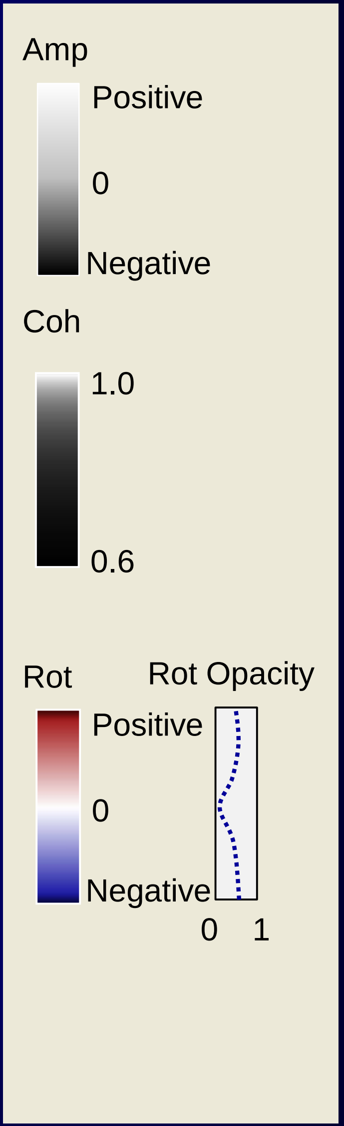

Attributes based on volumetric dip and azimuth

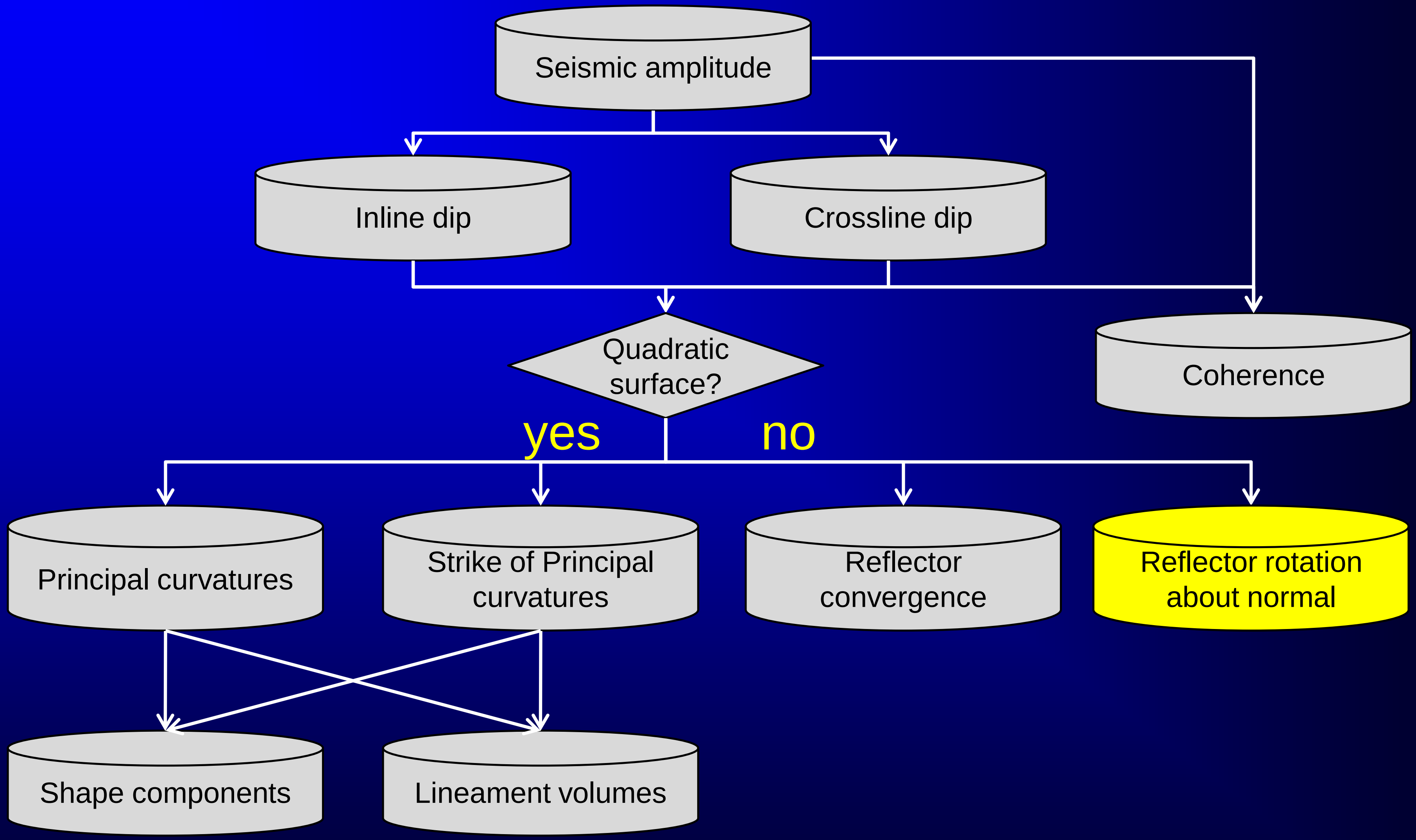

Computational vs. Interpretational curvature

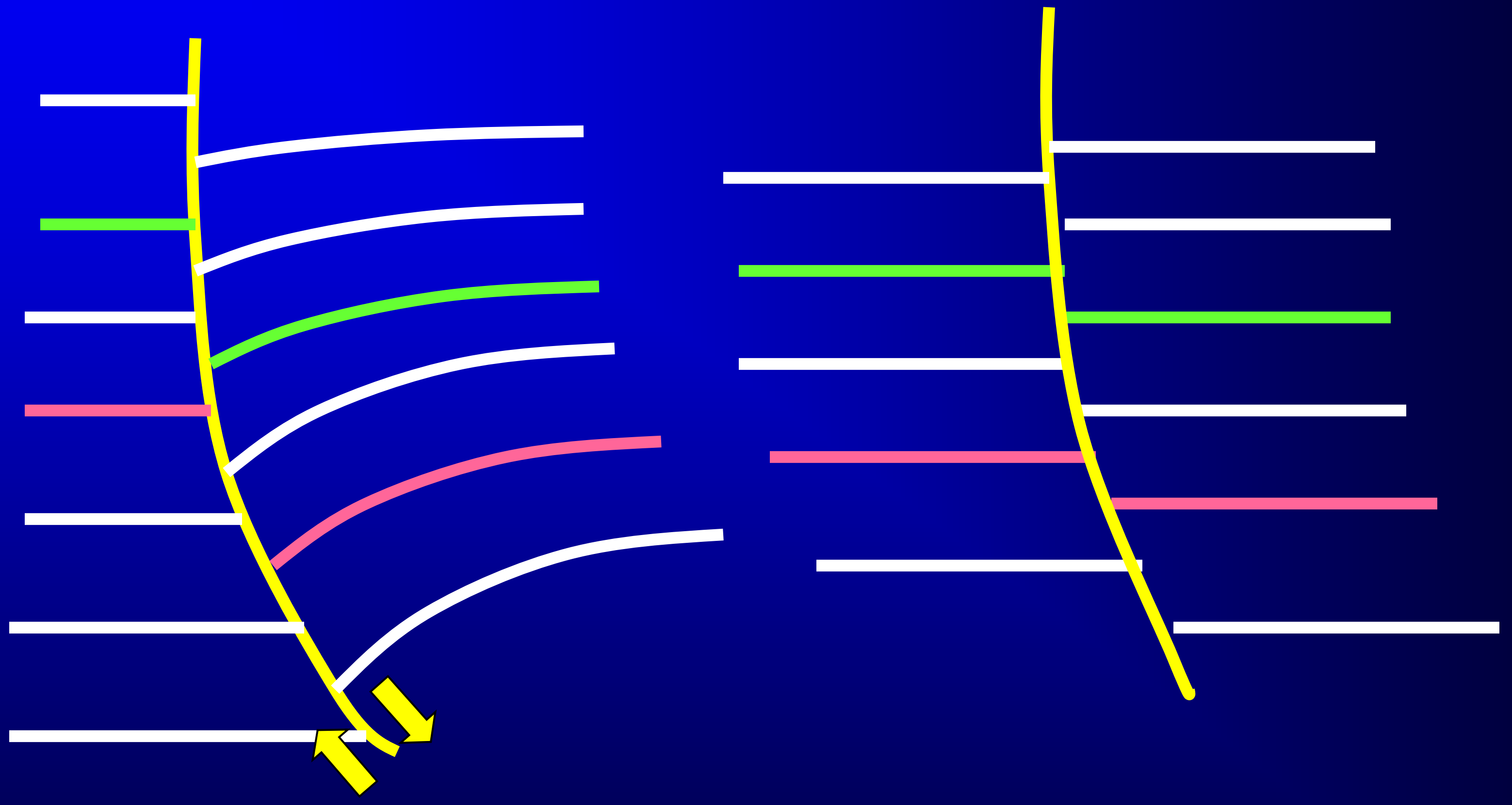

Normal fault seen by curvature

Strike slip fault not seen by curvature

Computational vs. Interpretational curvature

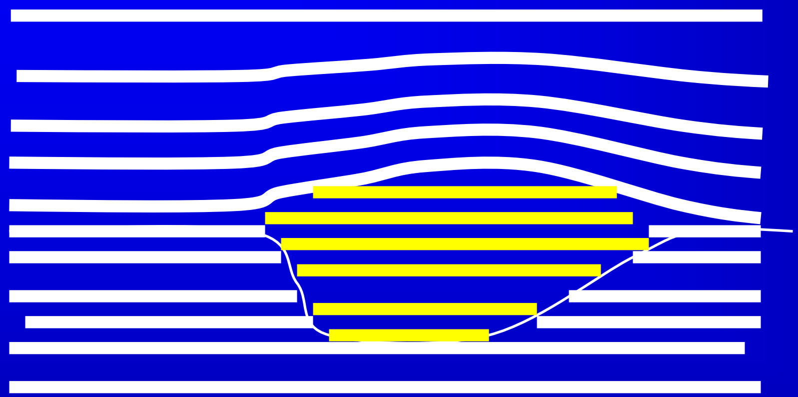

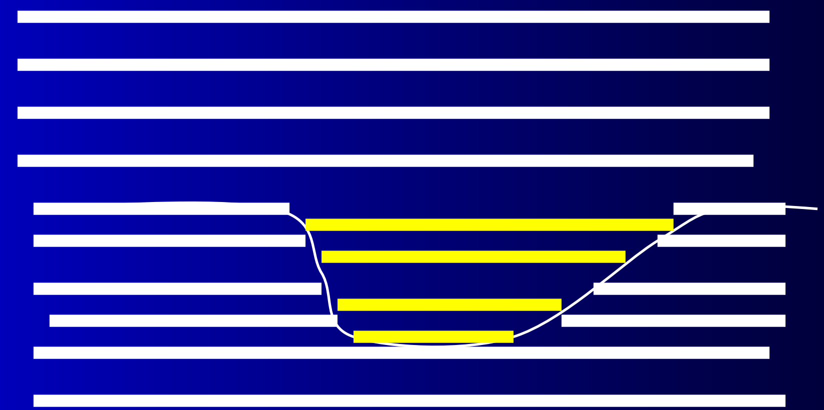

Channel *not* seen by curvature

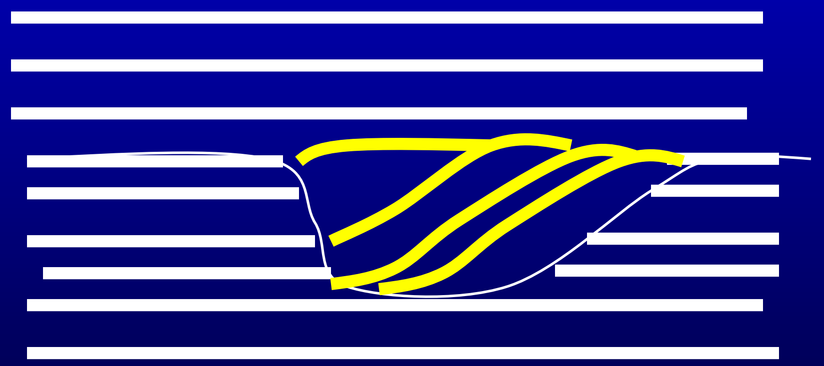

Channels seen by curvature

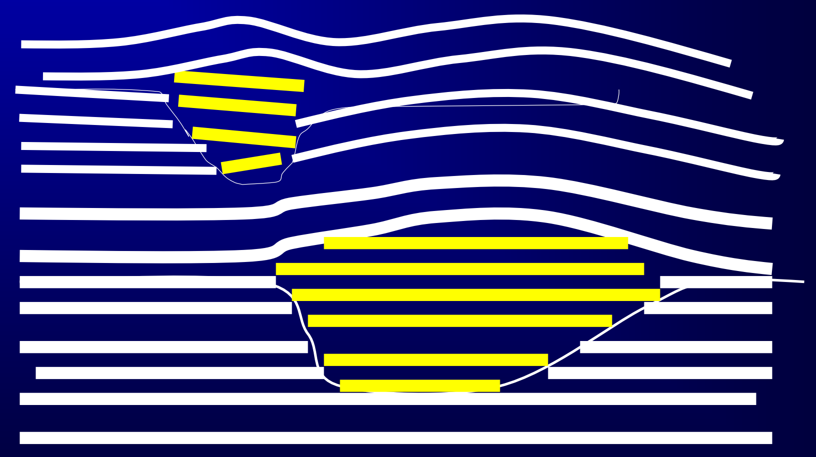

Stacked channels giving composite curvature anomaly

Curvature, Reflector Rotation, and Reflector Convergence

In Summary:

- Volumetric curvature extends a suite of attributes previously limited to interpreted horizons to the entire uninterpreted cube of seismic data.
- The most negative and most positive principal curvatures appear to be the most unambiguous of the curvature images in illuminating folds and flexures.
- Curvature attributes are a good indicator of paleo rather than present-day stress regimes.
- Open fractures are a function of the strike of curvature lineaments and the azimuth of minimum horizontal stress.
- Channels appear in curvature images if there is differential compaction.
- Faults appear in curvature images if there is a change in reflector dip across the fault, reflector drag, if the fault displacement is below seismic resolution, or if the fault edge is over- or under-migrated.